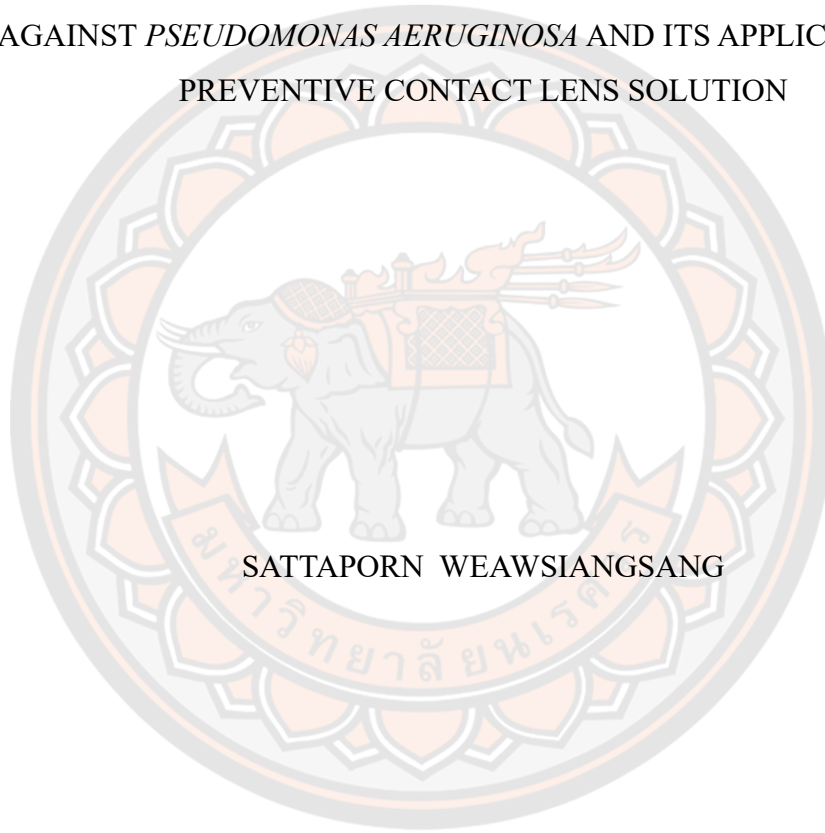




INVESTIGATING ANTIBACTERIAL MECHANISMS OF HYDROQUININE
AGAINST *PSEUDOMONAS AERUGINOSA* AND ITS APPLICATION AS
PREVENTIVE CONTACT LENS SOLUTION



SATTAPORN WEAWSIANGSANG

A Thesis Submitted to the Graduate School of Naresuan University
in Partial Fulfillment of the Requirements
for the Doctor of Philosophy in Biomedical Sciences

2023

Copyright by Naresuan University

INVESTIGATING ANTIBACTERIAL MECHANISMS OF HYDROQUININE
AGAINST *PSEUDOMONAS AERUGINOSA* AND ITS APPLICATION AS
PREVENTIVE CONTACT LENS SOLUTION



A Thesis Submitted to the Graduate School of Naresuan University
in Partial Fulfillment of the Requirements
for the Doctor of Philosophy in Biomedical Sciences
2023

Copyright by Naresuan University

Thesis entitled "Investigating antibacterial mechanisms of hydroquinine against *Pseudomonas aeruginosa* and its application as preventive contact lens solution"

By Sattaporn Weawsiangsang

has been approved by the Graduate School as partial fulfillment of the requirements
for the Doctor of Philosophy in Biomedical Sciences of Naresuan University

Oral Defense Committee

..... Chair
(Assistant Professor Robert Baldock, Ph.D.)

..... Advisor
(Assistant Professor Jirapas Jongjitwimol, Ph.D.)

..... Internal Examiner
(Assistant Professor Yordhathai Thongsri, Ph.D.)

..... Internal Examiner
(Krai Daowtak, Ph.D.)

..... External Examiner
(Assistant Professor Thanwa Wongsuk, Ph.D.)

Approved

.....
(Associate Professor Krongkarn Chootip, Ph.D.)
Dean of the Graduate School

Title INVESTIGATING ANTIBACTERIAL MECHANISMS OF HYDROQUININE AGAINST *PSEUDOMONAS AERUGINOSA* AND ITS APPLICATION AS PREVENTIVE CONTACT LENS SOLUTION

Author Sattaporn Weawsiangsang

Advisor Assistant Professor Jirapas Jongjitwimol, Ph.D.

Academic Paper Ph.D. Dissertation in Biomedical Sciences, Naresuan University, 2023

Keywords antibacterial mechanism, contact lens solution, hydroquinine, *Pseudomonas aeruginosa*

ABSTRACT

Pseudomonas aeruginosa is one of the most common causes of contact-lens-related microbial keratitis (CLMK). Previous studies reported that disinfecting solutions were ineffective in preventing biofilm formation. Solutions containing novel natural agents may be an excellent option for reducing the risk of CLMK. Hydroquinine has antimicrobial potential with demonstrated activity against several bacteria, including drug-sensitive (DS) and multidrug-resistant (MDR) *P. aeruginosa* reference strains. Despite this, there is limited evidence confirming the antibacterial activity of hydroquinine against clinical isolates and the underlying mechanism of action. Here, this study aimed to investigate the antibacterial effect of hydroquinine in clinical *P. aeruginosa* strains using phenotypic antimicrobial susceptibility testing and synergistic testing. This study examined the potential inhibitory mechanisms against MDR *P. aeruginosa* isolates using molecular docking analysis in combination with RT-qPCR. Furthermore, this study investigated the antibacterial, anti-adhesion, and anti-biofilm properties of hydroquinine formulated multipurpose solutions (MPSs) compared to MPSs alone.

These thesis finding uncovered that hydroquinine inhibits and kills clinical *P. aeruginosa* at 2.50 mg/mL (MIC) and 5.00 mg/mL (MBC), respectively. Hydroquinine also showed partial synergistic effects with ceftazidime against clinical MDR *P. aeruginosa* strains. Using molecular docking, this study identified potential

interactions between arginine deiminase (ADI) pathway-related proteins and hydroquinine. Furthermore, using RT-qPCR, hydroquinine directly affected the mRNA expression of the *arc* operon. This study demonstrated that the ADI-related genes, including the arginine/ornithine antiporter (*arcD*) and the three enzymes; arginine deiminase (*arcA*), ornithine transcarbamylase (*arcB*), and carbamate kinase (*arcC*) were significantly downregulated at half MIC of hydroquinine. Moreover, hydroquinine directly affected the expression levels of adhesion-related genes, namely *cgrC*, *cheY*, *cheZ*, *fimU*, and *pilV*. Using ISO 14729 stand-alone testing, hydroquinine met the criteria (>99.9% killing at disinfection time) against both *P. aeruginosa* reference and clinical strains. Using the crystal violet retention assay and FE-SEM, MPSs combined with hydroquinine were effective in inhibiting *P. aeruginosa* adhesion and destroying preexisting biofilms.

This study is the first report that the ADI-related proteins are potential molecular targets for the inhibitory effect of hydroquinine against clinically isolated MDR *P. aeruginosa* strains. Moreover, this is also the first report that hydroquinine-containing formulations have potential use as a contact lens disinfecting solution for adhesion inhibition and biofilm destruction. These findings may aid in the development of novel disinfectants aimed at combating *P. aeruginosa*, thereby potentially reducing the incidence of CLMK.

ACKNOWLEDGEMENTS

First of all, I would like to thank and offer my respect to my thesis advisor, Assistant Professor Dr. Jirapas Jongjitwimol who has supported me throughout the length of the study with his attention, his energy, his patience, and his kindness. He has given me helpful consultation and technical support on the lab experiment, results, and publications. I am indeed deeply grateful to my advisor for having always believed in my abilities. He provided several opportunities along this journey. This thesis would not have been feasible without his counsel and cooperation.

The author would like to attribute special thanks to Assistant Professor Dr. Sukunya Ross as well as Assistant Professor Dr. Gareth M. Ross, Faculty of Science, Naresuan University, for allowing me to be part of the EU-funded Molecular Design of Polymers for Biomedical Applications (MEDIPOL) project at Aston University, United Kingdom, which led me to expand my research knowledge and experience. Also, I would like to acknowledge Professor Brian J. Tighe from Aston University for his useful guidance and intellectual support.

I would like to thank Assistant Professor Dr. Robert A. Baldock for becoming chair of this thesis examination. Moreover, I would like to thank him for allowing me to be part of the Exchange Programme in the Faculty of Science and Health, School of Pharmacy and Biomedical Sciences, University of Portsmouth, United Kingdom, leading me to expand my new experience, new knowledge, and new technology to fulfil the missing gaps in the thesis.

I would like to thank Assistant Professor Dr. Thanwa Wongsuk, Assistant Professor Dr. Yordhathai Thongsri, and Dr. Krai Daowtak for being members of my external and internal committees in the thesis examination. I also would like to give special thanks to all members of the thesis committee and I am deeply grateful for their helpful comments.

I would like to thank Assistant Professor Dr. Nungruthai Nilsri, Assistant Professor Dr. Yordhathai Thongsri, Dr. Napaporn Apiratmateekul, and Dr. Krai Daowtak for their recommendations on the experiments, encouragements, and comments. I am also thankful to all Biomedical Sciences (BMS) staff in the Faculty of Allied Health Sciences, especially Assistant Professor Dr. Pachuen Potup and Miss Pilaipan

Kongtiam, for their support throughout my study here.

I am thankful to Miss Nontaporn Rattanachak, who has given me advice on the microbial experimental technique. I am also thankful for the friendship and encouragement given to me by my friends and all the graduate students in the BMS Program. Also, thanks to all the professors from the Faculty of Allied Health Sciences who provided lectures equipped with a considerable amount of precious knowledge that stands as the base of the research. I would like to thank the Faculty of Allied Health Sciences, Naresuan University for providing the facility for performing lab experiments, expense, and accommodation.

In addition, I would like to thankfully acknowledge funding from the Full Tuition Fee Scholarship for Naresuan University high-potential graduate-level students fiscal year 2023, Naresuan University, to support my study and an additional grant from the faculty of Allied Health Sciences, Naresuan University, for support my thesis.

Finally, I want to give special thanks and respect to myself, my family, and my friends for their mental and financial support during this whole study.

Sattaporn Weawsiangsang



TABLE OF CONTENTS

	Page
ABSTRACT.....	C
ACKNOWLEDGEMENTS.....	E
TABLE OF CONTENTS.....	G
List of tables.....	K
List of figures.....	L
CHAPTER I INTRODUCTION.....	1
Background and Significance of the Study.....	1
Purposes of the Study.....	2
Statement of the Problem.....	2
Scope of the Study.....	3
Hypotheses of the Study.....	3
CHAPTER II LITERATURE REVIEW.....	5
Hydroquinine (HQ).....	5
Anti-bacterial activity of hydroquinine.....	7
The arginine deiminase (ADI) pathway.....	8
Antibacterial mechanism of natural alkaloids.....	9
Inhibition of bacterial nucleic acid and protein synthesis.....	10
Inhibition of cell wall synthesis and disruption of cell membrane function.....	11
Inhibition of bacteria metabolisms.....	11
Inhibition of efflux pump.....	12
<i>Pseudomonas aeruginosa</i>	13
Introduction to <i>Pseudomonas aeruginosa</i>	14
Bacterial keratitis.....	16
Corneal structure.....	16
Corneal infection.....	18

Contact lens.....	18
Contact lens-related corneal infection.....	19
Contact-lens-related microbial keratitis (CLMK).....	22
Risk factors of CLMK.....	22
Pathogenesis of CLMK (Mechanism of infection).....	23
<i>Pseudomonas aeruginosa</i> virulence factor related with CLMK	26
Bacterial adhesion on contact lens	28
Biofilm formation on contact lens.....	29
Pathogenesis of <i>Pseudomonas aeruginosa</i> related CLMK.....	30
The diagnosis and treatment of CLMK	30
Commonly used disinfectants in contact lens solutions	31
CHAPTER III RESEARCH METHODOLOGY	33
Research materials	33
Culture medias.....	33
Chemicals and reagents	33
Equipments.....	34
Instruments	34
Experimental designs.....	35
Part 1: The characterization of hydroquinine against <i>P. aeruginosa</i> clinical strains	36
1.1 Preparation antibiotics and hydroquinine (HQ)	36
1.2 Strain and microorganism cultivation	36
1.3 Antibiotic susceptibility testing of the bacterial stains.....	36
1.4 Antibacterial activity	37
1.5 <i>In vitro</i> evaluation of synergistic effects using the checkerboard method ..	38
Part 2: The purpose mechanisms of hydroquinine against <i>P. aeruginosa</i> clinical strains.....	39
2.1 Molecular docking analysis.....	39
2.2 Testing the genes expression of <i>P. aeruginosa</i> strains.....	42
2.2.1 RNA extraction.....	43

2.2.2 Complementary DNA (cDNA) synthesis	44
2.2.3 Quantitative Reverse Transcription PCR (RT-qPCR)	44
Part 3: The application of hydroquinine as preventive contact lens solution	45
3.1 <i>P. aeruginosa</i> strains, cultivation, and inoculum preparation	45
3.2 Contact lenses and lenses cases preparation.....	45
3.3 Commercial multipurpose solutions preparation	46
3.4 Tested solution preparation.....	46
3.5 Studying adhesion-related gene expression levels	46
3.6 Stand-alone testing with microorganisms	47
3.7 Anti-adhesion efficacy of tested solutions.....	47
3.8 Anti-adhesion efficacy on contact lens.....	47
3.9 Anti-biofilm mass on contact lens	48
3.10 Morphological observation using the FE-SEM.....	48
Statistical analysis.....	48
CHAPTER IV RESULTS	49
Part 1: The characterization of hydroquinine against <i>P. aeruginosa</i> clinical strains	49
1.1 Antibiotic susceptibility testing of the bacterial stains	49
1.2 Antibacterial activity	50
1.3 <i>In vitro</i> evaluation of synergistic effects using the checkerboard method ..	51
Part 2: The purpose mechanisms of hydroquinine against <i>P. aeruginosa</i> clinical strains.....	53
2.1 Molecular docking analysis.....	56
2.1.1 Hydroquinine docked with the arginine deiminase (ADI) protein ..	59
2.1.2 Hydroquinine docked with the ornithine transcarbamylase (OTC) protein.....	60
2.1.3 Hydroquinine docked with the carbamate kinase (CK) protein	61
2.1.4 Hydroquinine docked with the arginine/ornithine antiporter (AOA) protein.....	62
2.2 Testing the genes expression of <i>P. aeruginosa</i> strains.....	63

Part 3: The application of hydroquinine as preventive contact lens solution	64
3.1 Testing the adhesion-related genes expression of <i>P. aeruginosa</i> strains	64
3.2 Anti-bacterial activity of multipurpose solutions	65
3.3 Anti-adhesion efficacy of multipurpose solutions.....	67
3.4 Anti-bacterial activity of hydroquinine alone and in combination with MPSs	68
3.5 Anti-adhesion efficacy of hydroquinine alone and in combination with MPSs	70
3.6 Anti-adhesion efficacy on contact lens surface	71
3.7 Destruction biofilm mass on contact lens surface	72
CHAPTER V DISCUSSIONS AND CONCLUSIONS	73
Hydroquinine inhibits and kills MDR <i>P. aeruginosa</i> isolated from clinical samples	73
Hydroquinine inhibits <i>P. aeruginosa</i> growth through decreased expression of ADI pathway-related genes	75
Hydroquinine enhances the effectiveness of contact lens solutions for inhibiting <i>Pseudomonas aeruginosa</i> adhesion and biofilm formation	78
ABBREVIATION LIST.....	82
REFERENCES	86
BIOGRAPHY	101

List of tables

	Page
Table 1 Virulence factors of <i>Pseudomonas aeruginosa</i>	15
Table 2 The risk factors associated with contact lens-associated infectious keratitis..	23
Table 3 Primer sequences and annealing temperature used in this study.....	43
Table 4 Commercial multipurpose solution (MPS) used in this study.....	46
Table 5 <i>P. aeruginosa</i> strains used in this study	49
Table 6 Phenotypic antibiotic susceptibility profiles of <i>P. aeruginosa</i> ATCC 27853 and eight clinical <i>P. aeruginosa</i> isolates to six classes of anti-pseudomonal drugs	50
Table 7 Antibacterial activity of hydroquinine against <i>P. aeruginosa</i> ATCC 27853 and clinical <i>P. aeruginosa</i> isolates.....	50
Table 8 The combined effect of hydroquinine and antibiotics against clinical MDR <i>P. aeruginosa</i> isolates.....	52
Table 9 The top 15 transcripts of the significantly up-regulated DEGs (hypothetical protein and undefined genes were excluded).....	53
Table 10 The top 15 transcripts of the significantly down-regulated DEGs (hypothetical protein and undefined genes were excluded).....	54
Table 11 DEGs of ADI pathway-related genes as determined by transcriptome analysis.....	55
Table 12 The molecular docking results between hydroquinine and ADI pathway-related proteins using SwissDock.	56
Table 13 S score and estimated ΔG value for binding (kcal/mol) between hydroquinine and ADI pathway-related proteins using MOE and SwissDock.....	57
Table 14 DEGs of adhesion-related genes as determined by transcriptome analysis..	64
Table 15 Anti-adhesion efficacy of MPSs against <i>P. aeruginosa</i> strains.....	67
Table 16 Anti-adhesion efficacy of hydroquinine solutions and their combinations against <i>P. aeruginosa</i> strains.....	70

List of figures

	Page
Figure 1 Chemical structures of quinine (Q) and hydroquinine (HQ).....	5
Figure 2 Structure of cinchona alkaloids	7
Figure 3 The nest entrances of <i>Tetrigona apicalis</i>	7
Figure 4 Antibacterial mechanism of substance	9
Figure 5 Bacterial cell membrane and cell wall component.....	10
Figure 6 Bacterial efflux pump systems	12
Figure 7 Structure of <i>Pseudomonas aeruginosa</i>	14
Figure 8 The many sites of <i>Pseudomonas aeruginosa</i> infection	16
Figure 9 Structure of the cornea.....	17
Figure 10 <i>Pseudomonas aeruginosa</i> keratitis	18
Figure 11 The pathogenesis of <i>P. aeruginosa</i> keratitis	20
Figure 12 Pathogenesis of contact lens-related microbial keratitis (CLMK)	21
Figure 13 Contact lens contaminated bacteria	23
Figure 14 Flow chart showing the relationship between the risk factors and the pathogenesis of CLMK.....	25
Figure 15 The main virulence factors in <i>Pseudomonas aeruginosa</i>	26
Figure 16 Summary of the stage of adhesion.....	28
Figure 17 Summary of the stage of biofilm formation	29
Figure 18 The bactericidal process of quaternary ammonium compounds	32
Figure 19 The mechanism of disinfectants	32
Figure 20 Experimental designs.....	35
Figure 21 96-well plate for broth microdilution assay.....	37
Figure 22 96-well plate for checkerboard method.....	38
Figure 23 Binding free energy formulation	40
Figure 24 Material and equipment used in contact lens study: (A) MPSs, (B) Contact lenses, (C) Standalone testing, and (D) Anti-adhesion efficacy on contact lens.	45

Figure 25 Minimum bactericidal concentration (MBC) of hydroquinine	51
Figure 26 Gene expression heatmap of <i>P. aeruginosa</i> ATCC 27853 in response to hydroquinine (1.25 mg/mL).....	55
Figure 27 The 3D electrostatic mapping of molecular docked hydroquinine to the ADI pathway-related target proteins.....	58
Figure 28 The 2D ligand interaction mapping of molecular docked hydroquinine to arginine deiminase (ADI).....	59
Figure 29 The 2D ligand interaction mapping of molecular docked hydroquinine to ornithine transcarbamylase (OTC).....	60
Figure 30 The 2D ligand interaction mapping of molecular docked hydroquinine to carbamate kinase (CK).....	61
Figure 31 The 2D ligand interaction mapping of molecular docked hydroquinine to arginine/ornithine antiporter (AOA)	62
Figure 32 The relative expression levels of the ADI pathway-related genes were treated with hydroquinine at 1.25 mg/mL for 1 h using RT-qPCR.....	63
Figure 33 The relative expression levels of the adhesion-related genes treated with 1.25 mg/mL of hydroquinine for an hour in <i>P. aeruginosa</i> ATCC 27853 compared to the corresponding untreated control.....	65
Figure 34 The log of reduction of the <i>P. aeruginosa</i> growth as a parameter of antibacterial efficacy of multipurpose solutions at (A) 6 h and (B) 24 h contact time compared to the corresponding untreated controls (PBS).	66
Figure 35 The log of reduction of the <i>P. aeruginosa</i> growth as a parameter of antibacterial efficacy of tested solutions at (A) 6 h and (B) 24 h contact time compared to the corresponding untreated controls (PBS).	68
Figure 36 The structural characterization of <i>P. aeruginosa</i> ATCC 27853 as a representative strain in different tested solutions: (A) PBS, (B) 100% MPS A, (C) hydroquinine (HQ) 2.50 mg/mL, and (D) HQ 2.50 mg/mL with 100% MPS A.	69
Figure 37 The adhesion of <i>P. aeruginosa</i> ATCC 27853 on contact lens surface as a representative strain in different tested solutions: (A) PBS, (B) 100% MPS A, (C) hydroquinine (HQ) 2.50 mg/mL, and (D) HQ 2.50 mg/mL with 100% MPS A.	71
Figure 38 The biofilm mass of <i>P. aeruginosa</i> ATCC 27853 on contact lens surface as a representative strain in different tested solutions: (A) contact lens surface, (B) PBS, (C) 100% MPS A, (D) hydroquinine (HQ) 2.50 mg/mL, (E) HQ 1.25 mg/mL with 50% MPS A, (F) HQ 2.50 mg/mL with 50% MPS A, (G) HQ 1.25 mg/mL with 100% MPS A, and (H) HQ 2.50 mg/mL with 100% MPS A.	72

Figure 39 The schematic of the arginine deiminase (ADI) pathway. 76



CHAPTER I

INTRODUCTION

Background and Significance of the Study

Pseudomonas aeruginosa is an opportunistic pathogen in hospitalized patients with high propensity for multi-drug resistance (MDR). Bacterial keratitis, also known as corneal ulcer represents the overwhelming majority of contact-lens-related microbial keratitis (CLMK). In particular, *P. aeruginosa* is the most common pathogen which causes CLMK (1, 2). For these reasons, the treatment of either *P. aeruginosa* or MDR *P. aeruginosa* infections should have effective antibiotics or combined antibiotics. A new alternative agent from natural products may be another choice to be observed for inhibiting the growth of MDR *P. aeruginosa*. According to several investigations, natural substances or bioactive compounds extracted from medicinal plants (e.g., flavonoids, alkaloids, terpenoids) have been shown to possess antibacterial properties and anti-quorum sensing activities (3, 4). Many natural products have been documented as a potential antimicrobial agent to inhibit the growth of pathogenic microorganisms and also act as a synergistic agent or a potentiator of the particular antibiotics (5).

A previous study of Jongjitvimol *et al.* (6) reported that the ethanolic nest entrances extracts from *Tetrigona apicalis* possessed antibacterial, antifungal, and anti-proliferative activities. Significantly, hydroquinine (HQ) was found as the major content of chemical compounds in the extracts. As a therapeutic drug, hydroquinine has been used in medical treatment for nocturnal cramps in the Netherlands. However, safety concerns have been raised regarding the use of hydroquinine for this purpose. Moreover, hydroquinine may reduce light-brown patches on the skin and skin discolorations associated with pregnancy. In addition, hydroquinine has been documented that it has anti-malarial and demelanizing activities (7). According to these reviews, hydroquinine might be one of the potential agents as antimicrobials for safely use in humans.

The studies of crude extracts from natural products, according to Kraikongjit *et al.* (8) and Jongjitvimol *et al.* (6) has been reported that the extracts showed antibacterial activity. Interestingly, hydroquinine is one of the major compounds found in the extracts. The chemical structure of hydroquinine is closely related to quinine alkaloid compounds. Some chemicals in alkaloids compounds demonstrated a significant role in the treatment of several infectious diseases through specifically different mechanisms (9). Recently, Rattanachak *et al.* (10) found that hydroquinine potentially became antibacterial properties. The particular concentration of hydroquinine could inhibit and kill both gram-positive bacteria, namely *Staphylococcus aureus*, and gram-negative bacteria, *Enterobacter cloacae*, *Escherichia coli*, *Klebsiella pneumoniae* as well as in particular, *P. aeruginosa*. Furthermore, Rattanachak *et al.* (10) uncovered the mechanism of action through the evaluation of the global transcripts of *P. aeruginosa* in response to hydroquinine-induced stress using RNA sequencing with transcriptomic analysis. One point of note, however, is that the study reported only the set of up-regulated expression genes, in

particular, the MexCD-OprJ and MexXY efflux pumps. In addition, they have not reported the efficacy and potential use of hydroquinine in the clinic yet. Therefore, the antibacterial activity of hydroquinine against *P. aeruginosa* clinical strains and the exact mechanism of hydroquinine against *P. aeruginosa* strains, in particular the group of down-regulated expression genes based on transcriptomic analysis (10), were investigated in this study. Additionally, this study investigated the application of hydroquinine as preventive contact lens solution. Theoretically, to lower the risk of CLMK, contact lens solutions should be able to sufficiently reduce the number of microorganisms and prevent biofilm formation on contact lenses.

The findings from this study were beneficial in targeting *P. aeruginosa* infections, facilitating further development, and potentially aiding the discovery of novel drugs to treat *P. aeruginosa* infections. Furthermore, the findings from this study may enable hydroquinine to be used in the development of contact lens disinfectants to minimize infection risk. Therefore, the aims of this study are to evaluate the anti-bacterial activity of hydroquinine against *P. aeruginosa* clinical strains and to investigate the mechanism of hydroquinine in inhibiting growth *P. aeruginosa*. Moreover, evaluating the disinfection efficacy of hydroquinine against *P. aeruginosa* including anti-bacterial, anti-adhesion, anti-biofilm mass properties on contact lens were determined.

Purposes of the Study

1. To evaluate the anti-bacterial activity of hydroquinine against *P. aeruginosa* clinical strains and to investigate the exact mechanism of hydroquinine against *P. aeruginosa* ATCC 27853 as bacterial models.
2. To evaluate the disinfection efficiency of hydroquinine against *P. aeruginosa* including anti-bacterial, anti-adhesion, anti-biofilm mass properties for applicable use as a preventive contact lens solution.

Statement of the Problem

The studies of crude extracts from natural products, according to Kraikongjit *et al.* (8) and Jongjitvimol *et al.* (6) has been reported that the extracts showed antibacterial activity. Interestingly, hydroquinine is one of the major compounds found in the extracts. The chemical structure of hydroquinine is closely related to quinine alkaloid compounds. Some chemicals in alkaloids compounds demonstrated a significant role in the treatment of several infectious diseases through specifically different mechanisms (9). Recently, Rattanachak *et al.* (10) found that hydroquinine potentially became antibacterial properties. The particular concentration of hydroquinine could inhibit and kill both gram-positive bacteria, namely *Staphylococcus aureus*, and gram-negative bacteria, *Enterobacter cloacae*, *Escherichia coli*, *Klebsiella pneumoniae* as well as in particular, *P. aeruginosa*. Furthermore, Rattanachak *et al.* (10) uncovered the mechanism of action through the evaluation of the global transcripts of *P. aeruginosa* in response to hydroquinine-induced stress using RNA sequencing with transcriptomic analysis. One point of note, however, is that the study reported only the set of up-regulated expression genes, in particular, the MexCD-OprJ and MexXY efflux pumps. In addition, they have not reported the efficacy and potential use of hydroquinine in the clinic yet. Therefore, the antibacterial activity of hydroquinine against *P. aeruginosa* clinical strains and the

exact mechanism of hydroquinine against *P. aeruginosa* strains, in particular the group of down-regulated expression genes based on transcriptomic analysis (10), were investigated in this study. Additionally, this study investigated the application of hydroquinine as preventive contact lens solution. Theoretically, contact lens solutions should be able to sufficiently reduce the number of microorganisms and prevent biofilm formation on contact lenses to lower the risk of CLMK among contact lens users.

Scope of the Study

The scope of this research, hydroquinine (HQ) was studied in three main parts: (1) characterization of hydroquinine against all *P. aeruginosa* clinical strains, (2) the purpose mechanism of hydroquinine against *P. aeruginosa* clinical strains, and (3) the application of hydroquinine as preventive contact lens solution.

The first part involved the characterization of hydroquinine. Firstly, the antimicrobial susceptibility profiles of all *P. aeruginosa* clinical strains tested in this study were performed using a method from the Clinical and Laboratory Standards Institute (CLSI) guideline M07-A9 (11). Secondly, the antibacterial activity of hydroquinine against *P. aeruginosa* clinical strains was investigated using the broth microdilution method. Next, synergistic effects of hydroquinine with certain antibiotics were observed against *P. aeruginosa* clinical multi-drug resistant (MDR) strains by checkerboard method.

In the second part, the down-regulated expression genes based on transcriptomic analysis results (10) were selected in order to investigate the purpose mechanisms of hydroquinine against *P. aeruginosa* clinical strains. The purpose mechanism was predicted in atomic level using molecular docking analysis and then the mechanism was investigated in RNA levels using quantitative reverse transcription polymerase chain reaction (RT-qPCR).

The last part was the application of hydroquinine as preventive contact lens solution. Firstly, disinfection efficacies against *P. aeruginosa* were performed using stand-alone testing method and anti-bacterial activity assay on contact lens. Next, anti-adhesion activity assay on contact lens was performed using crystal violet (CV) retention assay and field emission scanning electron microscopy (FE-SEM) study. Lastly, anti-biofilm mass on contact lens was tested using FE-SEM.

According to the Biosafety and Biosecurity aspects, this work was approved by the Naresuan University Institutional Biosafety Committee (NUIBC no. 64-16) and (NUIBC MI 65-10-35). The microbiology-related experiments in this research were performed in the Biosafety Level 2 (BSL2) Laboratory at Medical Technology department and other experiments in this research were performed at central research laboratory unit (C.R.L.U), Faculty of Allied Health Science, Naresuan University, Phitsanulok, Thailand.

Hypotheses of the Study

A recent study by Jongjitvimol *et al.* (2020) (6) reported that hydroquinine is the major content of chemical compounds in the natural extracts, which possessed antibacterial, antifungal, and anti-proliferative activities. In addition, Rattanachak *et al.* (10) found that hydroquinine potentially became antibacterial properties, in

particular, *P. aeruginosa* which is the most common cause of contact lens-related microbial keratitis (1).

This study, therefore, hypothesized that hydroquinine may have antibacterial activity against clinical *P. aeruginosa* strains. Moreover, hydroquinine might have some mechanism against *P. aeruginosa*. Additionally, this study also hypothesized that hydroquinine might have disinfection efficacy against *P. aeruginosa*. Therefore, hydroquinine might serve as candidate compounds could be used as prophylactic agent in the preventive contact lens solution for preventing microorganism, in particular, *P. aeruginosa* growth on contact lens.



CHAPTER II

LITERATURE REVIEW

Hydroquinine (HQ)

Hydroquinine is an organic substance, sometimes known as dihydroquinine. It is present in naturally occurring quinine-related alkaloids (cinchona alkaloids). Additionally, it has been identified in commercial quinine medicinal formulations. Its molecular weight is 326.4334 g/mole and its chemical formula is $C_{20}H_{26}N_2O_2$ (7). In clinical settings, hydroquinine has been used to relieve nocturnal cramps in the Netherlands having been approved for this use (12). Concerns have been raised around the potential safety of using hydroquinine for this purpose. Hydroquinine (Inhibin®) has been prescribed medically to treat nocturnal cramps at 200 mg with supper and 100 mg at bedtime for two weeks (7). In a clinical trial, 300 mg dairy of hydroquinine was safe to take in the short-term period (14 days) (13). Moreover, the hydroquinine proved effective for prevention of frequent ordinary muscle cramps in the treated group versus the placebo treated group (13). Hydroquinine has also been shown to have demelanizing and an anti-malarial activities (7). Hydroquinine can also reduce light-brown patches on the skin and skin discolorations associated with pregnancy (7). Hydroquinine reduces melanin by delaying the production of the tyrosinase enzyme, which catalyzes the protein molecule (tyrosine) and dihydroxyphenylalanine (DOPA) in the melanin synthesis pathway (14). As a result, hydroquinine has the resources to be utilized as a powerful bleaching agent, although further investigation is required to determine its potential clinical use. Hydroquinine has been used as a derivative of a variety of medications used in pharmacology, including cabotegravir, capmatinib, tazemetostat, etc. Additionally, it was utilized in derivatives of malaria drug, including quinidine, cyproquinatone, tafenoquine, mefloquine, and chloroquine (7). The *in vitro* model demonstrated that hydroquinine at dosage of 129 nM [IC₅₀] inhibit the *Plasmodium falciparum* growth (15). The study of Nontprasert, A. *et al.* (1996) demonstrated the similar anti-malarial effects of quinine and hydroquinine, which are about ten times more potent than the metabolite 3-hydroxyquinine (15). Consistently, the deoxyribonucleic acid (DNA), ribonucleic acid (RNA), and protein have also been affected by hydroquinine during the *in vitro* erythrocytic growth cycle of *Plasmodium knowlesi* (16). Hydroquinine structure is like the quinine ($C_{20}H_{24}N_2O_2$), naturally occurring compounds, which is one of the cinchona alkaloids (10, 17) (Figure 1).

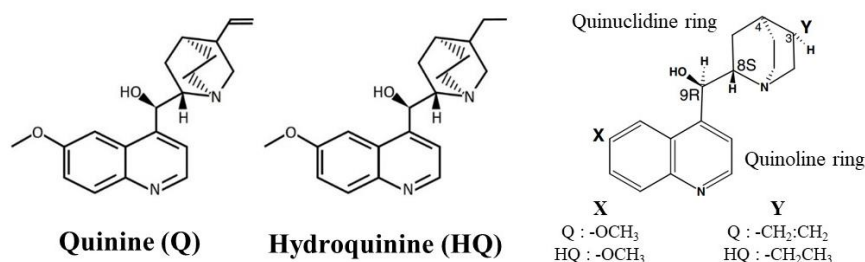


Figure 1 Chemical structures of quinine (Q) and hydroquinine (HQ)

In chemical structure, cinchona alkaloids consist of a conjugated heterocyclic quinoline ring joined to a bulky rigid bicyclo heterocyclic aliphatic quinuclidine ring by an alcoholic chiral carbon, C9. (17). The quinoline is organic compounds consist of a double-ring structure composed of a benzene (six carbon atoms) and a pyridine ring (five carbon atoms and a nitrogen atom) fused at two adjacent carbon atoms. The quinuclidine is a saturated organic heterobicyclic which contain two rings that share a pair of bridgehead carbon atoms and contains an amine group (17, 18). Quinine, quinidine, cinchonidine, and cinchonine are the four alkaloids found in cinchona (19, 20). The cinchona alkaloid structures are comparable in Figure 2. All of cinchona alkaloid contain the exocyclic unsaturated vinyl group attached to C3 of the quinuclidine ring. Cinchona bark also produces the analogous dihydro compounds namely hydroquinine in which the exocyclic double-bond has been reduced to the saturated ethyl group (Figure 1). Interestingly, quinoline ring has been found to possess antimalarial, anti-bacterial, antifungal, anti-inflammatory, analgesic activity, etc. (21). Most important use of the quinoline ring is its antimalarial potential. Quinine is the most common cinchona alkaloid, accounting for approximately 50-90% of the total amount of alkaloids (20). Quinine is cinchonidine in which the hydrogen at the 6-position of the quinoline ring is substituted by methoxy (-OMe). Quinine has been utilized as an anti-malarial medication in medicine for centuries (22, 23). Other cinchona alkaloids, including quinidine, cinchonine, and cinchonidine, were also used to treat malaria (23). Quinine has been demonstrated to have other medicinal benefits beyond its ability to treat malaria, including anti-inflammation and anti-cancer ability (24). Quinine has anticancer properties that effectively stop cancer cells from proliferating and lead to cell death due to its protease activity (25). Moreover, quinine can effectively handle obesity by triggering adipogenesis via ERK/S6 signaling (24). Several studies have shown that quinine has antibacterial effects against *Escherichia coli*, *Klebsiella pneumoniae*, and *Staphylococcus aureus*. Additionally, quinine derivatives demonstrated middle antimicrobial activity when compared with quinine itself on common pathogenic bacteria strains, e.g. *E. coli*, *S. aureus*, *P. aeruginosa*, and *Bacillus subtilis*. Among other quinine derivatives, ester quinine propionate was also discovered to have the highest antibacterial activity when compared to streptomycin (26). Considerably, the structure of cinchona alkaloid and hydroquinine might have potential anti-bacterial properties.

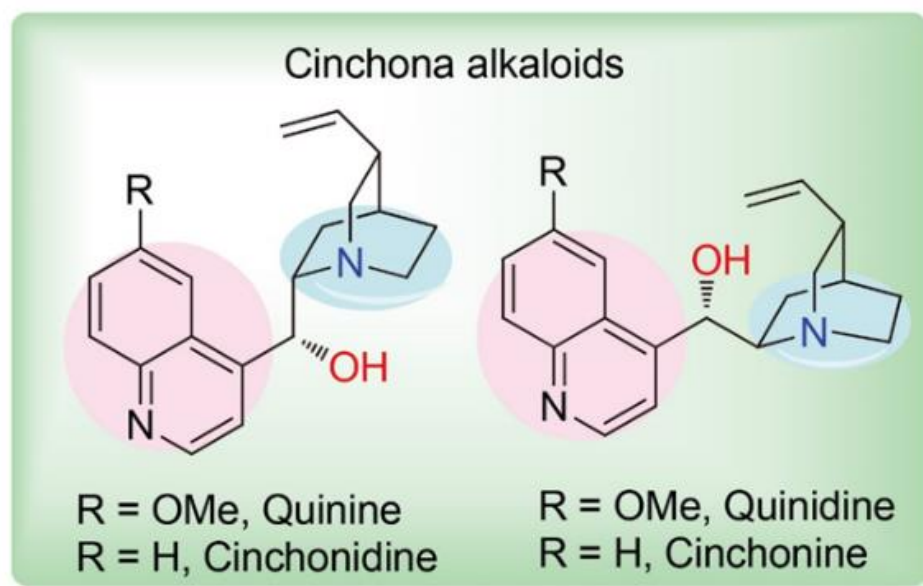


Figure 2 Structure of cinchona alkaloids

From: http://sioc-journal.cn/Jwk_yjhx/fileup/0253-2786/PIC/cjoc202007004_pic.jpg

Anti-bacterial activity of hydroquinine

In a recent study, the ethanolic nest entrance extracts (eNEEs) were examined. Surprisingly, hydroquinine is the one of key alkaloid compound that found in the eNEEs (6, 8). In 2017, Kraikongjit *et al.* investigated the antimicrobial properties of propolis, a resin-like extract, which produced by *Tetrigona apicalis* (smith 1857) for nest production. The *Tetrigona apicalis* (smith 1857) is a common species of stingless bee found in lower northern Thailand (8). In 2020, Jongjitvimol *et al.* investigated the phenolic content of the eNEEs from *Tetrigona apicalis* using high performance liquid chromatography (6). Interestingly, Kraikongjit *et al.* (2017) (8) and Jongjitvimol *et al.* (2020) (6) have previously demonstrated that these eNEEs exhibit antibacterial, antifungal, and anti-proliferative activities (6, 8). Hydroquinine was present in the greatest content in the resin extract (higher than 200 mg/kg of the dried eNEEs) (6, 8).



Figure 3 The nest entrances of *Tetrigona apicalis*

In 2022, Rattanachak *et al.* (10) found that hydroquinine possessed antibacterial properties. Hydroquinine had potential in inhibiting and killing both gram-positive and gram-negative bacteria, including *Staphylococcus aureus*, *Enterobacter cloacae*, *Escherichia coli*, *Klebsiella pneumoniae*, and *P. aeruginosa* (10). Furthermore, Rattanachak *et al.* (10) uncovered the mechanism of action through the evaluation of the global transcripts of *P. aeruginosa* in response to hydroquinine-induced stress using RNA sequencing with transcriptomic analysis. The minimum inhibitory concentration (MIC) and minimum bactericidal concentration (MBC) values of hydroquinine against all eight bacterial strains investigated ranged from 0.650–2.50 and 1.25–5.00 mg/mL, respectively (10). Interestingly, hydroquinine had the highest MIC values (2.50 mg/mL) against the drug-sensitive (DS) *P. aeruginosa* ATCC 27853. In contrast, hydroquinine showed a lower MIC (1.25 mg/mL) against the MDR *P. aeruginosa* BAA-2108 strain (10). According to the more effective of hydroquinine against the MDR *P. aeruginosa* strain than the DS *P. aeruginosa* strain, Jongjitwimol and Baldock (2023) proposed that hydroquinine has potential as an antimicrobial agent, highlighting the hydroquinine ability to target MDR *P. aeruginosa* strains (27). Furthermore, Rattanachak *et al.* also investigated the inhibitory effects of sub-inhibitory hydroquinine concentrations (half MIC) through the evaluation of the global transcripts of *P. aeruginosa* using RNA sequencing with high-throughput transcriptomic analysis (10). It was found that hydroquinine inhibited several virulence factors, including downregulating flagellar-related genes, affecting the bacterial motility, and downregulating quorum sensing-related genes, affecting the reduction of pyocyanin production and biofilm formation. Furthermore, transcriptomic analysis demonstrated that resistance nodulation division (RND) efflux pump transcripts were overexpressed. Hydroquinine induced upregulation of MexCD-OprJ and MexXY efflux pumps. In addition, several additional genes were identified as having up- or downregulated expression with high confidences (10).

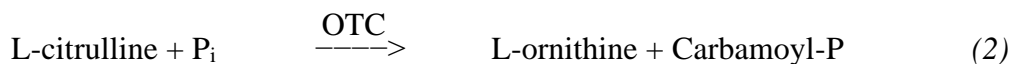
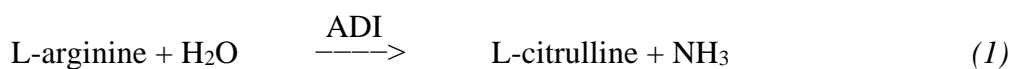
According to the transcriptomic result, hydroquinine significantly downregulated the genes which related to the arginine deiminase (ADI) pathway. Especially, the *arcD* gene was the most downregulated by a -4.24 Log₂-fold change (10).

The arginine deiminase (ADI) pathway

Among bacteria, including *P. aeruginosa*, the ADI pathway is widely distributed, where it is frequently a major source of bacterial energy (28).

There are four notable genes in the ADI pathway, including *arcA*, *arcB*, *arcC*, and *arcD*. The *arcA* encodes the arginine deiminase, *arcB* encodes the ornithine transcarbamylase, and *arcC* encodes the carbamate kinase. In *P. aeruginosa*, the expression of the functional genes (*arcA*, *arcB*, and *arcC*) is preceded by *arcD*, which encodes the arginine/ornithine antiporter (29). The expression of the ADI pathway-related genes and the function of their protein products are important for the adenosine triphosphate (ATP) or energy source (29-32). The ADI pathway also provides some energy in *P. aeruginosa* under anaerobic conditions because of the lack of oxygen or terminal electron acceptors (28).

The ADI pathway is conserved in several bacteria. This pathway produces one mole of ATP from every mole of L-arginine intake via three metabolic conversion steps. The equations of each step are showed as follows.



The first step, L-arginine is catalyzed by the enzyme namely arginine deiminase (ADI) and converted into L-citrulline and ammonia (NH₃). The second step, the carbamoyl part of L-citrulline is converted by the enzyme namely ornithine transcarbamylase (OTC), resulting in L-ornithine and carbamoyl phosphate (33). The final step, the phosphate moiety of carbamoyl phosphate is transferred to adenosine diphosphate (ADP) by the enzyme namely carbamate kinase (CK), yielding ATP, ammonia, and CO₂ (29-32). Overall, the ADI pathway allows the bacterial cells to sustain ATP production in the oxygen-dependent respiratory chain from carbamoyl phosphate (34) and produce ATP in anoxic environments (32, 35).

Antibacterial mechanism of natural alkaloids

Alkaloids distinctive chemical structures relate to antibacterial mechanisms (36, 37) by preventing the production of bacterial proteins and nucleic acids as well as altering the permeability of the bacterial cell membrane and preventing bacterial development. Alkaloids also stop bacteria from proliferating by rupturing bacterial cell walls and membranes, inhibiting bacterial metabolism, and inhibiting efflux pumps (38).

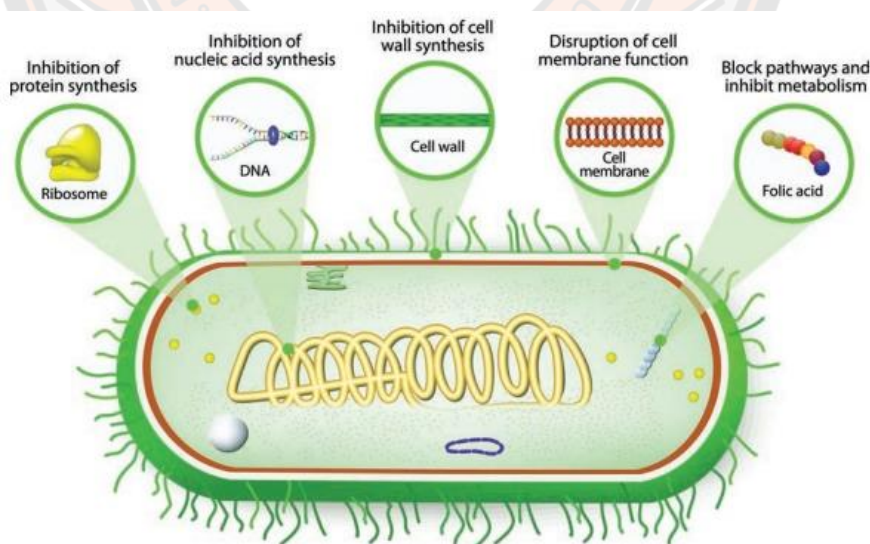


Figure 4 Antibacterial mechanism of substance

From: https://www.123rf.com/photo_46978345_antibiotic-mechanisms-of-action-of-antimicrobials.html

Inhibition of bacterial nucleic acid and protein synthesis

Bacterial nucleic acids are involved in the storage and expression of genetic information including deoxyribonucleic acid (DNA) and ribonucleic acid (RNA). DNA function contains all of the genetic information to develop, maintain, and reproduce for cell development and survival (39). There are three main different types of RNA molecules. Messenger RNA (mRNA), which act as messengers between DNA and cellular protein synthesis, a single-stranded molecule with the ability to carry out the functions of other RNA types and act as a protein template or blueprint during protein synthesis, is produced by the transcription of genetic material from DNA. When the genetic code is translated into a protein, transfer RNA (tRNA) serves as a specific adaptor. It transports the correct amino acid to mRNA, which then recognizes a codon on mRNA. Ribosomal ribonucleic acid (rRNA) is the RNA component of ribosomes, associated with a group of proteins to create ribosomes (40). Therefore, the inhibition of DNA replication or the DNA/RNA molecules was damaged result in preventing the expression of genes or genome activity which affect the characteristics of microorganisms and their growth and reproduction (41). For instance, DNA gyrase, enzymes supercoil and uncoil bacterial DNA during DNA replication, is crucial for DNA synthesis, replication, repair, and transcription, so it is a good target for anti-bacteria of antibiotics (42). Heeb, S. *et al.* (2011) reported that type II topoisomerase enzyme was the target of quinolone alkaloids consequently inhibiting DNA replication (43). Similarly, the isoquinoline alkaloid, berberine, has exhibited activity against viruses, bacteria, fungus, and protozoa. This compound demonstrated the ability to inhibit bacteria through preventing cell division and inhibiting protein and DNA synthesis, leading to bacterial death (44-46). Matrine also inhibited the synthesis of proteins necessary for cell growth and division in *E. coli* and *S. aureus* (36). Moreover, sanguinarine and berberine are naturally occurring alkaloids capable of altering the functionality of filamentous temperature-sensitive protein Z (FtsZ). FtsZ is associated with being crucial for the cell cycle, particularly in controlling the bacterial cell division process, the construction of a diaphragm, and the formation of a ring structure at the division site (47).

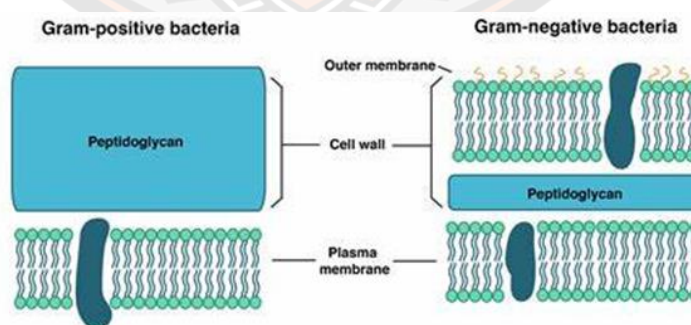


Figure 5 Bacterial cell membrane and cell wall component

From: <https://www.onlinebiologynotes.com/wp-content/uploads/2017/07/cell-wall.png>

Inhibition of cell wall synthesis and disruption of cell membrane function

The phospholipid bilayers and semi-permeable proteins that make up the bacterial cell membrane are responsible for the cell's protective barrier, recognition, identification, and electron transport (48). It offers a reasonably steady, continuous environment for bacterial life activities (48, 49). There is a significant loss of macromolecules when the bacterial cell membrane is ruptured. The transport and information transfer functions of the cell membrane are inhibited if the cell wall protection function is lost. All of which reduce bacterial growth or survival, which results in biological death (50). Additionally, it has several indicators that the bacteria's cell membrane was damaged. Significantly, when intracellular electrolytes leak into the culture media, the medium's conductivity rises. As a result, alterations in the conductivity of the culture supernatant can be used to detect changes in the permeability of bacterial cell membranes (51). Alkaline phosphatase (AKP), which is largely present between the cell wall and cell membrane of bacteria, leaks out of the cells when the permeability of the bacterial cell wall is elevated. Consequently, AKP activity may be used to determine the integrity of the bacterial cell wall (52, 53). Additionally, a variety of targets, including as proton motive force, electron transport, food absorption, or other unrelated enzyme activities, may contribute to the damaging the cell membrane of alkaloids mechanisms (54). For example, alkaloids from *Dicranostigma leptopodum* can modify the cell permeability and have a significant effect on antibacterial activity (*K. pneumonia*), which displayed the conductivity of the culture medium with and without the alkaloid was significantly different (55).

Inhibition of bacteria metabolisms

Alkaloids' antibacterial properties may interfere with bacteria's primary and energy metabolisms, which would hinder their ability to sustain or multiply their cells. Adenosine triphosphate (ATP), which is often produced through respiration, is one of the possible targets. It provides energy for a number of life activities in cells and is the most direct source of energy in organisms (56, 57). Respiration, primary metabolism, and the energy supply for several enzyme processes all depend on ATP. Therefore, ATP production inhibition affects a variety of essential metabolic processes in microorganisms, which may cause bacterial mortality (36, 58). For example, berberine has the ability to influence *Streptococcus pyogenes*' (Group A streptococcus, GAS) carbohydrate metabolism. The conversion and absorption of carbohydrates were enhanced because berberine stimulated the pathway by which other substances exchanged with monosaccharides and their derivatives. Interestingly, berberine increased the activity of ATP-binding cassette transported phosphotransferase systems that were also associated in the absorption of carbohydrates. Moreover, berberine's disruption of the metabolism of carbohydrates in GAS stimulates excessive reactive oxygen species (ROS), which ultimately inhibits the bacteria. Additionally, berberine reduces the production of ATP and reduced nicotinamide adenine dinucleotide (NADH), which inhibits the growth of intestinal bacteria (55).

Inhibition of efflux pump

Efflux pumps are transmembrane protein complexes, present in eukaryotic organisms and both gram-positive and gram-negative bacteria (59). The function of efflux pumps is to eliminate harmful substances from cells, such as antibiotics, into the surrounding environment. The pumps may be specific to one or several substrates, including different antibiotics or drugs with distinct structural molecules. Because the pumps can transport a variety of medicines out of the cell, they have consequently been correlated to multiple drug resistance (MDR) (60). There are five major families of an efflux transporter in the bacteria (61) including:

- 1) RND (Resistance nodulation division family)
 - 2) SMR (Small multidrug resistance family)
 - 3) MFS (Major facilitator superfamily)
 - 4) MATE (Multidrug and toxic compound extrusion) and
 - 5) ABC (Adenosine triphosphate [ATP]-binding cassette superfamily)
- (Figure 6)

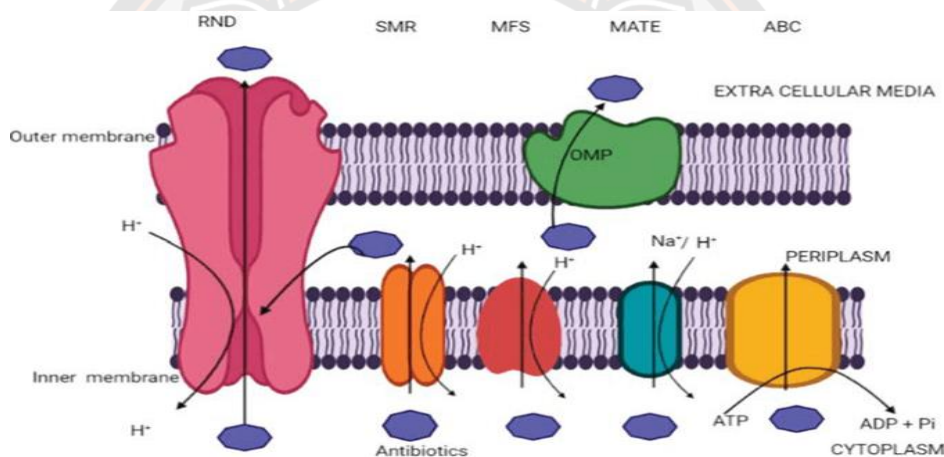


Figure 6 Bacterial efflux pump systems

From: <https://ebrary.net/htm/img/14/2015/110.png>

The bacterial cell may escape the exposure to the antibacterial agents in the membrane if the efflux pump mechanism is successful in pumping membrane-permeable antibacterial drugs out of the cell rapidly. This mechanism may increase the pathogen membrane's capacity for agent resistance and diminish the agent's impact on bactericidal activity (62). All of these efflux transporters receive energy source from the proton motive force except the ABC family, which use ATP hydrolysis to pump the substrates out of the cell (63). Rattanachak *et al.* (10) found that hydroquinine induced upregulation of MexCD-OprJ and MexXY efflux pumps. Furthermore, both gram-positive and gram-negative bacteria have been demonstrated to be susceptible to this conessine's potential antibacterial activity. Conessine is one of the alkaloids included in the bark of *Holarrhena antidysenterica*. Additionally, when used conessine combined with conventional antibiotics, conessine had notable synergistic effects (64). According to the research that are currently available, conessine has demonstrated efflux pump inhibitory efficacy against the AdeIJK efflux

pump, which is essential for pumping the various antibiotics into *Acinetobacter baumannii* (64). According to Siriyong *et al.* (2017) (5) reported that conessine significantly decreased the MICs of all antibiotics in *P. aeruginosa* MexAB-OprM overexpressed K1455 strain compared to *P. aeruginosa* PAO1 strain. Therefore, conessine could be an inhibitor of the MexAB-OprM efflux pump. The researchers discussed that the mechanism of conessine for efflux pump inhibition might cause inhibition by competition and/or block the substrate-binding site of MexB. As a result, conessine may take the position of MexB's substrate-binding site. Conessine compounds may interact with the efflux pump structure's "G-loop" or "switch loop," which has the distal and proximal binding sites separated, compared to the mechanism of MexB-specific PA β N. Therefore, *in vitro* studies shown that the inhibition of efflux pump are able to reduce the levels of MDR efflux pump activities. Consequently, antibacterial effects are improved, and bacterial resistance is prevented (65). For this reason, developing and using efflux pump inhibitors may be a new alternative for development and utilization to promote and recover the existing antibiotics (66).

Pseudomonas aeruginosa

The emergence of drug-resistant pathogens is one of the most severe public health problems in many countries, leading to the difficulty in treating microbial infections and a significant cause of human mortality. *Enterobacteriaceae*, *Pseudomonas aeruginosa*, and *Acinetobacter* have been classified by the World Health Organization (WHO) as the most concerning pathogens (67). In addition, there are currently many drug-resistant bacteria that were assessed by the Centers for Disease Control and Prevention (CDC) as presenting urgent, serious, and concerning threats. For example, *S. pneumoniae*, *S. aureus*, *Mycobacterium tuberculosis*, *Enterococcus* spp., *E. coli*, *Salmonella* spp., *K. pneumoniae*, *P. aeruginosa*, *Acinetobacter baumannii*, and *Neisseria gonorrhoeae* (68, 69). Some of these bacteria are the main causes of opportunistic infections in hospitalized patients and serious limitation of effectively therapeutic options. One of the reasons is the remarkable ability of microorganisms to resist antibiotics (70). They are able to adapt or avoid destruction from antibiotics through various mechanisms such as β -lactamase production, decreased outer membrane permeability, efflux pump expression, aminoglycoside-modifying enzymes, and target modification (71). These mechanisms are reviewed that they are resistant to many types of antibiotics, such as aminoglycosides, fluoroquinolones, β -lactams, chloramphenicol etc. This is considered as multidrug resistance (MDR) (72). The definition of MDR is 'the resistance to three or more antimicrobial classes', which frequently used for both gram-positive and gram-negative bacteria (73-76).

P. aeruginosa is one of the representative opportunistic bacteria and with a high propensity for the development of MDR strains in hospitalized patients. The National Nosocomial Infections Surveillance (NNIS) System reported that *P. aeruginosa* has been the second common microorganism isolated in nosocomial pneumonia (17% of cases) (77). It was the third common pathogen isolated in both urinary tract infections (UTI) and surgical site infection patients (11% of cases) (77). For overall, *P. aeruginosa* is the fifth microorganism isolated from all specimens in nosocomial infection patients (about 9% of cases) (78).

Introduction to *Pseudomonas aeruginosa*

P. aeruginosa is a prevalent opportunistic human pathogen. Using a variety of virulence factors and its intrinsic ability to adapt to new environments (79). *P. aeruginosa* is a gram-negative, rod-shaped, non-spore forming, oxidase-positive, and lactose non-fermenting bacterium (79). It has no membrane-bound nucleus and very few organelles such as a capsule, cell wall, plasma membrane, cytoplasm, ribosome, plasmid, nucleoid (DNA) as show in Figure 7.

P. aeruginosa has a single polar flagella and pili for motility as well as it has ability to thrive in moist environments like soil and water. Moreover, it can be found in various fresh fruits and vegetables (80). *P. aeruginosa* can colonize a wide range of habitats because of its high metabolic adaptability and a wide spectrum of environmental adaption abilities (80).

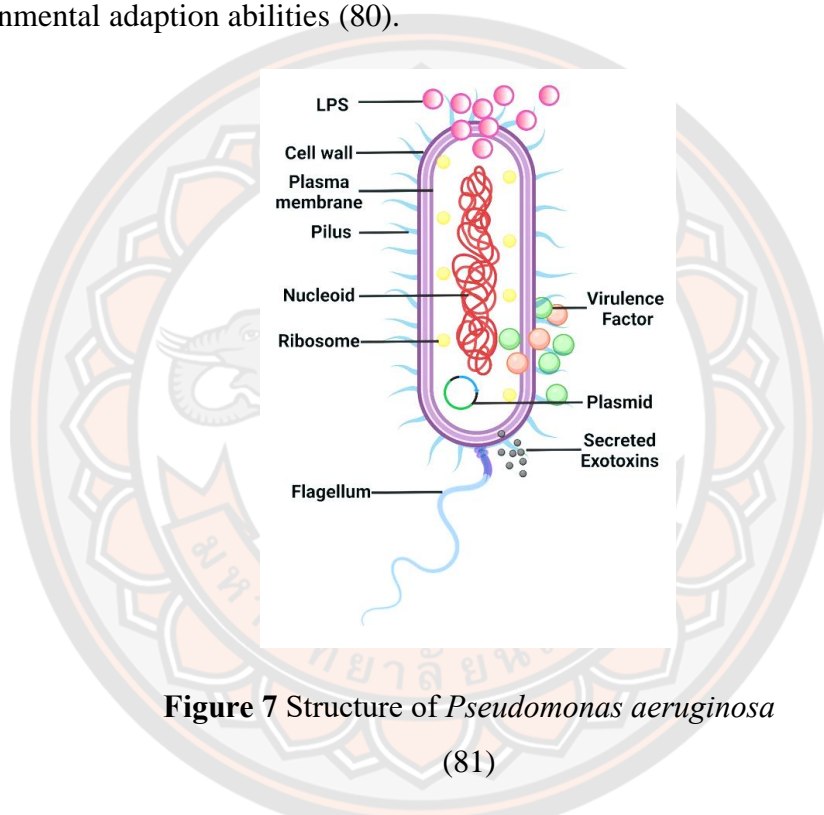


Figure 7 Structure of *Pseudomonas aeruginosa*

(81)

P. aeruginosa is a facultative anaerobe because it can survive in both aerobic and anaerobic environments. When there is insufficient oxygen, it receives energy from anaerobic respiration, and when oxygen is available, produces energy from aerobic respiration for cell growth or survival (80). *P. aeruginosa* can survive in temperatures from 4°C to 42°C, however 37°C is the ideal temperature for growth. Furthermore, it can generate the blue-green color colonies on the solid media that are caused by the water-soluble pigments pyocyanin and pyoverdine. Additionally, *P. aeruginosa* generates indophenol oxidase, a substance that distinguishes them from other gram-negative bacteria by making them positive in the oxidase test (82). Some *P. aeruginosa* strains may also produce biofilm, which encourages tolerance and survival under challenging environments. Remarkably, it can survive and reproduce inside of human tissues and medical equipment due to slime-encased biofilms. *P. aeruginosa* is in the form of a biofilm, which will protect phagocytes and antibodies formed by the host, adding to the organism's drug resistance (83).

Pseudomonas spp. are the group organisms with the least nutritional needs for growth. There are only acetate and ammonia as carbon and nitrogen sources, respectively, that *P. aeruginosa* needs for growth. Additionally, *P. aeruginosa* does not operate fermentation and can grow anaerobically by using nitrate or nitrite as a terminal electron acceptor. Without oxygen, *P. aeruginosa* may grow by using a substrate-level phosphorylation pathway to break down arginine and pyruvate (84). Furthermore, the adaptive nutritional requirements of *P. aeruginosa* make it difficult to eliminate and challenging to remove it from contaminated areas. As such, *P. aeruginosa* is capable of growing in various environments including those where aseptic conditions are required such as operating rooms, hospital rooms, clinics, and medical equipment (71).

P. aeruginosa has several virulence factors and produce many factors that may present its virulence pathogenesis to host cell as show in Table 1 (85, 86).

Table 1 Virulence factors of *Pseudomonas aeruginosa*

Virulence factors	Action to cell host
Flagella	Invasion, mobility, and adhesion
Pili	Adhesion and transfer of secretions
Exopolysaccharides	Pathogen persistence and adhesion
Lipopolysaccharide	Endotoxin; inflammatory agent, adherence, biofilm formation
Coagulase	Hemolytic
Elastase	Elastin and protein degradation, membranes disruption
Lipase A	Participation in degradation
Phospholipase C	Disruption of lung surfactant and hydrolysis of lecithin
Proteolytic	Degrades host tissue, and destroy immunity of host
Pigments	Inhibit lymphocyte proliferation via neutrophils apoptosis
Exotoxin A	Interrupt protein synthesis of eukaryotes cell
Exoenzyme S	Antiphagocytic factor
Biofilm	Protection cells from antibiotics and immune system effectors
Hemolysin	Toxic to alveolar macrophages
Leucocidin	Depression of host defenses

P. aeruginosa is associated with a wide range of clinical conditions that vary in severity and duration. It can infect and colonize almost all body systems in humans. *P. aeruginosa* can produce endotoxin, a significant virulence factor in bacteremia and septic shock (79).

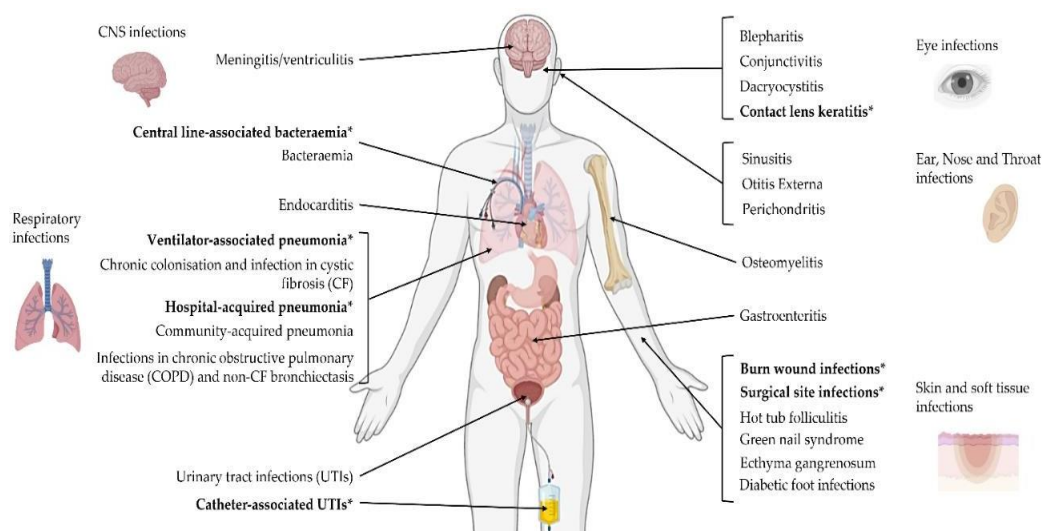


Figure 8 The many sites of *Pseudomonas aeruginosa* infection

(79)

P. aeruginosa is one of the opportunistic pathogen infections in hospitalized patients and can produce many virulence factors. Moreover, it has biofilms which helps it live and thrive in human tissues resulting in antibiotic resistance. Therefore, it can infect various site organisms. *P. aeruginosa* infection is associated with a 50% overall mortality rate of patients (86). Furthermore, nosocomial infection by MDR *P. aeruginosa* causes mortality rates of 18–61% (78). For these reasons, the treatment of either *P. aeruginosa* or MDR *P. aeruginosa* infections should have effective antibiotics or combined antibiotics.

Bacterial keratitis

Bacterial keratitis is an infection of the cornea tissue that caused by the bacteria (87). Bacterial keratitis also means the transient, recurrent, acute, or chronic infection of cornea (87). The cornea is one of the most important components of the visual system. Bacterial keratitis is the common sight-threatening ocular corneal pathology that cause visual impairment, vision loss and ultimately leads to blindness, especially in working age adults (88), if it not was diagnosed and treated promptly (87, 89).

Corneal structure

The cornea is a transparent, avascular, and highly innervated tissue located at the anterior outer part of the eye. This structure acts as a barrier and protects the structure inside the eye, including against infections (90). Histologically, cornea comprises of 5 difference layers including the epithelium, Bowman's membrane, the stroma, Descemet's membrane, and the endothelium (from the exterior to interior) (90, 91) as shown in Figure 9.

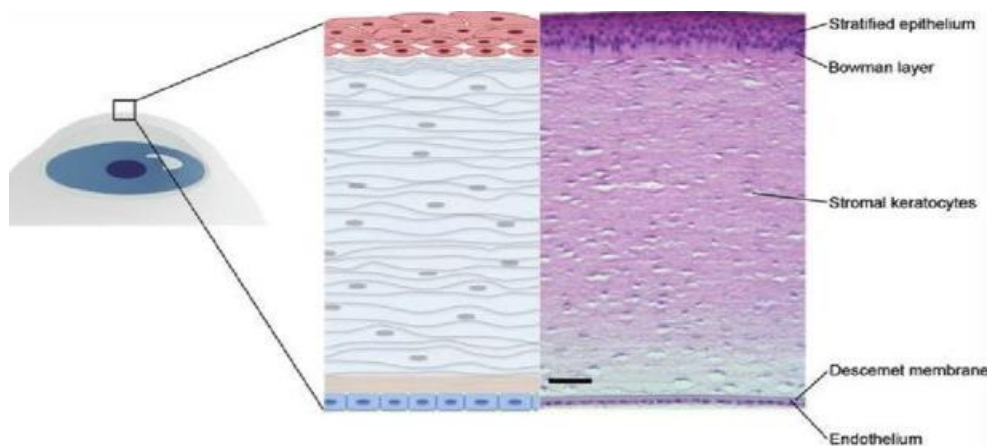


Figure 9 Structure of the cornea

(92)

The corneal epithelium is the principal barrier to fluid and pathogens and constant repopulation through differentiation and maturation of dividing cells in its basal cell layer (90). The epithelium is uniform to provide a smooth regular surface and represents the major refractive element of the cornea (90, 93). It is supported posteriorly by basement membrane and Bowman's layer and supports in maintenance of stromal dehydration (90). The stroma is most of the corneal volume, the thickest layer, which supports normal corneal homeostasis and assists in ocular immunity (90, 94). Recently, the pre-Descemet's membrane or Dua's layer was identified (95). Therefore, the cornea has 6 layers if the Dua's layer is included. This Dua's layer is like the stroma, but it has a higher spacing between collagen fibrils and higher lamellae's density (95). Descemet's membrane and endothelium, is essential for corneal dehydration, maintained through tight junctions and endothelial pumps (96).

According to the corneal epithelium is the principal barrier against pathogens, this corneal layer has various cell types. The corneal epithelium composes 4–6 layers of the cells (90). The superficial corneal epithelial cells form 2–3 flat layers with glycocalyx-covered microvilli (90). The glycocalyx is necessary for the stability of tear film. These surface cells form tight junctions that prevent tears, toxins, and microbes from entering the eye (97). Next layers are the middle wing cell layer and the basal cell layer. The basal cells are the only corneal cells capable of mitosis and contribute to constant epithelial regeneration which occurs every 7–10 day. These cells are firmly connected to each other by lateral gap junctions and zonulae adherence and strongly attached to underlying basal lamina by hemidesmosomes to modulating cellular signaling between the epithelium and stromal layers (97, 98). Disruptions in this protective layer can lead to infection, ulceration, perforation, scarring, and decreased visual acuity (99).

Corneal blindness, a major ophthalmic public health problem, is an important especially in developing countries. According to the World Health Organization, Corneal opacity is the 4th cause of blindness globally, affected around 1.9 million people (5.1% of the total number of blind people) and WHO has recognized that corneal blindness resulting from microbial keratitis is emerging as an important cause of visual disability (100, 101).

Corneal infection



Figure 10 *Pseudomonas aeruginosa* keratitis

(102)

There are many different conditions which can damage the cornea including infectious, nutritional, inflammatory, inherited, iatrogenic and degenerative conditions (103). However, infectious keratitis tends to be the most common problem in low-middle income countries (101). According to the a case report and review, Eltis *et al.* found that bacterial infections represent about 90% of all microbial keratitis cases (104). Especially, *P. aeruginosa* presents the most common pathogen, followed by *S. aureus*. The remaining 10% pathogens are associated with amoebae such as *Acanthamoeba castellanii* or with fungi, including *Fusarium solani* (104).

P. aeruginosa is the most common cause of gram-negative bacterial keratitis, which is an opportunistic bacterial pathogen in contact lens wearers (2). Furthermore, *P. aeruginosa* is the most frequent and the most pathogenic ocular pathogen which cause corneal perforation in just 72 h (87). Importantly, *P. aeruginosa* were identified as a leading cause of contact lens-associated microbial keratitis (1, 2, 105, 106). Not only living bacteria but also their components such as lipopolysaccharide (LPS), endotoxin, is the principal component of the outer membrane of gram-negative bacteria that can contribute to the development of inflammation and subsequent corneal damage in infectious keratitis (107). Simmons *et al.* have shown that LPS activation of TLR4 leads to increased expression of inflammatory cytokines, such as IL-1 β and TNF- α (108). Notably, bacterial keratitis is the overwhelming majority of contact lens-related microbial keratitis (CLMK) which is associated with overnight contact lens wear (104).

Contact lens

The contact lens was initially conceptualized by Leonardo DaVinci in 1508, and the first glass contact lenses were used for eyesight correction in the 19th century. Soft contact lens, as we know it today, was initiated in the early 1950s by Otto Wichterle and Drahoslav Lím (106). They designed the biocompatible and transparent hydrophilic hydrogel polymers for medical use in human (106).

Contact lenses represent a widely utilized form of vision correction with more than 140 million wearers worldwide (106). Contact lenses have many advantages, option to patients who desire to keep on clear vision with spectacle-free (109, 110). Although generally well-tolerated, however, it has the potential spectrum of complications that contact lens wearers may present (110, 111), particularly corneal ulcers associated with overnight wear of contact lenses (112). Moreover, pain, redness, mucopurulent discharge, photophobia and an anterior chamber reaction may be present (104). In particular, using contact lens is the particular greatest risk factor for developing corneal infection (microbial keratitis) (113), with an approximate annualized incidence ranging from 2 to 20 cases per 10,000 wearers, and sometimes resulting in permanent vision loss (113). The pathogenesis of contact lens-associated microbial keratitis is complex and multifactorial, likely requiring multiple conspiring factors that compromise the intrinsic resistance of a healthy cornea to infection (114). Numerous epidemiological studies have repeatedly demonstrated that the annualized incidence of CLMK increases significantly with overnight and/or extended wear versus daily wear (e.g., 5 to 10 times or more), and that additional risk factors can also be present such as patient compliance and hand hygiene, type of lens care solution used, microbial contamination of the lenses or lens cases (115). Importantly, although commercial contact lens solutions meet the international standard (ISO 14729) and FDA criteria for their adequate antimicrobial efficacy, contact lens solutions are only subjected to assessment against reference strains (116-119). Furthermore, the antimicrobial activity does not guarantee efficacy against clinical strains (119). In addition, commercially available contact lens solutions may be ineffective against bacterial biofilms (117-119).

Contact lens-related corneal infection

The cornea is constantly exposed to the outside environment and is subject to particulate matter and allergens, not only microbes and their antigens (90). The cornea must simultaneously preserve the clarity necessary for vision. It depends not only on the highly specialized arrangement of collagen fibrils that provides the necessary optical characteristics but also on barrier function and proper control of ion and fluid transport by cells in both the endothelium and epithelium (120). This remarkable biological feat also depends on the immune-privileged nature of the cornea to minimize potentially damaging inflammation caused on by unwelcome immunological reactions to environmental antigens whether microbial or not (120). Importantly, the regulation of epithelial barrier function against microbes depends on regulators and effectors of innate immune responses (MyD88 and IL-1R) (114) somewhat surprisingly even in the constitutive state. *P. aeruginosa* could readily traverse the otherwise healthy corneal epithelium of MyD88 knockout mice even in the absence of any form of superficial injury. In this way, MyD88 regulates defenses against bacterial adhesion and also their subsequent traversal through the layer (121).

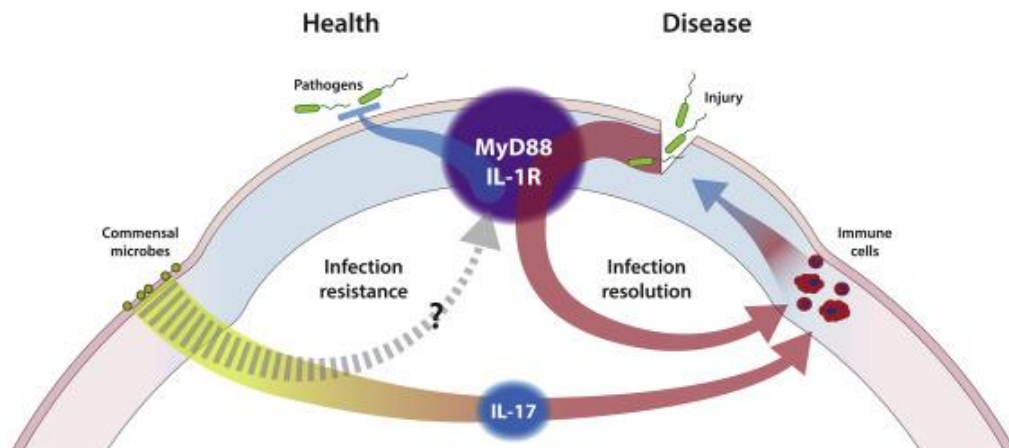


Figure 11 The pathogenesis of *P. aeruginosa* keratitis

(114)

Contact lens effects on epithelial barrier function in the absence of overt injury (114). IL-1R and MyD88 participate in ocular defense in both health and disease. The protective response against inflammation involving an interleukin-17 (IL-17) response, defense responses to acute infection, from gamma-delta T cells in the ocular mucosa, reducing damaging pathology from *P. aeruginosa* infection (114). Furthermore, the combination of blinking, tear fluid or tear flow, the corneal epithelium, and the basal lamina work together with regulatory elements to form a formidable barrier protecting the vulnerable corneal stroma against microbial penetration (114). On the morphology and function of bacteria, tear fluid has several effects (114). In *P. aeruginosa*, tear fluid can lead to bacterial chain formation and clumping, can interfere with contact lens-associated biofilm formation and result in the loss of two types of motility including swimming motility, which is used to move through fluid, and twitching motility, which is used to traveling on surfaces (122). Moreover, twitching motility is important for *P. aeruginosa* to traffic through corneal epithelial cell layers to exit host cells after internalization and for virulence (122).

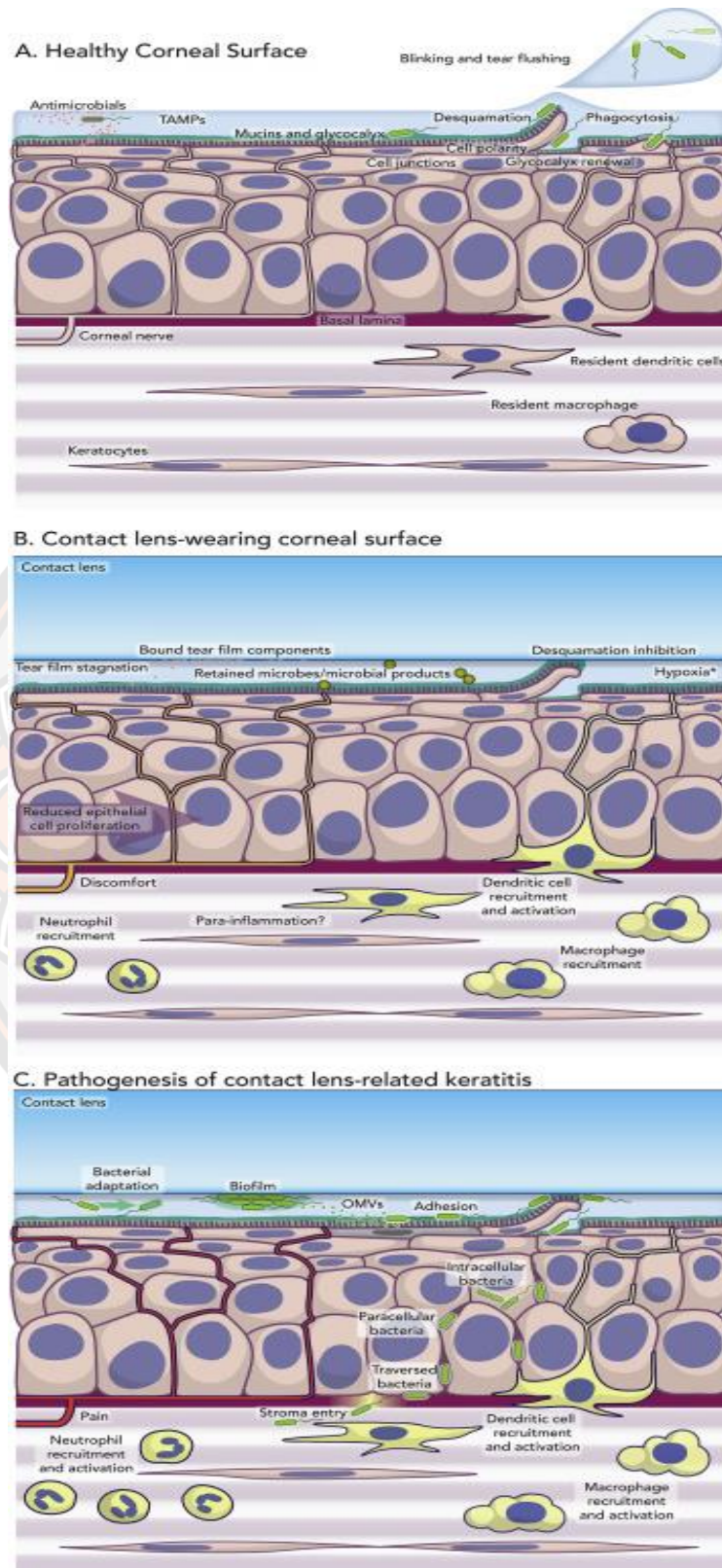


Figure 12 Pathogenesis of contact lens-related microbial keratitis (CLMK)

Contact-lens-related microbial keratitis (CLMK)

Contact-lens-related microbial keratitis (CLMK) is an infection of the cornea, the clear front part of the eye, that is caused by bacteria that are associated with the use of contact lenses. An illustration of the known constitutive defenses in a healthy cornea are shown in Figure 12A. The tear fluid and corneal epithelium combine to form a formidable barrier to microbial attack supported by the basal lamina and resident immune cells (114). Many of these defenses can also be upregulated in response to TAMPs (Tear-Associated Molecular Patterns) which are likely to include both microbial and non-microbial ligands. In contrast, Figure 12B, schematic representation of known, and potential effects of contact lens wear on constitutive defenses of the cornea that could help predispose to *P. aeruginosa* keratitis. Effects of contact lenses in binding tear components, reducing basal epithelial cell proliferation and surface cell desquamation (exfoliation, sloughing). However, effects of bound microbes (commensal bacteria), tear film stagnation, and lens-induced para-inflammation (e.g. dendritic cell activation, quiescent neutrophil infiltration), and their consequences, remain to be determined (Figure 12B).

The potential events underlying the initiation of *P. aeruginosa* keratitis during contact lens wear are shown in Figure 12C. Pathology of *P. aeruginosa* keratitis requires bacterial entry into the corneal stroma by traverse the multilayered epithelium via intracellular or paracellular pathways and then activate the inflammatory and immune cells. Biofilm formation on contact lenses or on lenses in storage cases could promote phenotypic and genotypic changes that stimulate bacterial survival and virulence, as could adaptations to the ocular environment over time (114). Release of outer membrane vesicles could prime the corneal epithelium for bacterial adhesion, the latter also promoting expression of the Type Three Secretion System (T3SS) in *P. aeruginosa* (114).

Risk factors of CLMK

There are several risk factors associated with the incidence of CLMK. Hygiene practices were highly important affect the magnitude of risk, especially overnight wearing and poor hygiene (123, 124). The poor hygiene including inadequate of hand washing, lack of hand washing, lack of frequent case replacement, smoking, showering with contact lens (124, 125). Furthermore, swimming with contact lenses are also the risk factors (126). Other risk factors include being a male (127), probably related to poor compliance and unwillingness to seek regular care consideration (127). The modifiable and non-modifiable risk factors associated with contact lens-associated infectious keratitis are demonstrated in Table 2 (128).

Table 2 The risk factors associated with contact lens-associated infectious keratitis.

Risk factors	Highest risk	Lowest risk
Modifiable risk factors		
Wear schedule	Overnight use	Daily wear only
Days of weekly use	6–7 days	< 2 days
Hand washing before cleaning	Not always	Always
Contact lens type	Daily disposable	Rigid lenses (129)
Current smoker	Yes	No
Case hygiene/replace time	Poor	Excellent
Purchase of contact lens	Internet/mail order	Optometrist (130)
Showering with lenses	Yes	No (125)
Water exposure*	Yes	No (131)
Ocular surface and systemic diseases	Presence	absence (132)
Non-modifiable risk factors		
Gender	Male	Female
Age	< 49 years	> 50 years (129)
Caucasian race*	Yes	No (131)
Previous ocular trauma	Presence	Absence (132)

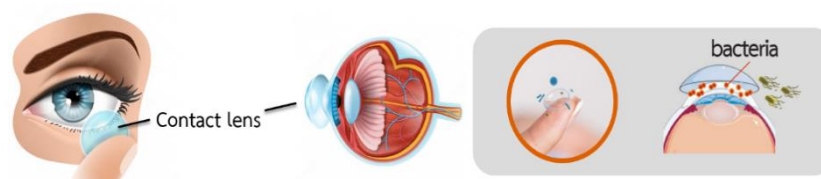
*Especially related to *Acanthamoeba* keratitis.

High risk when exposure to ocean/sea/river/lake water and highest risk when swimming in public or private pool and hot tub.

Hypothetically, to lower the risk of CLMK, contact lens solutions must be able to sufficiently reduce the number of microorganisms. Additionally, contact lens solutions should have ability to reduce or prevent biofilm formation on contact lenses. Therefore, new natural agents that prevent biofilm formation may be an excellent option to reduce the risk of CLMK.

Pathogenesis of CLMK (Mechanism of infection)

The pathogenesis of CLMK is complex and involves intrinsic contact lens properties, including lens material and oxygen transmissibility (128). Moreover, contact lens may be contaminated from eyelids, hands, storage case, cosmetic and contaminated water, or contact lens solutions.

**Figure 13** Contact lens contaminated bacteria

Normally, the combination of blinking, tear flow, the corneal epithelium, and the basal lamina work together with regulatory elements to form a formidable barrier protecting the vulnerable corneal stroma against microbial penetration (114, 133). Contact lenses have an impact on the protective response on ocular surface. They disrupt tear fluid or tear flow and impair the function of the cornea epithelial barrier against bacteria. Contact lenses cause local hypoxia led to decreased epithelial metabolic rate, resulting in alteration of normal corneal physiology, epithelial thinning, loss of tight cell junctions, and hemidesmosome (128), all of which led to epithelial abrasions, predisposing to opportunistic infections and the development of microbial keratitis. Microorganisms possibly adhere to the contact lens, then transfer from the contact lens to a corneal surface, penetrate into the deeper layers (microbial invasion) and damage the cornea (134).

P. aeruginosa, the most common cause of gram-negative bacterial keratitis, which is an opportunistic bacterial pathogen in contact lens wearers (2). Importantly, *P. aeruginosa* were identified as a leading cause of contact lens-associated microbial keratitis about 23% of isolates in one study and more than 50% in another (106). Not only living bacteria but also their components such as lipopolysaccharide (LPS), endotoxin, is the principal component of the outer membrane of gram-negative bacteria can contribute to the development of inflammation and subsequent corneal damage in infectious keratitis (107). Furthermore, contact lens wearing induce hypoxic conditions in human corneas that increase wild-type cystic fibrosis transmembrane conductance regulator (CFTR) expression, which is the cellular receptor for *P. aeruginosa* (135). Furthermore, *P. aeruginosa* has several virulence factors that may present its virulence pathogenesis to host cell (136).

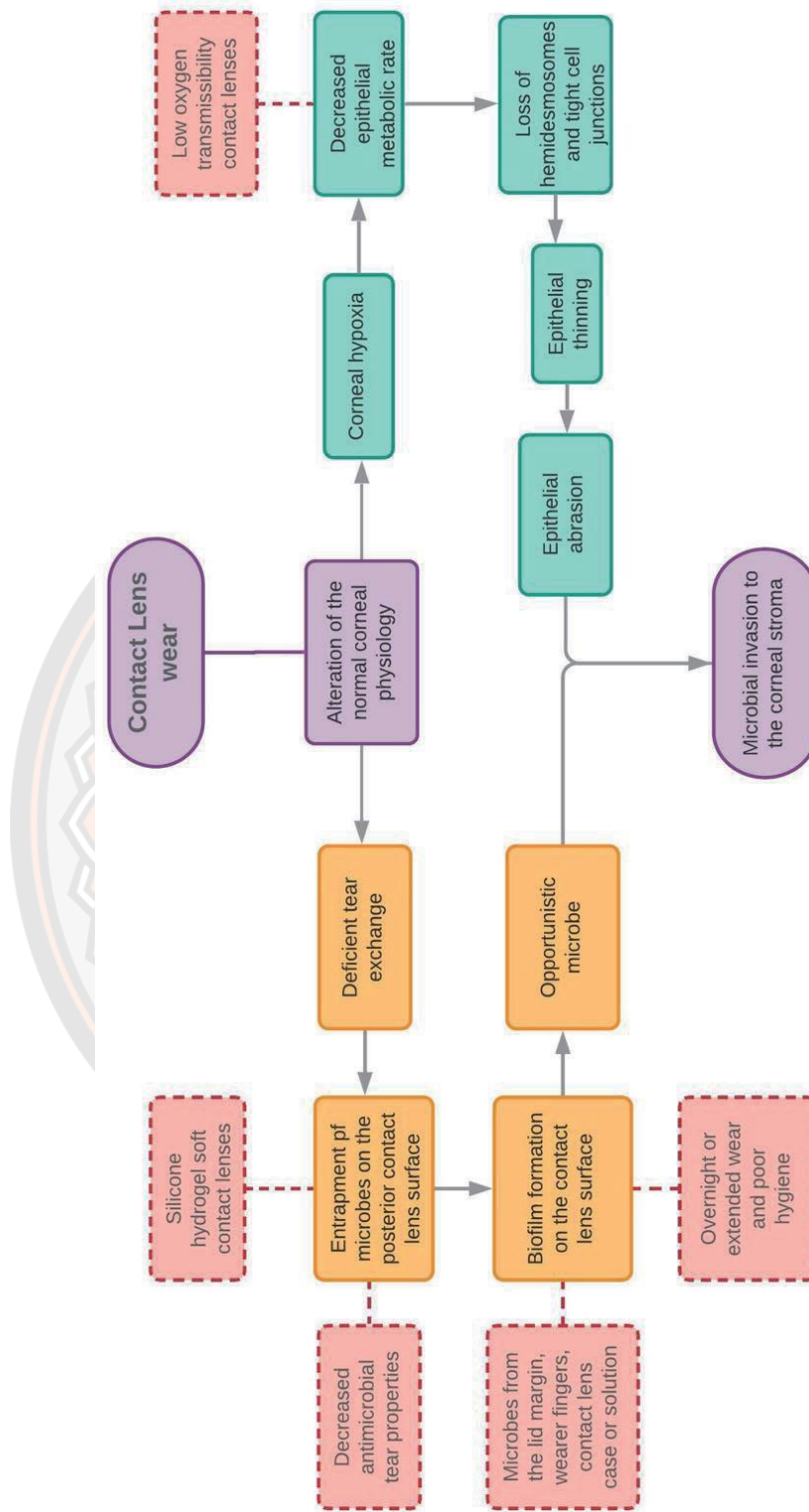


Figure 14 Flow chart showing the relationship between the risk factors and the pathogenesis of CLMK (128)

***Pseudomonas aeruginosa* virulence factor related with CLMK**

Pseudomonas spp. stands apart from other species due to its large genome and highly dynamic proteome (137), giving it more opportunities to adapt to environmental challenges or overcome antibiotic resistance. *P. aeruginosa* expresses an arsenal of virulence traits that are powerful weapons damaging host cells, which can be classified in two categories. *P. aeruginosa* is a ubiquitous gram-negative bacterium found in the water, soil, plants, insects, and sewage (138). This bacterium can be found in such diverse locations because of its low nutritional requirements. Additionally, it can grow both aerobically and anaerobically (138). As mentioned previously, *P. aeruginosa* can cause infections in the eyes, particularly in contact lens wearers. *P. aeruginosa* can colonize on the ocular surface and cause infections through their adhesion to the surface of contact lenses.

There are several adhesive factors associated with *P. aeruginosa* that may modulate its ability to adhere to surfaces (139-141). A set of important factors includes its motility appendages are flagellum and pili. *P. aeruginosa* is capable of swimming motility through a single flagellum (139-141). The flagellum is essentially a tail extending out from one of the bacterium's poles (139-141). Swimming allows *P. aeruginosa* to seek nutrients, avoid toxins, find optimal locations for colonization, and engage in chemotaxis, or movement caused by chemical gradients (139-141). *P. aeruginosa* is also capable of surface associated mobility attributed to its pili for twitching motility (141). The pili are hair-like appendages also on the surface of the bacterium (141). *P. aeruginosa* is capable of specifically interacting with a substrate through adhesins. Adhesins located internally and externally such as on their pili allow for chemical specificity to substrates (136). Furthermore, lipopolysaccharides (LPS) on the membrane of *P. aeruginosa* have been shown to be a major component in its virulence in addition to aiding bacterial adhesion (142). It may be possible that a hydrophobic O-side chain in LPS help *P. aeruginosa* adhere to hydrophobic surfaces in some contact lens materials (136). Additionally, *P. aeruginosa* is capable of quorum sensing (QS) or signaling to one another by excreting chemicals (143) and it can secrete vary virulence factors such as exotoxins or degrading enzymes to destroy host cells (136) as show in Figure 15. The two main virulence factors related to the CLMK are cell-associated determinants and secreted virulence factors (Figure 15).

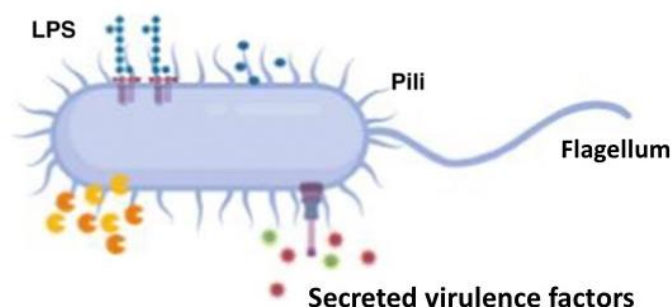


Figure 15 The main virulence factors in *Pseudomonas aeruginosa* (136)

1) Cell-associated determinants

The cell-associated determinants or surface-bound virulence determinants including flagella and pili, bacterial surface appendages, are not only needed for their motility but are also involved in other biological functions (136). *P. aeruginosa* uses flagella-driven swimming to reach epithelial cells located close to the damaged area plus amino acid sensor-driven chemotaxis (144). Moreover, the binding of these appendages to certain target molecules such as toll-like receptor 5 (TLR5) can induce a strong proinflammatory response in epithelial cells (145), especially, cornea cells. Additionally, type IV pilus (T4P) is particularly relevant to ocular pathogenesis (146). Pili is utilized for binding to epithelial cells near damage area (147, 148). In addition, LPS, major component of the outer surface membrane has been found to elicit an immunogenic response via toll-like receptor 4 (TLR4) on the corneal host cell (142, 147, 148).

2) Secreted virulence factors

P. aeruginosa can secrete virulence factors comprise a series of cytotoxins such as those of the type 3 secretion system (T3SS) which include several protein toxins that play important roles on the pathogenesis of keratitis (136). The effector proteins of T3SS including, ExoU, ExoS, ExoT, and ExoY (149). Keratitis infections are commonly caused by isolates carrying the *exoU* gene. Moreover, *P. aeruginosa* with ExoU show resistance to disinfection (149). The expression of many of these virulence factors is regulated by the QS network (150). This system is involved in a series of events related to the production of biofilm, toxins, and pigments, as well as to the development of antimicrobial resistance (136, 150). Exotoxin is another secreted virulence factor that inhibits host protein synthesis resulting in apoptosis, superoxide production and mitochondrial dysfunction (151, 152). Finally, *P. aeruginosa* secretes several nonspecific proteases and phospholipases, which display a vast array of cytotoxic effects on cell surfaces and intracellular matrices (151, 152).

P. aeruginosa can produce a variety of virulence factors that allow it to infect the eye. These include exotoxins, enzymes and adhesins that allow it to adhere to the cornea and evade the host's immune response. Normally, bacterial contamination of the contact lens is followed by bacterial adhesion to the corneal epithelium and then microtrauma or erosion to the epithelium occurs, resulting in the bacterial invasion of the corneal stroma (128).

Bacterial adhesion on contact lens

P. aeruginosa can adhere to the surface of the contact lens or the cornea via flagellum, pili, or body (139-141). *P. aeruginosa* adhesion on contact lenses result in promoting bacteria to the nearby cornea, in that way promoting greater chances of ocular infection (128).

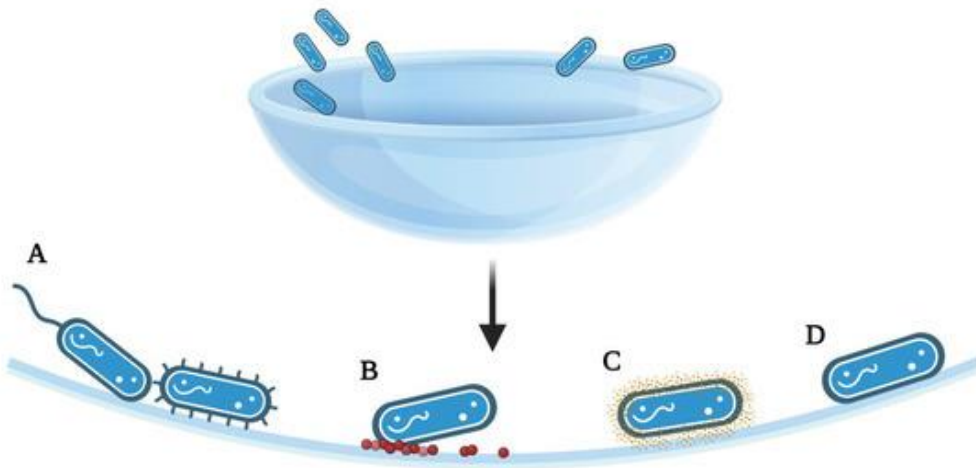


Figure 16 Summary of the stage of adhesion (146)

In general, the bacterial attachment process to any surface can be divided into two stages (Figure 16) (146). The first stage is one of temporary adhesion, in which bacteria can break away from the surface. This stage is largely mediated by London Van der Waals forces (146). In the second stage, irreversible adhesion, *P. aeruginosa* using their flagella or pili to attachment (A). Moreover, surface deposits of proteins or lipids following CL wear allowing for bacterial attachment (B). Next, bacteria produce adhesive proteins such as polysaccharides, or extracellular polymeric substances (EPS) exposed on the surface (C) and after these stages of initial adhesion (D), the adherent bacteria can then progress to form a biofilm which further contributes to the anchoring of the bacteria to the surface (146).

Adhesion to contact lenses surface differs between various species or strains of bacteria (153). *P. aeruginosa* adhesion to the lens is rapid, usually occurring within 1 h. Furthermore, the biofilm formation of *P. aeruginosa* can formed within 24 h of their adhering to lens surface (153).

Biofilm formation on contact lens

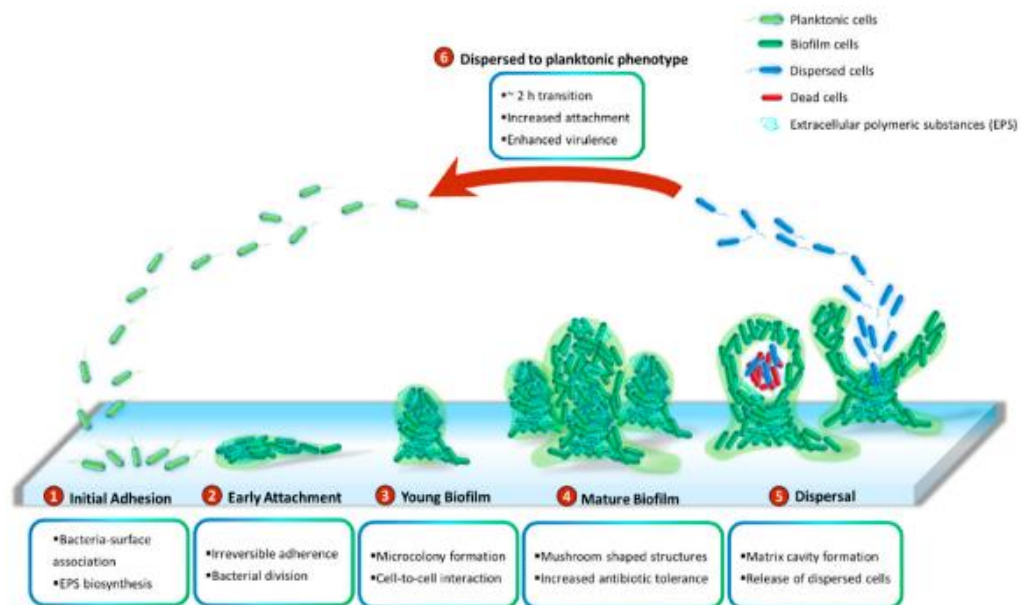


Figure 17 Summary of the stage of biofilm formation (154)

The cycle of biofilm formation is normally divided into six stages (Figure 17) (154). In the beginning, the bacteria couple with the surface (initial adhesion) and EPS biosynthesis. Bacteria produce EPS including extracellular DNA (eDNA), proteins, polysaccharides, and lipids. Secondary, early attachment, the bacterial cell division and the transition of reversible adherence into irreversible adherence take place. The third step, young biofilm, the microcolony formation and cell-to-cell interaction take place. Next, mature biofilm is the further maturity of these microcolonies into mushroom shaped structures. Importantly, biofilms protect the bacteria cells and cause the increasing antibiotic resistance and increasing tolerance to disinfectant chemical (155). The interaction between cells or QS network and the production of their virulence factors plays critical roles in biofilm maturation and biofilm robustness. Matrix cavity is then formed in the center of microcolony through cell autolysis to disrupt the matrix for the freeing of the dispersed population. Finally, the released cells undergo about 2 h transition into planktonic phenotypes, subsequently inhabit uncolonized areas (154).

The presence of bacterial biofilm on the contact lens surface has a key role in the development of microbial keratitis (156). The biofilm-producing bacteria cells can survive after being disinfected with the commercial contact lens solutions (157).

Pathogenesis of *Pseudomonas aeruginosa* related CLMK

The process of any CLMK generally starts with the adhesion of opportunistic pathogens to contact lens surface. According to *P. aeruginosa* adhere contact lenses, it can supply bacteria to the contact ocular surface such as cornea, thereby promoting greater chances of infection. Contact lens wear also enhances adherence of *P. aeruginosa* and binding of lectins – component of *P. aeruginosa* to the cornea (158). Moreover, the greatest amount of protein and lipid deposition after wearing on contact lens surface increases the bacterial adherence to corneal epithelial cells directly (159). As described previously, the main important virulent factor of the bacteria is their ability to form biofilms and produce adhesion factors. Bacterial biofilms facilitate prolonged contamination of contact lens and the persistence of organisms in the contact lens storage case (160). Moreover, contact lenses create a barrier for corneal respiration, limiting direct exposure to the atmosphere and decreasing corneal oxygenation (157). Contact lens wear for an extended period, combined with decreased oxygen permeability, may result in corneal hypoxia. This can result in discomfort, dryness, and corneal edema, as well as an increased risk of serious ocular infection. When *P. aeruginosa* adhesion in the cornea, it produce toxin or virulence factors that injures the surrounding tissue or ocular surface and cause inflammatory responses. Epithelial injury also results in loss of their functions so *P. aeruginosa* can invasion to stroma layers (161). Moreover, biofilm formation after adhesion leading to a persistent infection and inflammation (156). Additionally, contact lenses sit is in close proximity to the eye therefore the bacteria can spread to other parts of the eye, causing more serious infections.

The diagnosis and treatment of CLMK

The proper diagnosis of CLMK according to Contact Lens-Associated Infectious Keratitis: Update on Diagnosis and Therapy (2021) is based on a complete ocular history of contact lens wear, the patient's symptoms, a complete ophthalmological examination, corneal scrape, and culture (128). The typically made by taking a sample of the infected tissue (usually a scraping of the corneal epithelium) and performing a culture and sensitivity analysis test (128).

Microbial keratitis symptoms include sudden onset of ocular pain, red eye, tearing, foreign body sensation, conjunctival mucopurulent discharge, and photophobia with a variable degree of vision loss (128). The symptoms are commonly accompanied by these signs including, eyelid swelling, ciliary injection, conjunctival chemosis, corneal epithelial ulceration, stromal inflammatory, endothelial keratic precipitates, and anterior chamber reaction (128). Bacterial keratitis is characterized by a round, or oval epithelial defect with an underlying stromal infiltrate and anterior chamber reaction or hypopyon. However, these clinical findings are often misleading. Thus, corneal scrapings and cultures remain the gold standard for microbial identification and the only method for determining antibiotic sensitivity. An early diagnosis and appropriate treatment of infectious keratitis are essential. Broad-spectrum topical antibiotics are the first-line therapy for bacterial keratitis and should be initiated immediately after cultures are obtained, while waiting for the results. Antibiotics should be indicated, taking into consideration the local epidemiological data, frequency of specific pathogens, and antibiotic sensitivities (128).

The treatments according to Contact Lens-Associated Infectious Keratitis: Update on Diagnosis and Therapy (2021) (128) with adapted and modified from Mannis MJ and Holland EJ (Eds.). (2017). Cornea. Elsevier. include:

Penicillins: Inhibit bacterial cell wall formation by disrupting the peptidoglycan synthesis.

Cephalosporins: Inhibit bacterial cell wall formation by disrupting the synthesis of peptidoglycans. Less susceptibility to β -lactamases compared with Penicillins.

Glycopeptides: Inhibit cell wall formation of gram-positive bacteria

Fluoroquinolones: Inhibit bacterial DNA gyrase and topoisomerase IV, enzymes required for bacterial DNA synthesis.

Aminoglycosides: Bind to ribosomal subunits, resulting in defective mRNA translation and inhibition of protein biosynthesis.

Macrolides: Inhibit bacterial protein synthesis by binding to the 50S ribosomal subunit.

Bacterial folic acid inhibitors: Folic acid, used in DNA synthesis is required by bacteria for growth and replication.

Severe keratitis should be treated with an initial loading dose every 5 to 15 minutes for the first hour, followed by hourly instillation for 24 to 48 h; a topical fortified antibiotic or fluoroquinolone may be used (162). Treatment for microbial keratitis usually involves topical antibiotics, usually in the form of drops or ointments. In severe cases, oral antibiotics may be required (163). Antibiotics are efficient for treating almost all patients with CLMK if they are appropriately chosen based on common germs in every geographical region and the sensitivity and resistance of these germs against them. In addition, the patient should be educated on the proper use of contact lenses (164, 165). They should be counseled to avoid overnight wear and exposure to water and be educated on appropriate hygiene practices when handling contact lenses and timely contact lens replacement (128, 164). Moreover, the development of contact lens solutions targeting suppression of bacterial virulence factor are needed for prevention of CLMK (149).

Commonly used disinfectants in contact lens solutions

Quaternary Ammonium Compounds (QACs) also known as quaternary ammonium salts are chemical agents commonly used in healthcare domestic (166). QACs are commercially available used in contact lens solution as disinfectants. They possess antibacterial, antifungal, antiviral capabilities (167). The hydrophobic alkyl chains of the QACs interact with the bacterial outer membrane or phospholipid bilayer of the gram-negative bacteria. Then, this increases membrane permeability and induces the release of autolytic enzymes, resulting in loss of membrane integrity, intracellular component leakage, and bacterial cell lysis (Figure 18) (166, 168, 169). The QACs usually used in contact lens solutions including polyquaternium-1 (PQ-1) and biguanides (PHMB) (170). However, QACs are not always effective for clinical use due to the formation of biofilms, especially *P. aeruginosa* biofilms, which have demonstrated increased resistance to QACs (166). In addition, commercially available contact lens solutions may be ineffective against bacterial biofilms (117-119).

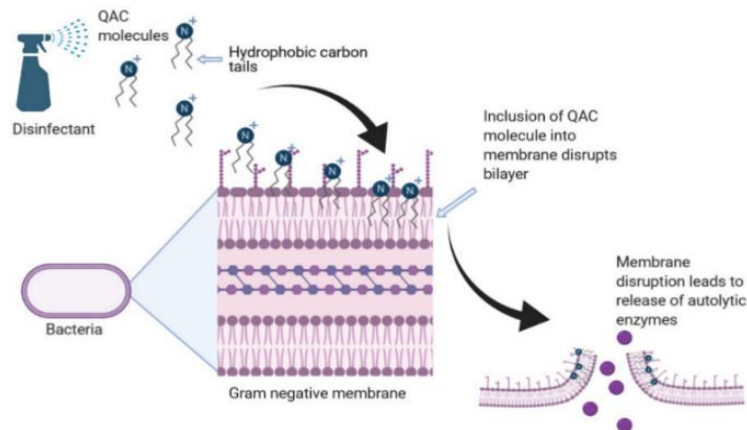


Figure 18 The bactericidal process of quaternary ammonium compounds (166)

The mode of action of disinfectants are shown in Figure 19 including the major mechanisms (left) and the reversible/irreversible mechanisms (right). The major mechanism is the disruption at the outer membrane of gram-negative bacteria which leads to a bactericidal effect. On the other hand, the time-dependent and concentration-dependent process by biocides causes a sequence of reversible and irreversible events. To illustrate, the initial release of intracellular potassium causes a depletion of the membrane potential and loss of proton motive force necessary for ATP biosynthesis (step 1–2). Then this event leads to an arrest of active transport, normal metabolic processes, and replication (step 3–5). Moreover, bacterial continued exposure to the biocide leads to irreversible damage, including changes to cytosolic pH which cascade into disruption of enzymatic function and coagulation of intracellular material (step 6–7). Finally, when the cytoplasmic membrane is significantly damaged, the proteins, nucleotides, pentoses and other ions may be lost from the bacterial cell (step 8) (171).

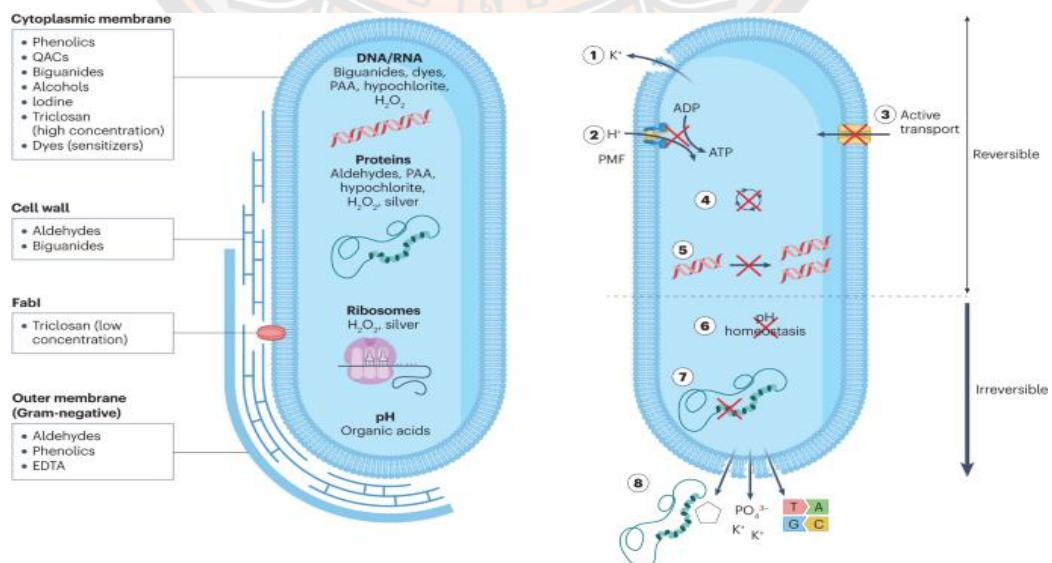


Figure 19 The mechanism of disinfectants (171)

CHAPTER III

RESEARCH METHODOLOGY

This part presents the methodology of this research including research materials, experimental designs, and methods.

Research materials

Culture medias

1. 5% sheep blood agar (BioMérieux, Inc. Hazelwood, MO, USA)
2. Luria Bertani; LB (Himedia Laboratories Pvt. Ltd., Maharashtra, India)
3. Mueller-Hinton Agar; MHA (Oxoid, Basingstoke, UK)
4. Mueller-Hinton Broth; MHB (Oxoid, Basingstoke, UK)
5. Tryptose Soya Agar; TSA (Himedia Laboratories Pvt. Ltd., Maharashtra, India)
6. Tryptose Soya Broth; TSB (Himedia Laboratories Pvt. Ltd., Maharashtra, India)

Chemicals and reagents

1. 100bp DNA Ladder RTU (GeneDireX, Taiwan)
2. 5xFIREPol® Master Mix (Solis BioDyne, Estonia)
3. 95% Ethanol (RCI Labscan, Thailand)
4. Agarose (Research Organics, Inc., USA)
5. Ceftazidime powder (Merck KGaA, Germany)
6. Ciprofloxacin powder (Merck KGaA, Germany)
7. Distilled water
8. DMSO (Dimethyl sulfoxide: Fisher scientific, UK)
9. Ethidium bromide (Vivantis Technologies Sdn. Bhd., Malaysia)
10. FIREScript RT cDNA synthesis Kit (Solis Biodyne, Tartu, Estonia)
11. Gentamicin powder (Merck, Germany)
12. HOT FIREPol® EvaGreen® qPCR Mix Plus (Solis Biodyne, Tartu, Estonia)
13. Hydroquinone; HQ (Sigma-Aldrich, Merck, Darmstadt, Germany)
14. Imipenem powder (Merck KGaA, Germany)
15. Multipurpose contact lens solutions: Opti-free® Replenish® solution (Alcon Laboratories, Inc., Texas, USA), Q-eye multipurpose solution (Stericon Pharma Pvt. Ltd., Karnataka, India), and ReNu® solution (Bausch & Lomb Inc., NJ, USA)
16. Phosphate buffer saline (Sigma-Aldrich, Merck, Darmstadt, Germany)
17. QuantiNova™ Reverse Transcription Kit (QIAGEN)
18. RNeasy Mini Kit (QIAGEN)
19. Sodium dodecyl sulfate; SDS (Sigma-Aldrich, Lyon, France)

Equipments

1. 12-well plates
2. 96-well plates
3. Beaker
4. Centrifuge tube 15 mL
5. Centrifuge tube 50 mL
6. Contact lens (Maxim Sofeye; Vision Science Co., Ltd, Gyeongsangbuk-do, South Korea)
7. Duran bottles
8. Erlenmeyer flask
9. Filter 0.22 micrometer
10. Microbiological needles and loops
11. Microcentrifuge tube
12. PCR tubes (Bio-Rad Laboratories, Hercules, CA, USA)
13. Petri dishes
14. Pipette and pipette tips
15. Syringe

Instruments

1. Automatic Vitek[®]2 compact device (BioMérieux, Inc. Hazelwood, MO, USA)
2. Biological safety cabinet (BSC) class II (NuAire Inc., USA)
3. Bio-Rad PCR Thermocyclers (Bio-rad Laboratories, Inc., USA)
4. CO₂ incubator (MEMMERT GmbH & Co. KG, Germany)
5. DEN-1 & DEN-1 B Densitometer Suspension turbidity detector
6. Electrophoresis system (Bio-rad Laboratories, Inc., USA)
7. Enspire[®] plate reader (PerkinElmer, Waltham, MA, USA)
8. Field emission scanning electron microscopy (FE-SEM; Apreo S, Thermo Fisher Scientific, MA, USA)
9. LineGene 9600 Plus Real-Time PCR Detection System (Bioer Technology, Hangzhou, China)
10. Microvolume Spectrophotometer (Colibri, Berthold Technologies)
11. Vortex mixer
12. Shaking bacterial incubator (Amerex Instruments Inc., USA)
13. SpectraMax iD3 Multi-Mode Microplate Reader (Molecular Devices, LLC., USA)

Experimental designs

The experimental designs were divided into three main parts.

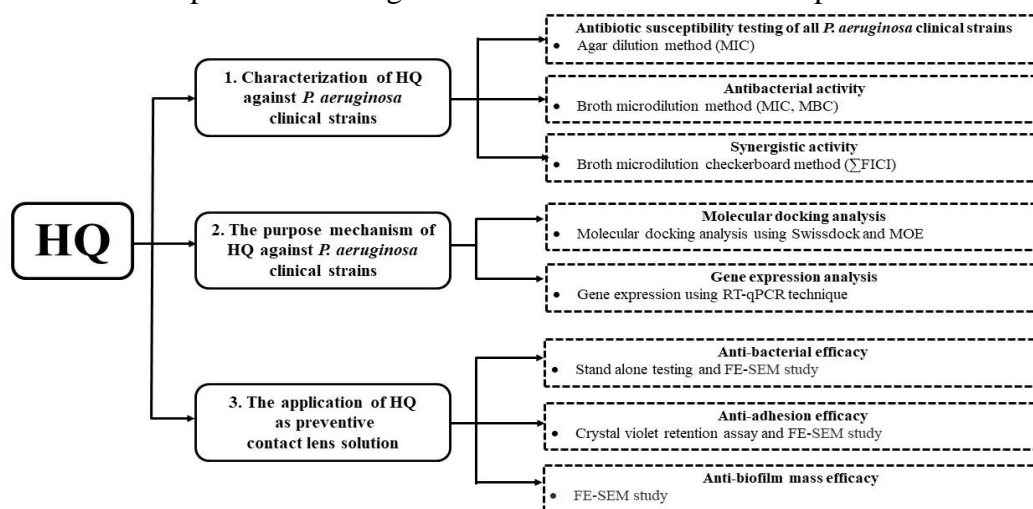


Figure 20 Experimental designs

For the scope of this research, hydroquinine (HQ) was studied in three main parts: (1) characterization of hydroquinine against several *P. aeruginosa* clinical strains, (2) the purpose mechanism of hydroquinine against *P. aeruginosa* clinical strains, and (3) the application of hydroquinine as part of a preventive contact lens solution. According to the Biosafety and Biosecurity aspects, this work was approved by the Naresuan University Institutional Biosafety Committee (NUIBC no. 64-16) and (NUIBC MI 65-10-35).

The first part involved the characterization of hydroquinine. Firstly, the antimicrobial susceptibility profiles of all *P. aeruginosa* clinical strains tested in this study were performed using a method from the Clinical and Laboratory Standards Institute (CLSI) guideline M07-A9 (11). Secondly, the antibacterial activity of hydroquinine against *P. aeruginosa* clinical strains was investigated using the broth microdilution method. Next, synergistic effects of hydroquinine with certain antibiotics were observed against *P. aeruginosa* clinical multi-drug resistant (MDR) strains by checkerboard method.

In the second part, the down-regulated expression genes based on transcriptomic analysis results (10) were selected in order to investigate the purpose mechanisms of hydroquinine against *P. aeruginosa* clinical strains. The purpose mechanism was predicted in atomic level using molecular docking analysis and then the mechanism was investigated in RNA levels using quantitative reverse transcription polymerase chain reaction (RT-qPCR).

The last part was the application of hydroquinine as preventive contact lens solution. Firstly, disinfection efficacies against *P. aeruginosa* were performed using stand-alone testing method and anti-bacterial activity assay on contact lens. Next, anti-adhesion activity assay on contact lens was performed using crystal violet (CV) retention assay and field emission scanning electron microscopy (FE-SEM) study. Lastly, anti-biofilm mass on contact lens was tested using FE-SEM.

Part 1: The characterization of hydroquinine against *P. aeruginosa* clinical strains

1.1 Preparation antibiotics and hydroquinine (HQ)

The antibiotics used in this study were dissolved in sterile deionized water or proper solvents recommended by CLSI (172).

Hydroquinine powder was purchased from Sigma-Aldrich (CAS No. 522-66-7). The working solution of hydroquinine (20 mg/mL) was prepared in 25% dimethyl sulfoxide (DMSO) in Mueller–Hinton broth (MHB, Oxoid, Basingstoke, UK). The working hydroquinine solution was freshly prepared for each experiment and filter before using. After that, the concentration of hydroquinine was diluted with MHB to achieve the required initial concentration. The concentration range of hydroquinine employed in this study was based on published studies by Rattanachak *et al.* (2022) (173).

In the last part, the application of hydroquinine as preventive contact lens solution, hydroquinine solutions were prepared according previous described, but hydroquinine was diluted with phosphate buffer saline (PBS; Sigma-Aldrich, Merck, Darmstadt, Germany) in pH 7.4 instead.

1.2 Strain and microorganism cultivation

The eight *P. aeruginosa* clinical strains (PAS1–8) were kindly provided by Kamphaeng Phet Hospital. These strains were isolated from specimens, such as blood, pus, and sputum, obtained from hospitalized patients at Kamphaeng Phet Hospital, Kamphaeng Phet, Thailand in 2022 as well as the drug-sensitive (DS) *P. aeruginosa* ATCC 27853 (PA-27853) was purchased from the American Type Culture Collection (ATCC) and was used as reference strain.

One colony of each clinical bacterium tested in this study was cultured on 5% sheep blood agar (BioMérieux, Inc. Hazelwood, MO, USA) as well as a colony of *P. aeruginosa* ATCC 27853 was cultured on tryptone soya agar (TSA, Himedia Laboratories Pvt. Ltd., Maharashtra, India) at 35 ± 2 °C for 18–24 h.

For subculturing, isolated bacterial colonies were re-streaked on the Mueller–Hinton Agar (MHA, Oxoid, Basingstoke, UK) and then incubated at 35 ± 2 °C for 24 h. For inoculum preparation in each experiment, the turbidity was adjusted to 0.5 McFarland standard, approximately $1-2 \times 10^8$ CFU/mL.

1.3 Antibiotic susceptibility testing of the bacterial stains

The antibiotic susceptibility testing (AST) of all *P. aeruginosa* strains tested in this study was performed by agar dilution method with the automatic Vitek[®]2 compact device (BioMérieux, Inc. Hazelwood, MO, USA). This automatic instrument for susceptibility testing was used to measure the changing turbidity value that occurs from bacteria growth compare with the initial value. Briefly, 40 µL of the prepared inoculum (0.5 McFarland) was added into the Vitek[®]2 identification test card which containing premeasured dried amounts of a specific antibiotic combined with the culture medium. The growth turbidity was measured every 15 min for a maximum incubation of 18 h at 35.5 ± 1 °C by the wavelength of 660 nm in each well at 16 different positions and repeated in triplicate.

The antibiotics and interpretation used in this study were undertaken from the Clinical and Laboratory Standards Institute (CLSI) document M100 recommendation

(174). The used antibiotics were divided into six classes, namely: (i) aminoglycosides (amikacin), (ii) carbapenems (doripenem, imipenem, meropenem), (iii) cephalosporins (ceftazidime, cefepime), (iv) fluoroquinolones (ciprofloxacin and levofloxacin), (v) penicillin with β -lactamase inhibitors (piperacillin/tazobactam), and (vi) cephalosporins with β -lactamase inhibitor (cefoperazone/sulbactam). The result from this method, called as MIC value of each antibiotic which inhibit the bacterial growth. For interpretation, the MDR definition is the resistance to three or more antimicrobial classes (175-178).

1.4 Antibacterial activity

The antibacterial activity of hydroquinine against *P. aeruginosa* tested in this study was determined by characterizing the minimum inhibitory concentration (MIC) and minimum bactericidal concentration (MBC) using broth microdilution assays with some modification of the CLSI guideline M07-A9 (11). All tests were performed in the triplicate experiments.

For the determination of MICs, the different dilutions of hydroquinine (a set of concentration 0.25, 0.50, 1, 1.25, 2, 4, 5, 8 and 10 mg/mL) in MHB were added to 96-well microtiter plates. For the quality control (QC), *P. aeruginosa* ATCC 27853 was tested with ciprofloxacin (CIP) (ranging from 0.0002 to 2 μ g/mL), while all strains were cultured in MHB containing 25% DMSO as vehicle controls. The negative and positive controls were wells containing only MHB without and with inoculum, respectively. Then, 10 μ L of bacterial inoculum was added to each well to achieve the final inoculum concentration of approximately 5×10^4 CFU/well. Then, the plates were incubated at 35 ± 2 °C for 16–20 h. The MIC values were the lowest concentrations of hydroquinine that inhibited bacterial growth, which can be seen clearly or without the growth of the bacteria by unaided eyes.

For the determination of MBCs, 10 μ L of each tested well was dropped to MHA plates and then incubated at 35 ± 2 °C for 24 h to observe the number of colonies. The MBC value was the lowest concentration without colonies growth.

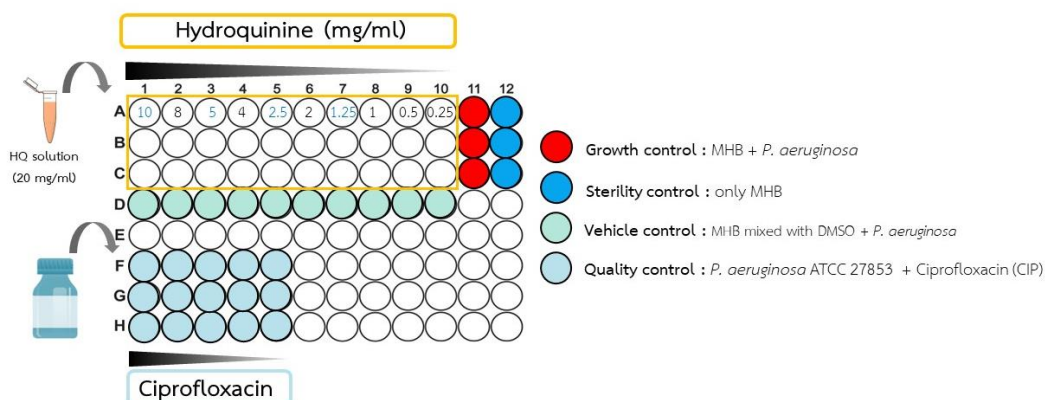


Figure 21 96-well plate for broth microdilution assay

1.5 *In vitro* evaluation of synergistic effects using the checkerboard method

This experiment focused only on *P. aeruginosa* clinical MDR strains as known from previous antibiotic susceptibility testing because there was one of the representative bacteria that is the opportunistic and MDR pathogen in hospitalized patients. Moreover, it had serious limitation of effectively therapeutic options because of its remarkable capacity to resist antibiotics (70).

The antibiotics used in this experiment were selected based on some antimicrobial resistance reported of MDR *P. aeruginosa* according to the ATCC (179) including ceftazidime, ciprofloxacin, and imipenem which were dissolved in sterile deionized water.

The synergistic effect of hydroquinine and antibiotic was tested against clinical MDR *P. aeruginosa* strains by reading the MIC value of a single indicated agent and a combination of the indicated agents and then calculating the fractional inhibitory concentration index (Σ FICI).

The broth microdilution checkerboard technique was performed using a 96-well plate, modified from Fratini *et al.* (2016) and Cheypratub *et al.* (2018) (180, 181). Briefly, the final concentrations of antibiotic and hydroquinine in combination were ranged as 2×MIC, MIC, MIC/2, MIC/4, MIC/8, MIC/16, MIC/32, and MIC/64. After that, 10 μ L of the final inoculum (5×10^4 CFU/well) was added into each well. Moreover, the vehicle as well as the positive and negative controls were performed similarly to the previous method. Then, the plates were incubated at 35 ± 2 °C for 16–20 h. The turbidity was observed by unaided eyes to determine the MIC values. The synergistic effect was determined by the fractional inhibitory concentration (FIC) index value, resulting from the changes in the MIC value (180, 181). The Σ FICI values were calculated from the formula Σ FICI = (MIC_{HQ + antibiotic} / MIC_{HQ}) + (MIC_{antibiotic + HQ} / MIC_{antibiotic}) and interpreted in terms of synergy, <0.50; partial synergy, 0.50–0.75; additive effect, 0.76–1.00; indifferent, >1.00; and antagonism was defined as Σ FICI > 4.00, respectively (182-184).

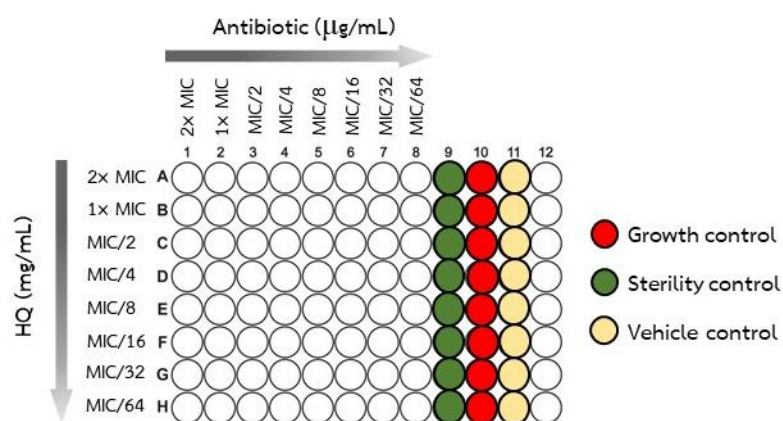


Figure 22 96-well plate for checkerboard method

Part 2: The purpose mechanisms of hydroquinine against *P. aeruginosa* clinical strains

According to previous our transcriptomic result (10) which identified the hydroquinine activity against *P. aeruginosa*. Briefly, the *P. aeruginosa* ATCC 27853 (PA-27853) strains were treated with either half MIC of hydroquinine (1.25 mg/mL) or MHB mixed with DMSO as an untreated control. Each culture was incubated for an hour then the total RNA from each sample was extracted. The RNA sequencing and transcriptomic analysis were performed as previously described (10, 173). Briefly, Gene expression profiles were represented as fragments per kilobase of transcript per million (FPKM). Then, gene expression that known genes and showed an average fold change >2 (p value ≥ 0.05) was used as the original raw data to identify differentially expressed genes (DEGs) between control and treated samples by the DESeq2 package (version 2.11.39).

The functional annotation of the significant down-regulated expression genes based on differentially expressed genes (DEGs) in Gene ontology (GO) terms and Kyoto Encyclopedia of Genes and Genomes (KEGG) pathway were also re-analyzed using the Database for Annotation, Visualization, and Integrated Discovery (DAVID) (<https://david.ncifcrf.gov/> 2021 updated database, accessed on 22 February 2023) in order to investigate the inhibitory mechanisms of hydroquinine against *P. aeruginosa*.

The interesting target proteins were selected for further analysis using molecular docking analysis and the differential expression was validated by quantitative reverse transcription polymerase chain reaction (RT-qPCR) respectively.

2.1 Molecular docking analysis

The molecular docking studied used to predict the active structure molecules of hydroquinine (ligand) against molecular bacterial targets and function by modelling the interaction between a ligand and target protein at the atomic level. This aim to characterize the behavior of small molecules in the binding site of target protein as well as to elucidate fundamental biochemical processes (185, 186).

The molecular docking was performed using Molecular Operating Environment (MOE) software and SwissDock web server. These were used to predict the active structure molecules of hydroquinine against the target protein by modelling the interaction between hydroquinine and target protein at the atomic level.

2.1.1 SwissDock server

The SwissDock server is based on the protein-ligand docking software EADock DSS developed by the Swiss Institute of Bioinformatics (SIB) (187). SwissDock server was used to perform the in-silico docking, whereas UCSF chimera was used for visualization and analysis of docking results.

There were three main steps for molecular docking, including preparing the target protein, preparing the ligand, and creating the molecular docking model.

1) Preparation of target protein structure file

The researcher searched the target protein structure from the research collaborative for structural bioinformatics protein databank (RCSB PDB) database. Then, the researcher prepared the *P. aeruginosa* proteins of interest, which originated from the X-ray crystal structures and the predicted structures using AlphaFold protein structure predictions (188, 189). Next, all protein files were then downloaded in “.pdb” files from database. Lastly, the researcher adjusted the target protein structure

into monomeric form such as all the non-protein atoms were removed using UCSF-Chimera program and then saved as “.pdb” files.

2) Preparation of ligand structure file

The researcher also prepared the ligand structure, hydroquinine, which was retrieved from the chemical component in the protein data bank from EMBL-EBI resources as “.pdb” files (190). The program UCSF-Chimera was then used to convert the ligand files from “.pdb” to “.mol2” files. Lastly, the researcher saved the ligand structure as “.mol2” files.

3) Creating the 3D molecular docking model

The interesting target proteins (.pdb) and the ligand (.mol2) were uploaded onto the SwissDock web server. Then, the result obtained in .zip files were viewed in UCSF-Chimera program. The binding free energy results were received and the “.chimeraX” files were also generated. The “.chimeraX” files were used to create the representative molecular docking models using the UCSF-Chimera program in order to analyze the interaction of the compounds studied and to show the three-dimensional (3D) structures (191). Lastly, analyzed and interpreted the binding affinity of target protein and ligand from binding structure of ligand and target protein, FullFitness, and binding free energy (ΔG).

Following each docking experiment, output clusters rated by a particular SwissDock method are received. The FullFitness scoring function is used to rank the clusters, with cluster 0 having the best FullFitness score. The individual conformer of each cluster was further arranged according to the FullFitness score. A better fit is provided by a binding mode with a greater negative FullFitness score (192).

Furthermore, the balance between structure and dynamics in biomolecular recognition is captured by the thermodynamic definition of the Gibbs free energy (ΔG), which is directly related to the binding affinity (Figure 17).

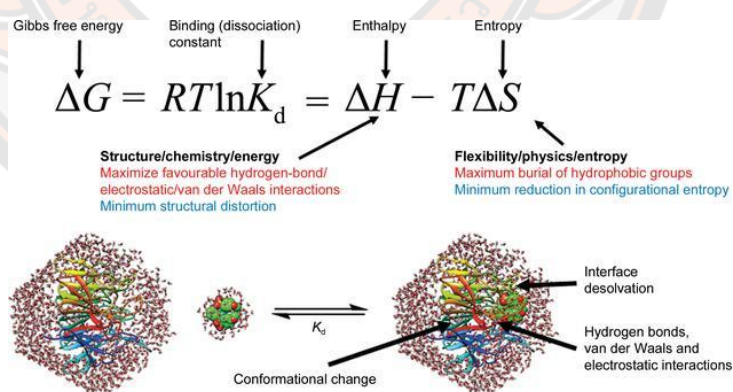


Figure 23 Binding free energy formulation (193)

The changes in free energy (ΔG) drive molecular recognition. However, the equilibrium is biased towards ligand binding when the thermodynamically favorable interactions (for example electrostatic attraction, hydrogen bonding, burial of hydrophobic groups and van der Waals forces) are larger than the thermodynamically unfavorable contributions (for example ligand desolvation, reduction in entropy associated with complexation and structural distortion of the ligand or protein, for example during induced-fit interactions).

Assessment of the binding capacity of ligand and protein by using ΔG value for predict the affinity capacity of ligand result in using it to predict the function of ligand interacts with target protein whether activator or inhibitor or antagonist (block or competitive). The lower ΔG value indicates the lesser requirement of energy for their bindings, as well as shows the easier binding or the greater binding possibility with the target protein (194-196).

2.1.2 Molecular Operating Environment (MOE) software

To further study the interaction between target proteins and hydroquinine, molecular docking simulations using MOE software were performed. The MOE 2015.10 software was developed by chemical computing group (197). MOE helped to visualize, characterize, and evaluate protein interactions. Furthermore, MOE identifies salt bridges, hydrogen bonds, hydrophobic interactions, sulfur-LP, cation- π , and solvent exposure, and gives the S score (198).

There were three main steps for molecular docking in MOE, including preparing the target protein and ligand, creating the molecular docking model, and creating the 2D ligand interaction mapping.

1) Preparation of target protein and ligand structure file

Ligands and receptors were prepared as previous described and then 3D protonating in MOE. Hydroquinine was retrieved from the chemical component in the protein data bank from EMBL-EBI resources as “.sdf” files (190). The target proteins were saved as “.pdb” files.

2) Creating the 3D molecular docking model

Firstly, the target proteins (.pdb) was uploaded onto the MOE software. Briefly, open the protein structure and identify the binding pocket by using alpha site technology to locate binding site. The Alpha Site Finder function was used to screen the surface of a protein for potential binding sites. This function also indicated preferred locations for hydrophilic or non-hydrophilic interaction points. Then, the generation of dummy atoms to mark site of target protein was perform (create dummy atoms at alpha sphere centers). Secondary, the ligand (.sdf) was uploaded onto the MOE software by “open molecule” menu. Lastly, creating the 3D molecular docking model was perform by using “compute” and then “dock” menu. The setting in the MOE software in receptor, site, and ligand were receptor atom, dummy atom, and ligand atom, respectively. After finished running, the S scores results were shown in the “viewer” window.

In this software, the interactions of hydroquinine with target protein were predicted on the basis of the S score (199). The binding S scores were computed based on binding affinities with all possible binding geometries. For interpretation, the lower S score tend to established a stronger interaction with ligand (200).

3) Creating the 2D ligand interaction mapping

To represent the main residues involved in the ligand-protein interaction of hydroquinine with target proteins, the lowest S score was used to create the two-dimensional (2D) view by using “ligand interaction” menu. The 2D ligand interaction mapping represented a good graphical view of results by showing ligand and receptor binding residues with their positions and interactions.

2.2 Testing the genes expression of *P. aeruginosa* strains

To verify the down-regulated gene expression levels, the drug sensitive *P. aeruginosa* ATCC 27853 and clinical MDR strains were treated with and without hydroquinine. These included three main steps: RNA extraction, complementary DNA synthesis, and RT-qPCR, respectively. Briefly, prior to performing, the researcher designed the interest primer which specific to the target gene.

In brief, the interesting down-regulated expression genes were selected. Then, the researcher obtained the whole genome sequencing of interest genes from the National Center for Biotechnology Information (NCBI) database. Subsequently, copied the whole genome sequencing of interest into the SnapGene viewer program (version 5.2.5.1) for primer design according to the suitable PCR primers design guidelines which described below (201).

- 1) The length of PCR primers should be 18–22 base pair.
- 2) Primer Melting Temperature (T_m): the optimal range of T_m is 52–58°C.
- 3) Primer Annealing Temperature (T_a): the optimal of T_a is about 5°C below the T_m of primers.
- 4) GC Content: the total bases G's and C's of primer should have many G's and C's in the primer of about 40–60%.
- 5) GC Clamp: should have many of G's or C's base at the 3' end of the primer about not exceed 3 bases.
- 6) Avoid primer secondary structures.
- 7) Avoid repetition of continues of four or more bases and dinucleotide repetitions (for example, AGGGG or CGCGCGCG).
- 8) Avoid homology of self-primer and forward and reverse primers (more than three bases). These conditions cause to self-dimers or primer-dimers.

After primer had designed already, the oligonucleotide properties calculator software (<http://biotools.nubic.northwestern.edu/>) was used to ensure the suitable melting temperature of the primer. Subsequently, the Basic Local Alignment Search Tool (Nucleotide BLAST) was used to confirm a specific primer to the gene of interest. Moreover, the Pseudomonas database (<https://www.pseudomonas.com>) was used to confirm whether the gene is designed primer have in *P. aeruginosa* or not. Lastly, all primer sequences were sent to Gibthai company to produce the primer. Primer sequences and annealing temperature were shown in Table 3.

Table 3 Primer sequences and annealing temperature used in this study.

Genes	Primer name	Oligonucleotide sequences (5' to 3')	Annealing temperature (°C)	
Genes related in arginine deiminase pathway	<i>arcA</i>	Forward	GAGCAACTGCGACGAGTTGC	57.9
		Reward	TCTGGATGGTCTCGGTCAGC	57.9
	<i>arcB</i>	Forward	CCAAGTTCATGCACTGCCTG	54.6
		Reward	TGATGGTATGCATGCGGTTTC	54.6
	<i>arcC</i>	Forward	CGGCTACATGATCGAACAGG	56.0
		Reward	CGGCTTCTTCCCTGGAGTAG	56.0
	<i>arcD</i>	Forward	CCTCGATGATCCTGATCCCG	57.9
		Reward	CAGCAGCAGGTACTIONCAGGC	57.9
Genes related in adhesion	<i>cgrC</i>	Forward	CGAGCGGATTGAAGCCATC	57.0
		Reward	ACGATGGGCTGGGTGAATC	57.0
	<i>cheY</i>	Forward	CCACGATGAGACGCATCATC	56.0
		Reward	ATGTTCCAGTCGGTGACGAG	56.0
	<i>cheZ</i>	Forward	ACTGGTGGACTGTCTCGAAC	57.0
		Reward	CGATCTGCGACATTTCTGC	57.0
	<i>pilV</i>	Forward	ACGACGTCAAGGACCAGATG	57.0
		Reward	GGCAGTTCGTTCTTCACCTG	57.0
	<i>fimU</i>	Forward	GGAAGTCAATGCGATGCTGC	56.0
		Reward	GAAGGTCAGATGTTCCACGG	56.0
Ref. gene	<i>16S rRNA</i>	Forward	CATGGCTCAGATTGAACGCTG	58.0
		Reward	GCTAATCCGACCTAGGCTCATC	58.0

2.2.1 RNA extraction

Bacterial inoculum was prepared to achieve turbidity about 0.5 McFarland standard ($1-2 \times 10^8$ CFU/mL). The equal volume of the cultures was then aliquoted into two falcon conical tubes (treated and untreated group). For one, hydroquinine solution was added at a final concentration of half of MIC, representing the treated group. The second tube had only the culture MHB mixed with DMSO without adding hydroquinine, which represents to untreated group. Each culture was shaken and incubated at $35 \pm 2^\circ\text{C}$ for 1 h. The pellet was collected using centrifugation at 5,000 rpm 4°C for 10 min.

Total RNA from the pellet was extracted by RNeasy Mini Kit (QIAGEN) and DNA residues were also removed using DNase reagent following the manufacturer's protocol. The quantity and purity of total RNA samples were analyzed by microvolume spectrophotometers (Colibri LB 915, Berthold Technologies GmbH & Co. KG). The ratio of absorbance at A₂₆₀/A₂₈₀ nm around 2.0 ± 0.2 was used to estimate the purity of the extract RNA.

2.2.2 Complementary DNA (cDNA) synthesis

The cDNA synthesis was performed using a FIREScript RT cDNA synthesis Kit (Cat. No. 06-15-00050, Solis Biodyne, Tartu, Estonia) by following the manufacturer's instruction. Briefly, 2 μ L of 10 \times reverse transcription buffer, 500 ng of RNA, 1 μ L of reverse transcriptase, 1 μ L of 100 μ M oligo (dT) primers, 0.5 μ L of dNTP Mix, 0.5 μ L of 40 U/ μ L RNase inhibitor and RNase-free water up to 20 μ L final volume were added to the reaction tube.

There were three steps in the cDNA synthesis:

- (i) the annealing step was performed at 25 $^{\circ}$ C for 5 min
- (ii) the reverse transcription step was performed at 45 $^{\circ}$ C for 30 min
- (iii) the enzyme inactivation step at 85 $^{\circ}$ C for 5 min.

The concentration of cDNA synthesized was measured prior to downstream analysis. After that, 2 μ L of cDNA were used for determining gene expression with specific primers by RT-qPCR.

2.2.3 Quantitative Reverse Transcription PCR (RT-qPCR)

The RT-qPCR was performed in low-profile PCR tubes (Bio-Rad Laboratories, Hercules, CA, USA) using HOT FIREPol[®] EvaGreen[®] qPCR Mix Plus (Cat. No. 08-25-00001, Solis Biodyne, Tartu, Estonia) by following the manufacturer's instructions. The reaction tubes were placed in a the LineGene 9600 Plus Real-Time PCR Detection System (Bioer Technology, Hangzhou, China). Briefly, each cDNA synthesized was used as a PCR template. The specific primers for each gene and the corresponding annealing temperatures were shown in Table 3. The *16S rRNA* of *P. aeruginosa* was used as a reference gene (housekeeping gene).

The RT-qPCR cycling conditions were as follows: 40 cycles of denaturation at 95 $^{\circ}$ C for 15 s, proper annealing step ranging at 54.6–58.0 $^{\circ}$ C for 20 s, and extension at 72 $^{\circ}$ C for 20 s. The housekeeping *16S rRNA* gene was used to calculate the relative expression levels of the genes using the $\Delta\Delta$ Ct method ($2^{-\Delta\Delta\text{Ct}}$) by following equation:

$$\Delta\text{Ct} = \text{Ct} (\text{gene of interest}) - \text{Ct} (\text{housekeeping gene})$$

$$\Delta\Delta\text{Ct} = \Delta\text{Ct} (\text{treated group}) - \Delta\text{Ct} (\text{untreated group})$$

The fold change of gene expression ($2^{-\Delta\Delta\text{Ct}}$) levels was used to calculate the fold change of gene expression levels which relative to the untreated sample. All the experiments were performed in triplicate.

Part 3: The application of hydroquinine as preventive contact lens solution

The last part was the application of hydroquinine as preventive contact lens solution. Firstly, anti-bacterial efficacy was performed using stand-alone testing method which reported as log of reduction. Next, anti-adhesion efficacy was performed using crystal violet (CV) retention assay and anti-adhesion efficacy on contact lens surface was observed using field emission scanning electron microscopy (FE-SEM) study. Lastly, anti-biofilm mass efficacy was tested using FE-SEM study. In this part, phosphate buffer saline (PBS; pH 7.4 Sigma-Aldrich, Merck, Darmstadt, Germany) was used as control. Hydroquinine solution (MIC and half MIC) dissolved in PBS was tested compare with commercial multipurpose solution. Moreover, screening test solutions were also tested including hydroquinine solution (MIC and half MIC) combined with some multipurpose solution (50% and 100%). The concentration range of hydroquinine in MIC and half MIC was based on previous results. All tested solutions were prepared for each challenge *P. aeruginosa*.

3.1 *P. aeruginosa* strains, cultivation, and inoculum preparation

P. aeruginosa ATCC 27853 was obtained from the American Type Culture Collection (ATCC; Manassas, VA, USA) and a clinical *P. aeruginosa* strain was isolated from eye infected-hospitalized patient from previous study (PA-S4). The bacterial isolates were streaked on the Mueller Hinton Agar (MHA, Oxoid, Basingstoke, UK) and then incubated overnight at $35 \pm 2^\circ\text{C}$. The turbidity of inoculum was adjusted to 0.5 McFarland standard around $1-2 \times 10^8$ CFU/mL.

3.2 Contact lenses and lenses cases preparation

Sterilized soft contact lenses (Maxim Sofeye; Vision Science Co., Ltd, Gyeongsangbuk-do, South Korea) were purchased. The lenses were the U.S. Food and Drug Administration (FDA) group 1 which had 14.1 mm diameter and 8.6 mm base curvature. The hydrogel contact lenses were made from polyacon which had 2-hydroxyethyl methacrylate (HEMA) as the main monomer (58% HEMA and 42% Water). Contact lens cases were obtained from the manufacturer's supplies. All contact lenses and lens cases were new and unused before testing. (Figure 24B).



Figure 24 Material and equipment used in contact lens study: (A) MPSs, (B) Contact lenses, (C) Standalone testing, and (D) Anti-adhesion efficacy on contact lens.

3.3 Commercial multipurpose solutions preparation

The three commercial soft contact lens MPSs, which were available in Thailand, were tested. The tested solutions were Opti-free® RepleniSH® solution (Alcon Laboratories, Inc., Texas, USA) which coded as MPS A, Q-eye multipurpose solution (Stericon Pharma Pvt. Ltd., Karnataka, India) which coded as MPS B, and ReNu® solution (Bausch & Lomb Inc., NJ, USA) which coded as MPS C. In this study, the 100% original product was tested as well as 50% of MPS was prepared by dissolved original product with phosphate buffer saline pH 7.4 (PBS; Sigma-Aldrich, Merck, Darmstadt, Germany). The component of each solution was shown in Table 4.

Table 4 Commercial multipurpose solution (MPS) used in this study.

Code	MPS A	MPS B	MPS C
Product name	OPTI-FREE® RepleniSH®	Q-EYE	ReNu®
Manufacturer	Alcon Laboratories, Inc., Texas, USA	Stericon Pharma Pvt. Ltd., Karnataka, India	Bausch & Lomb Inc., NJ, USA
Disinfection and preservatives	Polyquaternium-1 - POLYQUAD® 0.001% Myristamidopropyl dimethylamine - ALDOX® 0.0005%	Polyhexamethylen e biguanide (PHMB) 0.0001 %	Alexidine dihydrochloride 0.0002% Polyquaternium-1 (POLYQUAD®) 0.00015%
Wettings agents	Poloxamine - TETRONIC® 1304	Poloxamer, Dexpanthenol	Poloxamer 181
Lubricants	Propylene glycol	Sorbitol	Poloxamine
Buffer and saline	Sodium borate, Sodium chloride	Disodium Edetate, Sodium Dihydrogen Phosphate	Diglycine, Sodium borate, Sodium chloride

3.4 Tested solution preparation

The initial solution of hydroquinine (CAS No. 522-66-7) (Sigma-Aldrich, Merck, Darmstadt, Germany) was prepared in 25% DMSO in PBS to achieve 20 mg/mL. The working solution of hydroquinine was diluted in PBS to achieve the required concentration. The MIC of hydroquinine (2.50 mg/mL) and half MIC (1.25 mg/mL) employed in this study were based on previous results. For all the disinfection efficacy testing, the tested solutions were compared with control (PBS).

3.5 Studying adhesion-related gene expression levels

To verify the adhesion-related gene expression levels, the drug sensitive *P. aeruginosa* ATCC 27853 was treated with and without hydroquinine. The gene expression steps were as follows: RNA extraction, complementary DNA synthesis,

and RT-qPCR, respectively as previously described in section 2.2 Testing the genes expression of *P. aeruginosa* strains.

3.6 Stand-alone testing with microorganisms

The antimicrobial efficacy of tested solutions was determined using stand-alone testing with some modification according to the International Organization for Standardization (ISO) 14729 (116). The ISO 14729 is Ophthalmic optics – Contact lens care products – Microbiological requirements and test methods for products and regimens for hygienic management of contact lenses (116).

Briefly, the antimicrobial effectiveness was performed by inoculating 1.0×10^5 to 1.0×10^6 CFU/mL of each *P. aeruginosa* tested strain into the test tube which containing 10 mL of each tested solution. The test samples were stored at 20–25 °C. All test samples were assessed to determine the number of surviving bacterial at 6 h (recommended disinfection time) and 24 h (additional time point). To count the number of living bacteria, aliquots of the tested solution (1 mL) were transferred to new test tubes containing 9 mL of MHB. Serial 1:10 dilutions were then performed using additional test tubes containing MHB. Dilutions were then plated to quantify the colony forming unit (CFU/mL). Plate counts were conducted and calculated to log of reduction compared to the test control (PBS).

3.7 Anti-adhesion efficacy of tested solutions

The anti-adhesion efficacy was determined using crystal violet retention assay in 96-well plates with the following minor modifications (173). Briefly, in wells, each tested solution and control (200 μ L) challenged with 10% inoculum (20 μ L) approximately 1.0×10^5 to 1.0×10^6 CFU/mL of each *P. aeruginosa* strain. The plates were incubated at $35 \pm 2^\circ\text{C}$ for 24 h. The planktonic cells were carefully removed and washed three times with sterile distilled water. The plate was then dried at 60 °C for 45 min. Next, the adherent cells were stained with 0.1% (w/v) crystal violet for 20 min at room temperature. The crystal violet was washed three times with sterile distilled water, and then re-dissolved with 95% ethanol (v/v). The optical density of residue biofilm quantification was measured at 595 nm using a microplate reader (PerkinElmer, Waltham, MA, USA) and then calculated as the percentage of anti-adhesion efficacy.

3.8 Anti-adhesion efficacy on contact lens

The antimicrobial effectiveness of tested solutions on contact lenses was established using ISO 18259 (203) with minor modification. ISO 18259 is the protocol methodology for Ophthalmic optics – Contact lens care products – Method to assess contact lens care products with contact lenses in a lens case, challenged with bacterial and fungal organisms (117, 203). Briefly, contact lenses were aseptically removed from the package and immersed in PBS for 18 h before testing. The lenses were placed with the concave side up in the matching manufacturer's contact lens cases. Lenses were then inoculated to contain a final count of 1.0×10^5 to 1.0×10^6 CFU/mL of the *P. aeruginosa* tested strains. Following a contact time of 5 min, the required tested solution was added to the cases (4 mL) and the cases were then closed, ensuring the cap is not contaminated. Closed contact lens cases were stored at 20–25 °C for 6 h. PBS was used as a test control and experimentation was performed in

the same manner. Following this time point, test solutions and controls were evaluated to determine the morphology of bacteria at the recommended disinfection time (6 h). The contact lenses were carefully removed from their cases. Next, the field emission scanning electron microscopy (FE-SEM; Apreo S, Thermo Fisher Scientific, MA, USA) was used to determine the characterization of *P. aeruginosa* morphology.

3.9 Anti-biofilm mass on contact lens

To compare the architecture of the biofilm mass in *P. aeruginosa* strains on different tested solutions after recommended disinfection time (6 h), the anti-biofilm efficacy was performed in the same manner as previous method with minor modification. Briefly, sterile contact lenses were rinsed with PBS and then placed in 12-well plates containing 1.0×10^5 to 1.0×10^6 CFU/mL of the *P. aeruginosa* tested strain at 35 ± 2 °C for 24 h (biofilm formation phase). Following this, contact lenses were then transferred to new 12-well plates containing the required tested solution (4 mL) and then stored at 20–25 °C for 6 h. As a control, PBS was employed. After this immersion, the morphology of bacterial biofilm mass was examined using the FE-SEM.

3.10 Morphological observation using the FE-SEM

The morphology of *P. aeruginosa* tested strains on contact lens surface was measured using the FE-SEM. For sample preparation, the contact lens samples were cut into 8 mm diameter and put on an aluminum stub. The contact lens was then dehydrated in a desiccator to eliminate the moisture before being coated with gold. At this stage, the contact lens was ready for testing. The FE-SEM measurements were performed at 2.0–10 kV in magnification 1,200X, 5,000X, and/or 10,000X. The FE-SEM images were used to measure the bacterial morphology including their structure, size, and shape. Based on these characteristics, the morphology was utilized to differentiate between PBS (control) and tested solutions.

Statistical analysis

All of the experiments were performed in triplicate with three independent repeats for an accurate laboratory result. Data are presented as mean \pm standard deviation. GraphPad Prism version 8.0.1 (San Diego, CA, USA) was used to analyze the data and create all graphs. The comparison of the data between two experimental groups was performed by student's t-test. One-way analysis of variance (ANOVA) and Tukey test was used to verify the mean differences between groups. For all analyses, *p* values less than 0.05 were considered statistically significant.

CHAPTER IV

RESULTS

Part 1: The characterization of hydroquinine against *P. aeruginosa* clinical strains

1.1 Antibiotic susceptibility testing of the bacterial stains

There were eight representatives of clinical *P. aeruginosa* strains isolated from a blood sample (PA-S1), three samples of pus (PA-S2, PA-S3, and PA-S4), and four samples of sputum (PA-S5, PA-S6, PA-S7 and PA-S8) as shown in Table 5.

Table 5 *P. aeruginosa* strains used in this study

Strain code	Bacterial source
PA-27853	ATCC reference strain
PA-S1	Blood
PA-S2	Pus from abdominal surgery wound
PA-S3	Pus from bed sore
PA-S4	Pus from eye infection
PA-S5	Sputum
PA-S6	Sputum
PA-S7	Sputum
PA-S8	Sputum

The antibiotic susceptibility profiles of *P. aeruginosa* from one reference strain and the eight clinical isolates were phenotypically investigated with several antibiotic classes. This study demonstrated that all *P. aeruginosa* strains were sensitive to amikacin. In contrast, particular clinical *P. aeruginosa* isolates were resistant to specific anti-pseudomonal drugs. For example, four clinical isolates, namely PA-S2, PA-S4, PA-S5, and PA-S7, were resistant to ceftazidime.

Three clinical *P. aeruginosa* isolates, PA-S3, PA-S6, and PA-S8, were sensitive to all antibiotic agents tested, which was similar to the reference drug-sensitive (DS) strain (PA-27853). PA-S1 was sensitive to all drugs except, partially, levofloxacin. PA-S2 was only resistant to ceftazidime. On the other hand, PA-S7 was defined as drug-resistant (DR) strain because it showed resistance to two antimicrobial classes: cephalosporins and penicillin/ β -lactamase inhibitors group. Furthermore, two clinical *P. aeruginosa* isolates, PA-S4 and PA-S5, were defined as multidrug-resistant (MDR) strains as they showed resistance to ≥ 1 agent in ≥ 3 antimicrobial classes. Particularly, the PA-S4 resisted ceftazidime, piperacillin/tazobactam, and cefoperazone/sulbactam, whereas the PA-S5 resisted all agents in the carbapenems group (doripenem, imipenem, and meropenem), and it also resisted the cephalosporins group (ceftazidime and cefepime), fluoroquinolones group (ciprofloxacin and levofloxacin), as well as cefoperazone/sulbactam. A summary of the results was shown in Table 6. The numbers in table indicated the minimum inhibitory concentration (MIC) value. Colours indicate sensitivity: sensitive (green), intermediate (yellow), and resistant (red).

Table 6 Phenotypic antibiotic susceptibility profiles of *P. aeruginosa* ATCC 27853 and eight clinical *P. aeruginosa* isolates to six classes of anti-pseudomonal drugs

Anti-biotics	Amino-glycosides	Carbapenems			Cephalo-sporins		Fluoro-quinolones		Penicillins + β -lactamase inhibitors	Cephalosporins + β -lactamase inhibitors
	Amikacin	Doripenem	Imipenem	Meropenem	Ceftazidime	Cefepime	Ciprofloxacin	Levofloxacin	Piperacillin/Tazobactam	Cefoperazone/Sulbactam
PA-27853	≤ 2	0.5	2	0.5	≤ 1	2	≤ 0.25	1	≤ 4	≤ 8
PA-S1	≤ 2	0.5	2	≤ 0.25	4	2	≤ 0.25	2	8	≤ 8
PA-S2	≤ 2	1	2	1	32	4	≤ 0.25	0.5	32	≤ 8
PA-S3	≤ 2	0.25	2	≤ 0.25	4	2	≤ 0.25	1	8	≤ 8
PA-S4	≤ 2	4	2	1	32	4	≤ 0.25	2	≥ 128	≥ 64
PA-S5	≤ 2	≥ 8	≥ 16	≥ 16	≥ 64	≥ 64	≥ 4	≥ 8	32	≥ 64
PA-S6	≤ 2	0.25	2	≤ 0.25	4	2	≤ 0.25	0.5	8	≤ 8
PA-S7	≤ 2	0.5	2	≤ 0.25	≥ 64	32	≤ 0.25	2	≥ 128	32
PA-S8	≤ 2	≤ 0.12	2	≤ 0.25	4	2	≤ 0.25	1	8	≤ 8

1.2 Antibacterial activity

Hydroquinine could inhibit and kill all clinical isolates at the MIC 2.50 mg/mL and minimum bactericidal concentration (MBC) at 5.00 mg/mL. Comparable to the clinical strains, reference DS *P. aeruginosa* strain (PA-27853), was inhibited and killed by the same concentrations of hydroquinine (Table 7).

Table 7 Antibacterial activity of hydroquinine against *P. aeruginosa* ATCC 27853 and clinical *P. aeruginosa* isolates

Strain code	Minimum inhibitory concentration (mg/mL)	Minimum bactericidal concentration (mg/mL)
PA-27853	2.50	5.00
PA-S1	2.50	5.00
PA-S2	2.50	5.00
PA-S3	2.50	5.00
PA-S4	2.50	5.00
PA-S5	2.50	5.00
PA-S6	2.50	5.00
PA-S7	2.50	5.00
PA-S8	2.50	5.00

According to the phenotypic characterization of the antibiotic susceptibility profiles, PA-S4 and PA-S5 were identified as clinical *P. aeruginosa* MDR strains. Importantly, Comparable to the DS strains, these clinical MDR strains were still inhibited and killed by the same MIC and MBC of hydroquinine (Figure 25).

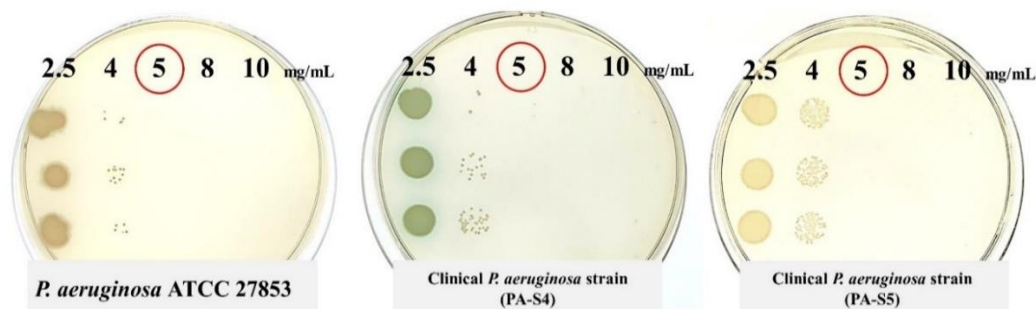


Figure 25 Minimum bactericidal concentration (MBC) of hydroquinine

1.3 *In vitro* evaluation of synergistic effects using the checkerboard method

The MDR strains, PA-S4 and PA-S5, showed considerable resistance to ceftazidime, with high MIC ($\geq 32 \mu\text{g/mL}$). Moreover, comparable to other strains, only PA-S5 showed highly resistant to imipenem (MIC $\geq 16 \mu\text{g/mL}$) and ciprofloxacin (MIC $\geq 4 \mu\text{g/mL}$) (Table 6). Therefore, imipenem, ceftazidime, and ciprofloxacin were selected for representative of carbapenem, cephalosporin, and fluoroquinolone anti-*P. aeruginosa* classes.

In combination, the MICs of hydroquinine and ceftazidime were reduced compared to those of the individual agents by two to eight times in both strains (PA-S4 and PA-S5) as shown in Table 8. The MIC values of ceftazidime were decreased by at two-fold (MIC/2) when combined with the hydroquinine treatment. According to the fractional inhibitory concentration index (ΣFICI), hydroquinine had notable partial synergistic effects with ceftazidime (ΣFICI of 0.7500 and 0.6250 against clinical MDR *P. aeruginosa* strains, PA-S4 and PA-S5, respectively).

Unfortunately, hydroquinine had remarkable indifferent effects with imipenem (ΣFICI of 1.0156 and 1.0019 against PA-S4 and PA-S5, respectively) as well as ciprofloxacin (ΣFICI of 1.0156 and 1.0078 against PA-S4 and PA-S5, respectively). However, when combined with hydroquinine treatment, the MIC values of imipenem were extremely decreased by 64-fold (MIC/64) and 512-fold (MIC/512) in PA-S4 and PA-S5, respectively. Furthermore, the MIC value of ciprofloxacin was also decreased by 128-fold (MIC/128) in PA-S5.

This study discovered that hydroquinine may enhance the effectiveness of currently available anti-pseudomonal antibiotics against clinical MDR *P. aeruginosa* strains.

Table 8 The combined effect of hydroquinine and antibiotics against clinical MDR *P. aeruginosa* isolates.

Strains	Agents	MIC ($\mu\text{g/mL}$)		FICI	ΣFICI	Interpretation
		Alone	Comb.			
PA-S4	Hydroquinine	2500	2500	1.0000	1.0156	Indifferent
	Imipenem	1	0.0156	0.0156		
PA-S5	Hydroquinine	2500	2500	1.0000	1.0019	Indifferent
	Imipenem	1024	2	0.0019		
PA-S4	Hydroquinine	2500	625	0.2500	0.7500	Partial synergy
	Ceftazidime	32	16	0.5000		
PA-S5	Hydroquinine	2500	312.5	0.1250	0.6250	Partial synergy
	Ceftazidime	64	32	0.5000		
PA-S4	Hydroquinine	2500	39.0625	0.0156	1.0156	Indifferent
	Ciprofloxacin	0.0625	0.0625	1.0000		
PA-S5	Hydroquinine	2500	2500	1.0000	1.0078	Indifferent
	Ciprofloxacin	8	0.0625	0.0078		

Part 2: The purpose mechanisms of hydroquinine against *P. aeruginosa* clinical strains

To find out the potential impact on gene expression according to the global transcriptomic profile of *P. aeruginosa* ATCC 27853 under untreated or treated with the half of MIC value (1.25 mg/mL) of hydroquinine for 1 h (10), in this study, the researcher excluded the hypothetical protein and undefined genes and represented in only top 15 transcripts of the significantly up- and down- regulated differentially expressed genes (DEGs) which were shown in Table 9 and 10, respectively.

Table 9 The top 15 transcripts of the significantly up-regulated DEGs (hypothetical protein and undefined genes were excluded)

No.	Genes	Product name	Log ₂ FC*
1	<i>mexC</i>	Resistance-Nodulation-Cell Division (RND) multidrug efflux membrane fusion protein MexC precursor	9.474
2	<i>morB</i>	Morphinone reductase	6.693
3	<i>mexD</i>	Resistance-Nodulation-Cell Division (RND) multidrug efflux transporter MexD	6.266
4	<i>oprJ</i>	Multidrug efflux outer membrane protein OprJ precursor	6.020
5	<i>armR</i>	Antirepressor for MexR, ArmR	5.711
6	<i>cifR</i>	CifR	5.311
7	<i>creD</i>	Inner membrane protein CreD	5.294
8	<i>mexX</i>	Resistance-Nodulation-Cell Division (RND) multidrug efflux membrane fusion protein MexX precursor	5.259
9	<i>ohr</i>	Organic hydroperoxide resistance protein	5.241
10	<i>mexY</i>	Resistance-Nodulation-Cell Division (RND) multidrug efflux transporter MexY	4.898
11	<i>pauB1</i>	FAD-dependent oxidoreductase	4.891
12	<i>ibpA</i>	Heat-shock protein IbpA	4.817
13	<i>esrC</i>	EsrC	4.276
14	<i>pyeM</i>	PyeM	4.098
15	<i>bamI</i>	Biofilm-associated metzincin Inhibitor, BamI	3.615

Note: *Log₂ FC was Log₂ relative fold changes of the gene expression levels in response to hydroquinine, compared to the untreated control.

Table 10 The top 15 transcripts of the significantly down-regulated DEGs (hypothetical protein and undefined genes were excluded)

No.	Genes	Product name	Log ₂ FC*
1	<i>arcD</i>	Arginine/ornithine antiporter (AOA)	-4.245
2	<i>nrdG</i>	Class III (anaerobic) ribonucleoside-triphosphate reductase activating protein, 'activase', NrdG	-3.936
3	<i>arcA</i>	Arginine deiminase (ADI)	-3.849
4	<i>yhhJ</i>	Permease of ABC transporter	-3.538
5	<i>arcC</i>	Carbamate kinase (CK)	-3.412
6	<i>arcB</i>	Ornithine transcarbamylase (OTC)	-3.319
7	<i>yhiH</i>	ATP-binding/permease fusion ABC transporter	-3.171
8	<i>rfaD</i>	ADP-L-glycero-D-mannoheptose 6-epimerase	-3.161
9	<i>nirG</i>	NirG	-3.150
10	<i>nirL</i>	Heme d1 biosynthesis protein NirL	-2.973
11	<i>nirF</i>	Heme d1 biosynthesis protein NirF	-2.937
12	<i>flgC</i>	Flagellar basal-body rod protein FlgC	-2.929
13	<i>nrdD</i>	Class III (anaerobic) ribonucleoside-triphosphate reductase subunit, NrdD	-2.845
14	<i>nirH</i>	NirH	-2.784
15	<i>ada</i>	O6-methylguanine-DNA methyltransferase	-2.740

Note: *Log₂ FC was Log₂ relative fold changes of the gene expression levels in response to hydroquinine, compared to the untreated control.

Further analysis was performed to generate a gene expression heatmap of *P. aeruginosa* ATCC 27853 in response to hydroquinine (1.25 mg/mL). The heatmap shown top 15 of significantly up and down regulated DEGs as in Figure 26.

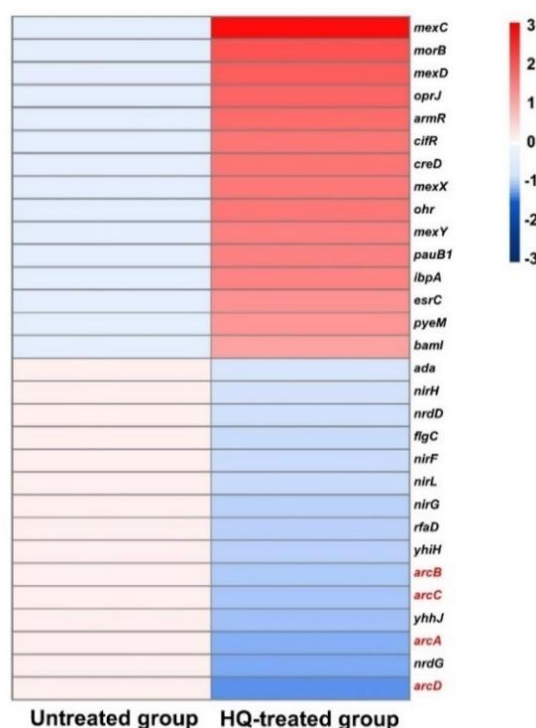


Figure 26 Gene expression heatmap of *P. aeruginosa* ATCC 27853 in response to hydroquinone (1.25 mg/mL)

Interestingly, it was recognized that the *arcD* gene (arginine/ornithine antiporter; AOA) was the most downregulated in the transcriptomic analysis by a -4.24 Log₂-fold change in response to hydroquinone (Table 11). Consistently, the differentially expressed genes (DEGs) of other arginine deiminase (ADI) pathway-related genes including *arcA* (arginine deiminase; ADI), *arcB* (ornithine transcarbamylase; OTC), and *arcC* (carbamate kinase; CK) were also depleted in response to hydroquinone, by -3.85, -3.32, and -3.41 Log₂-fold changes, respectively (Table 11).

Table 11 DEGs of ADI pathway-related genes as determined by transcriptome analysis

Genes	Product name	Log ₂ FC*	FDR [#]	<i>p</i> -value
<i>arcA</i>	Arginine deiminase (ADI)	-3.85	2.06 x 10 ⁻⁵	1.43 x 10 ⁻⁷
<i>arcB</i>	Ornithine transcarbamylase (OTC)	-3.32	4.00 x 10 ⁻⁴	3.36 x 10 ⁻⁶
<i>arcC</i>	Carbamate kinase (CK)	-3.41	2.00 x 10 ⁻⁴	1.96 x 10 ⁻⁶
<i>arcD</i>	Arginine/ornithine antiporter (AOA)	-4.24	2.51 x 10 ⁻⁶	1.22 x 10 ⁻⁸

Note: *Log₂ FC was Log₂ relative fold changes of the gene expression levels in response to hydroquinone, compared to the untreated control. [#]FDR was false discovery rate showed statistical significances.

2.1 Molecular docking analysis

The molecular docking using SwissDock web server and Molecular Operating Environment (MOE) software were used to predict the active structure molecules of hydroquinine against the target ADI pathway-related protein by modelling the interaction between a ligand and target protein at the atomic level.

Using the solved protein crystal structures for ADI and CK alongside the AlphaFold predicted structures of OTC and AOA (202), the molecular docking results shown the predict various values of the interaction in Table 12.

Table 12 The molecular docking results between hydroquinine and ADI pathway-related proteins using SwissDock.

SwissDock results	Target proteins			
	ADI	OTC	CK	AOA
Energy	18.0157	23.6354	19.3324	16.3821
SimpleFitness	18.0157	23.6354	19.3324	16.3821
Full Fitness (FF)	-1862.2413	-1792.0676	-1569.1299	-1182.9026
InterFull	-42.2811	-31.5186	-40.7556	-39.8486
IntraFull	68.6997	68.9478	72.7438	68.297
solvFull	-2176.79	-2059.64	-1834.29	-1513.5
surfFull	288.13	230.143	233.172	302.149
extraFull	0.0	0.0	0.0	0.0
deltaG _{compsolvpol}	-2176.79	-2059.64	-1834.29	-1513.5
deltaG _{compsolvnonpol}	288.13	230.143	233.172	302.149
deltaG _{protsolvpol}	-2190.84	-2063.37	-1843.89	-1523.11
deltaG _{protsolvnonpol}	289.461	230.599	233.664	304.359
deltaG _{ligsolvpol}	-9.49661	-8.16566	-8.60523	-8.10315
deltaG _{ligsolvnonpol}	9.32902	9.34359	9.01344	9.08695
deltaG _{vdw}	-42.2811	-31.5186	-40.7556	-39.8486
deltaG _{elec}	0.0	0.0	0.0	0.0
deltaG	-7.557174	-7.170672	-7.630536	-7.744327

The molecular docking results demonstrated the possibility of an interaction between the ADI pathway-related target proteins, including ADI, OTC, CK, and AOA, and hydroquinine based on the full fitness (FF) score and binding free energy (ΔG) value from SwissDock. According to FF scores, ADI, OTC, CK, and AOA had FF score of -1862.2413, -1792.0676, -1569.1299, and -1182.9026 kcal/mol, respectively (Table 13). Furthermore, ADI, OTC, CK, and AOA had ΔG binding energies of -7.5571, -7.1706, -7.6305, and -7.7443 kcal/mol, respectively (Table 13).

Table 13 S score and estimated ΔG value for binding (kcal/mol) between hydroquinine and ADI pathway-related proteins using MOE and SwissDock

Ligand	Targets	S score	Estimated ΔG value for binding (kcal/mol)
Hydroquinine	ADI	-5.8274	-7.5571
	OTC	-5.9134	-7.1706
	CK	-6.0185	-7.6305
	AOA	-6.5950	-7.7443

The molecular docking results from MOE software also demonstrated the possibility of an interaction between the ADI pathway-related target proteins and hydroquinine based on the predicted S score. The binding S scores were computed based on binding affinities with all possible binding geometries. For interpretation, the lower S score tend to established a stronger interaction with ligand (200). This study demonstrated that the S scores of ADI, OTC, CK, and AOA were -5.8274, -5.9134, -6.0185, and -6.5950, respectively. Interestingly, the observed trend in the S scores from MOE software was consistent with the predicted binding free energy (ΔG) from SwissDock.

It was notable that the S score and the binding free energy (ΔG) values of hydroquinine binding with AOA was the lowest value compared to that that of the target proteins (suggesting a more favourable interaction), potentially correlating with the prioritization of targets from the transcriptomic data.

Using UCSF-Chimera, the three-dimensional (3D) molecular interaction graphics showed the protein-ligand docking simulations with electrostatic interactions shown in red and blue (indicating negative and positive potential, respectively). The models shown suggest that hydroquinine potentially interacts with the binding pockets of all predicted target proteins: (A) arginine deiminase, (B) ornithine transcarbamylase, (C) carbamate kinase, and (D) arginine/ornithine antiporter (Figure 27). The 3D model representation of the hydroquinine ligand (cyan color) and the ribbon proteins (orange color) was visualized using UCSF-Chimera which shown in Figure 27.

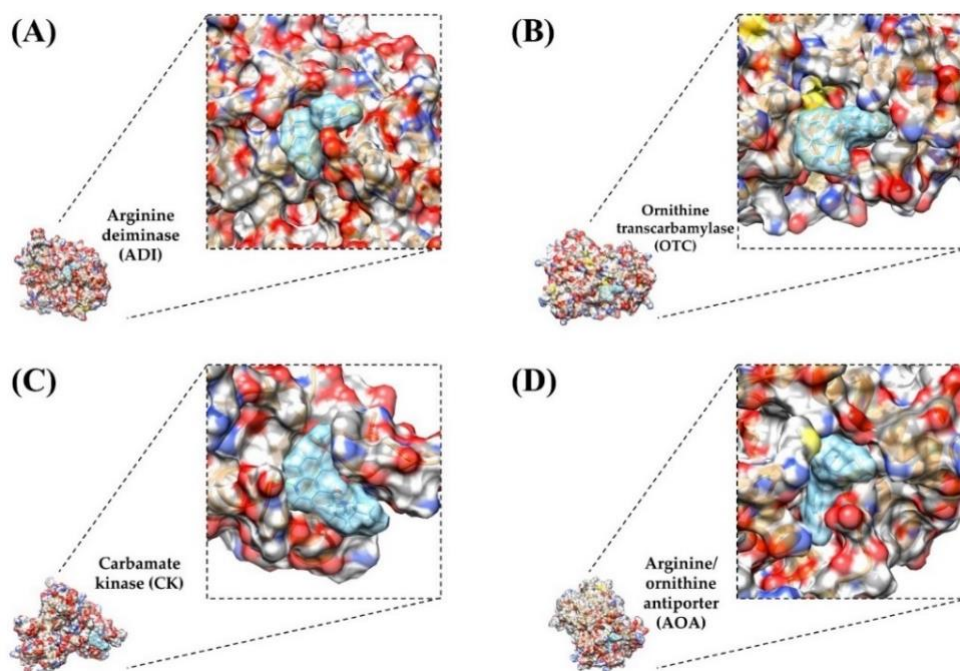


Figure 27 The 3D electrostatic mapping of molecular docked hydroquinine to the ADI pathway-related target proteins

To further study the interaction between ADI pathway-related target proteins and hydroquinine, molecular docking simulations using MOE software were performed. The two-dimensional (2D) view represented the main residues involved in the ligand-protein interaction of hydroquinine with the ADI pathway-related target proteins. Interestingly, the 2D ligand interaction diagrams demonstrated that the ADI preferred to interact with the quinoline ring of hydroquinine (Figure 28), whereas OTC, CK and AOA preferred to interact with nitrogen and hydrogen in quinuclidine ring ($\text{HC}(\text{C}_2\text{H}_4)_3\text{N}$), respectively (Figure 29–31).

2.1.1 Hydroquinine docked with the arginine deiminase (ADI) protein

The interaction mapping of molecular docked hydroquinine to ADI protein shown the total of 7 protein residues namely, Asp43, Arg274, Ala275, Met277, Gln354, Trp355, and Arg401, in proximity around the ligand. Interestingly, the arene-H interaction was detected at Ala275, as well as an arene-cation interaction with Arg401 also detected. The aromatic ring (quinoline ring) of hydroquinine interacted with hydrogen atom of alanine (R: $-\text{CH}_3$) and interacted with positive charge of arginine (R: $-(\text{CH}_2)_3\text{NH}-\text{C}(\text{NH})\text{NH}_2$). Moreover, the 2D ligand interaction diagrams demonstrated the highly ligand exposure around the specific side chain, especially the, R₂: $-\text{CH}_2-\text{CH}_3$, exocyclic unsaturated vinyl group ($-\text{CH}=\text{CH}_2$) at quinuclidine ring as well as the side chain, R₁ $-\text{OCH}_3$, at aromatic ring which shown in Figure 28.

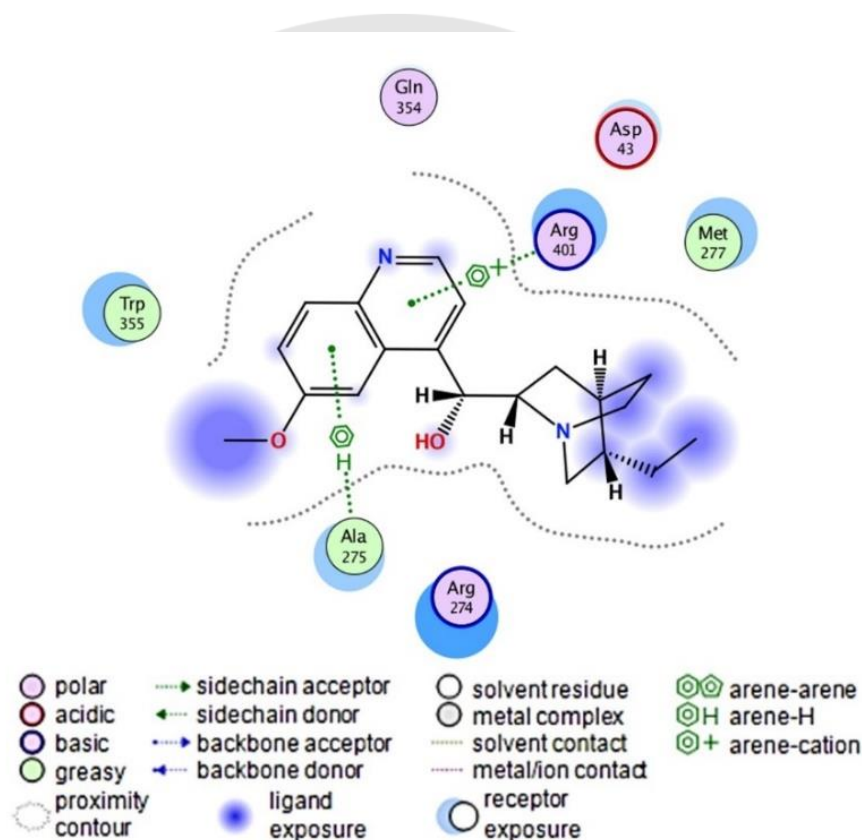


Figure 28 The 2D ligand interaction mapping of molecular docked hydroquinine to arginine deiminase (ADI)

2.1.2 Hydroquinine docked with the ornithine transcarbamylase (OTC) protein

The interaction mapping of molecular docked hydroquinine to OTC protein shown the highly magnitude of ligand exposure at alkaloid structure of hydroquinine. Moreover, the total of 12 protein residues were shown in proximity around the ligand. The 12 protein residues were Lys55, Asp132, Glu133, Arg166, Asn167, Asn168, Asn171, His195, Ser236, Met237, Gly238 and Glu239 (Figure 29). The 2D ligand interaction also demonstrated the highly ligand exposure at quinuclidine ring.

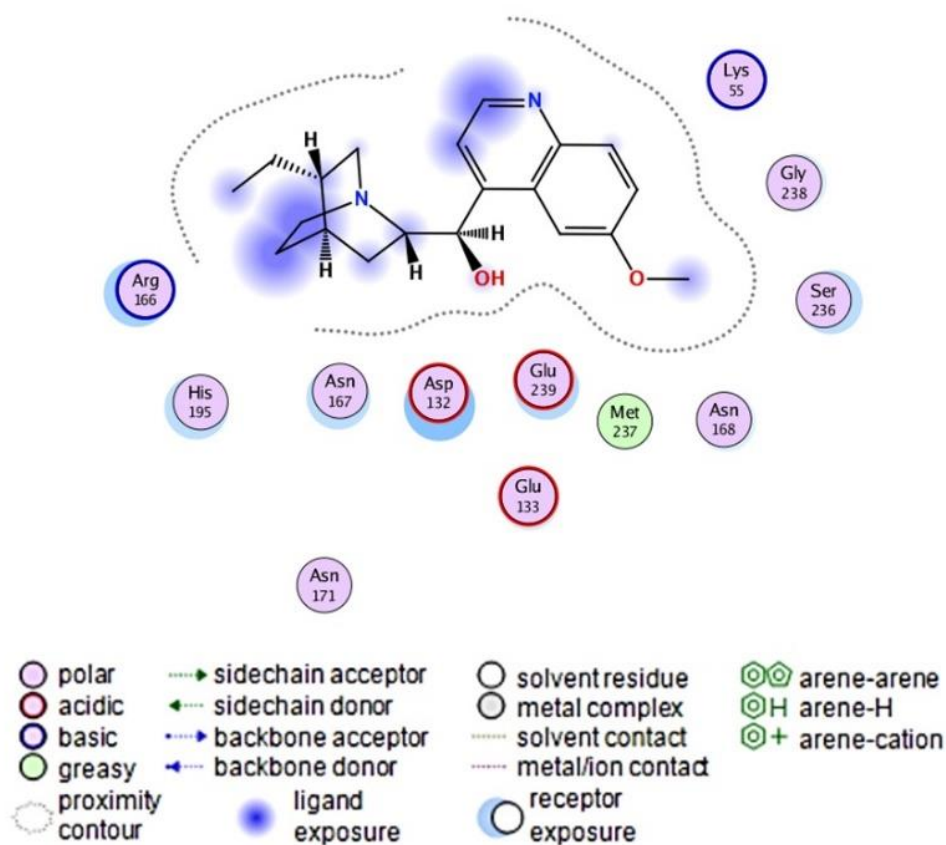


Figure 29 The 2D ligand interaction mapping of molecular docked hydroquinine to ornithine transcarbamylase (OTC)

2.1.3 Hydroquinine docked with the carbamate kinase (CK) protein

The interaction mapping of molecular docked hydroquinine to CK protein shown the total of 16 protein residues in proximity around the ligand. The protein residues namely, Gly9, Asn10, Leu13, Arg14, Arg15, Gly16, Gly49, Asn50, Gly51, Pro52, Lys122, Pro123, Arg152, Asp206, Lys207, and Gly260 were detected (Figure 30). Interestingly, the nitrogen (N) of hydroquinine at quinuclidine ring structure ($\text{HC}(\text{C}_2\text{H}_4)_3\text{N}$) shown hydrogen bond to side chains of carbamate kinase at Arg152. The arginine (R: $-(\text{CH}_2)_3\text{NH}-\text{C}(\text{NH}_2)=\text{NH}_2$) acted as the sidechain donor to hydroquinine.

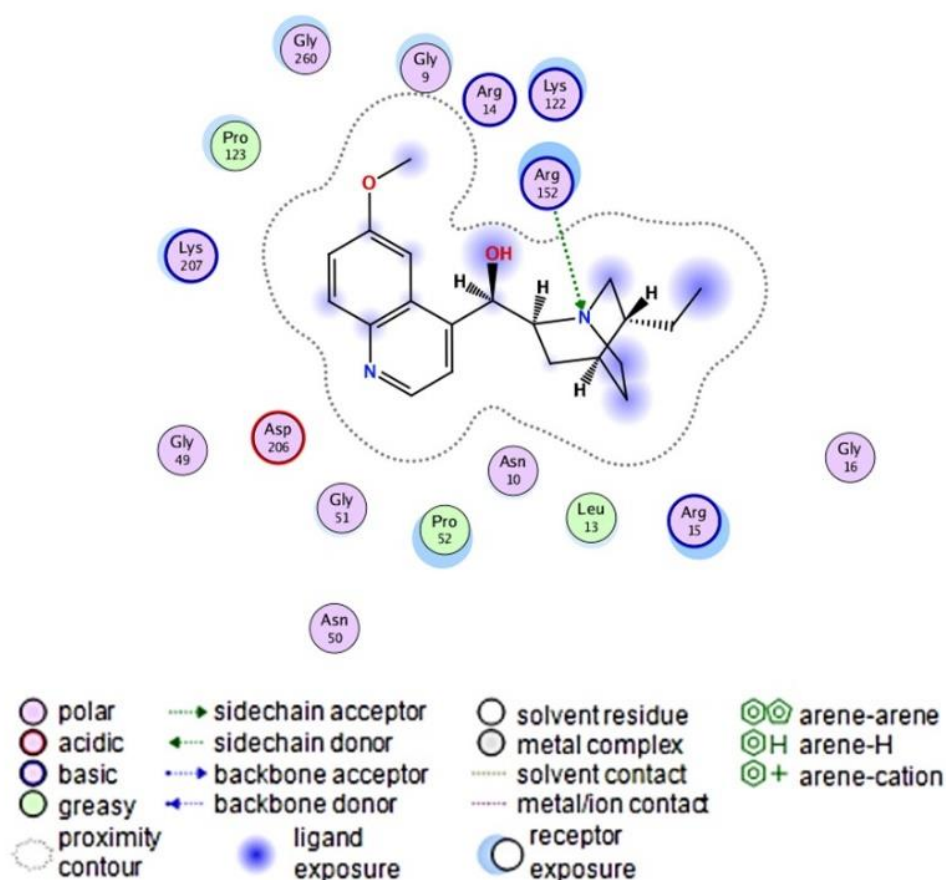


Figure 30 The 2D ligand interaction mapping of molecular docked hydroquinine to carbamate kinase (CK)

2.1.4 Hydroquinine docked with the arginine/ornithine antiporter (AOA) protein

Consistent with the predicted binding affinity, the 2D interaction shown the highest number of protein residues in proximity around the hydroquinine. The total of 18 protein residues of AOA were detected, namely, Leu17, Gly20, Ser21, Tyr95, Glu150, Asn155, Thr158, Thr159, Lys162, Gly214, Glu216, Gly217, Phe221, Gly296, Ala297, Ser300, Trp301, and Leu304. Furthermore, the arene-H interaction was detected at Trp301 (Figure 31). The aromatic of tryptophan at 301 shown interaction with hydrogen atom at the side chain of hydroquinine.

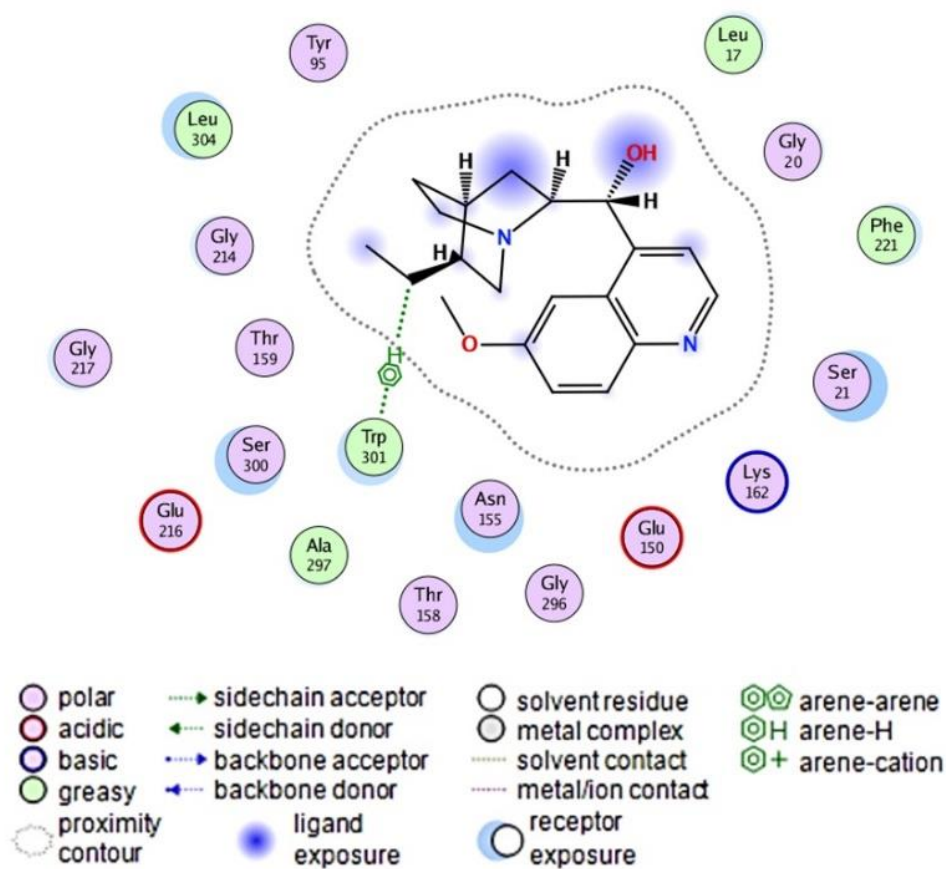


Figure 31 The 2D ligand interaction mapping of molecular docked hydroquinine to arginine/ornithine antiporter (AOA)

2.2 Testing the genes expression of *P. aeruginosa* strains

To validate the altered expression of the four *arc* genes in response to hydroquinine, the drug-sensitive (PA-27853) and clinical MDR (PA-S4, and PA-S5) *P. aeruginosa* strains were investigated further to represent reference and clinical isolates, respectively. Using quantitative reverse transcription polymerase chain reaction (RT-qPCR), the half MIC (1.25 mg/mL) of hydroquinine reduced *arcDABC* gene expression in PA-27853, PA-S4, and PA-S5 (Figure 32). Specifically, in PA-27853, the RT-qPCR results showed statistically significant decreases in the mRNA expression of the *arcA*, *arcB*, *arcC*, and *arcD* genes to 0.56 ± 0.20 , 0.37 ± 0.20 , 0.51 ± 0.07 , and 0.50 ± 0.21 -fold, respectively (Figure 32A). For the clinical MDR PA-S4 strain, the relative expression levels of the *arcA*, *arcB*, *arcC*, and *arcD* genes were downregulated to 0.02 ± 0.01 , 0.05 ± 0.01 , 0.53 ± 0.13 , and 0.17 ± 0.14 -fold, respectively (Figure 32B), whereas those in PA-S5 were statistically downregulated to 0.03 ± 0.02 , 0.40 ± 0.34 , 0.07 ± 0.06 , and 0.41 ± 0.31 -fold, respectively (Figure 32C). The Figure 32 demonstrates the relative expression levels of the ADI pathway-related genes which were treated with hydroquinine at 1.25 mg/mL for 1 h compared to the corresponding untreated controls. The asterisk *, **, *** and **** symbols were $p < 0.05$, $p < 0.01$, $p < 0.001$, and $p < 0.0001$, respectively. The data were presented as mean \pm SD.

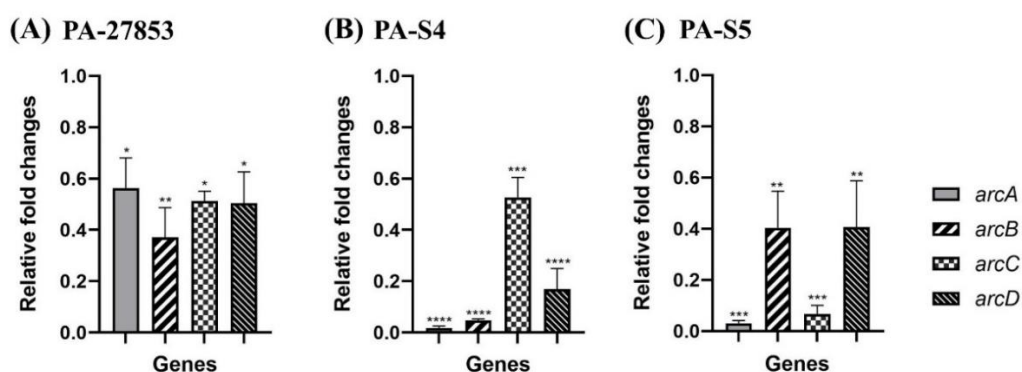


Figure 32 The relative expression levels of the ADI pathway-related genes were treated with hydroquinine at 1.25 mg/mL for 1 h using RT-qPCR.

Part 3: The application of hydroquinine as preventive contact lens solution

3.1 Testing the adhesion-related genes expression of *P. aeruginosa* strains

According to transcriptomic analysis result (10), comparable to other adhesion-related genes in this study, it was recognized that the *cgrC* gene (CupA gene regulator C) was the most downregulated by a -2.48 Log₂-fold change in response to hydroquinine (Table 14). Consistently, the differentially expressed genes (DEGs) of adhesion-related genes including *cheY* (two-component response regulator CheY), *cheZ* (chemotaxis protein CheZ), *fimU* (type 4 fimbrial biogenesis protein FimU), and *pilV* (type 4 fimbrial biogenesis protein PilV) were also depleted in response to hydroquinine, by -2.16, -2.46, -2.39, and -2.27 Log₂-fold changes, respectively (Table 14).

Table 14 DEGs of adhesion-related genes as determined by transcriptome analysis

Genes	Product name	Log ₂ FC*	FDR [#]	<i>p</i> -value
<i>cgrC</i>	CupA gene regulator C, CgrC	-2.48	1.57 x 10 ⁻²	5.00 x 10 ⁻⁴
<i>cheY</i>	Two-component response regulator CheY	-2.16	4.13 x 10 ⁻²	1.80 x 10 ⁻³
<i>cheZ</i>	Chemotaxis protein CheZ	-2.46	2.26 x 10 ⁻²	7.00 x 10 ⁻⁴
<i>fimU</i>	Type 4 fimbrial biogenesis protein FimU	-2.39	2.57 x 10 ⁻²	9.00 x 10 ⁻⁴
<i>pilV</i>	Type 4 fimbrial biogenesis protein PilV	-2.27	3.55 x 10 ⁻²	1.40 x 10 ⁻³

Note: *Log₂ FC was Log₂ relative fold changes of the gene expression levels in response to hydroquinine, compared to the untreated control. [#]FDR was false discovery rate showed statistical significances.

To validate the expression of the adhesion-related genes in response to hydroquinine, this study identified that hydroquinine at 1.25 mg/mL reduces expression of adhesion-related genes in *P. aeruginosa* ATCC 27853 (Figure 33). The RT-qPCR results showed statistically significant reduction in the mRNA expression of *cgrC*, *cheY*, *cheZ*, *fimU*, and *pilV* genes to 0.05 ± 0.02, 0.16 ± 0.04, 0.17 ± 0.06, 0.13 ± 0.10, and 0.18 ± 0.03 -fold, respectively compared to the corresponding untreated control which shown in Figure 33. The asterisk **** symbols were *p* < 0.0001. The triplicate data was presented as mean ± SD.

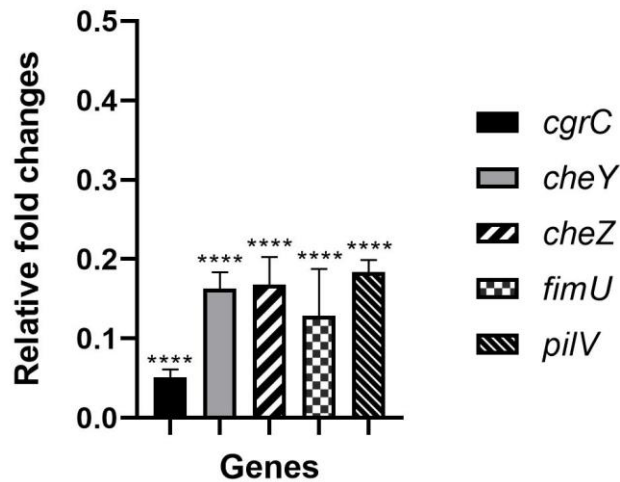


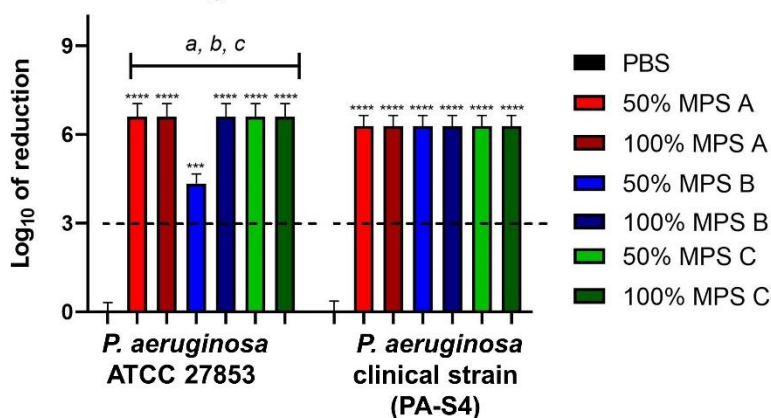
Figure 33 The relative expression levels of the adhesion-related genes treated with 1.25 mg/mL of hydroquinine for an hour in *P. aeruginosa* ATCC 27853 compared to the corresponding untreated control.

3.2 Anti-bacterial activity of multipurpose solutions

To investigate the disinfection efficacy of commercial MPSs, the solutions were determined by calculating the log reduction of bacterial growth. This study showed that all commercial solutions studied here met the ISO 14729 primary stand-alone criteria (3 log of reduction) for bacterial efficacy at both 6 and 24 h contact times against *P. aeruginosa* ATCC 27853 and clinical *P. aeruginosa* strains. Both MPS A and MPS C showed their similar disinfection efficacy at both 6 and 24 h.

Comparing the log reduction in *P. aeruginosa* strains after 6-h of disinfection time, the MPSs efficacies decreased in *P. aeruginosa* ATCC 27853. Specifically, 50% of MPS B significantly decreased in disinfection efficacy when compared to the original concentration. Moreover, 50% of MPS B had less efficacy compared to 50% of MPS A. However, there was no significant difference in comparing between MPS A and B in clinical *P. aeruginosa* strain (Figure 34A). On the other hand, the efficacies of MPS B were reduced in clinical *P. aeruginosa* strain at 24 h contact time. The MPS B efficacies dramatically reduced in both half and original concentration compared with the MPS A efficacies. Furthermore, it showed that 50% of MPS B statistically decreased in disinfection efficacy compared with its original concentration (Figure 34B).

(A) Stand alone testing at 6 hours



(B) Stand alone testing at 24 hours

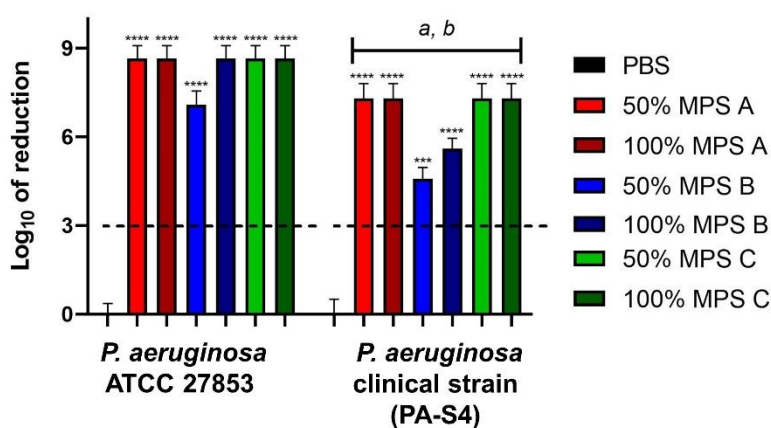


Figure 34 The log of reduction of the *P. aeruginosa* growth as a parameter of antibacterial efficacy of multipurpose solutions at (A) 6 h and (B) 24 h contact time compared to the corresponding untreated controls (PBS).

The data was presented as mean \pm SD. The dashed line represented the ISO 14729 criteria (3 log of reduction). The asterisk *** and **** symbols were $p < 0.001$, and $p < 0.0001$, respectively compared to PBS at the same time point and within the same strain. Statistical differences among tested solution families:
a: $p < 0.05$ for 50% MPS A vs. 50% MPS B within the same time and same strain,
b: $p < 0.05$ for 50% MPS B vs. 50% MPS C within the same time and same strain,
c: $p < 0.05$ for 50% MPS B vs. 100% MPS B within the same time and same strain.

3.3 Anti-adhesion efficacy of multipurpose solutions

To determine the anti-adhesion capacity of MPSs, the solutions challenged with *P. aeruginosa* strains and were then determined using crystal violet retention method. The percentage of residue biofilm quantification was calculated to the inhibition of adhesion as anti-adhesion efficacy (Table 15). The present study demonstrated that both MPSs had statistically strong anti-adhesion efficacy compared with the control ($p < 0.0001$). The percentages of anti-adhesion efficacy were between 89.76 and 91.89% in MPS A, 75.05 and 86.83% in MPS B, as well as 72.72 and 89.29% in MPS C, respectively. Interestingly, the MPS A in both 50% and 100% concentrations had more statistical anti-adhesion efficacy than MPS B and MPS C (Table 15). The 50% of MPS A had more efficacy than 50% of MPS B ($p < 0.0001$ in both strains). Moreover, the 50% of MPS A had more efficacy than 50% MPS C ($p < 0.0001$ in *P. aeruginosa* ATCC 27853). Consistent with the 100% original concentration, MPS A showed more adhesion inhibition than MPS B ($p < 0.0001$ in *P. aeruginosa* ATCC 27853 and at $p < 0.01$ in clinical *P. aeruginosa* strain) and MPS C ($p < 0.0001$ in *P. aeruginosa* ATCC 27853).

Furthermore, the disinfection efficacy of 50% of MPS B was significantly decreased when compared with 100% of MPS B ($p < 0.0001$) in both strains. The 50% of MPS C was also significantly decreased ($p < 0.05$) in *P. aeruginosa* ATCC 27853 when compared with its original concentration. Therefore, MPS A was further investigated at 50% and 100% original concentration combined with the hydroquinine solution in the same manner.

Table 15 Anti-adhesion efficacy of MPSs against *P. aeruginosa* strains

Test solutions	<i>P. aeruginosa</i> strains	
	PA-27853	PA-S4
PBS	00.00 ± 0.54	00.00 ± 0.63
50% MPS A	89.87 ± 0.03 ^{*, a, b}	89.76 ± 0.07 ^{*, a}
100% MPS A	91.89 ± 0.19 ^{*, c, d}	91.37 ± 0.08 ^{*, e}
50% MPS B	75.30 ± 1.36 ^{*, a, f}	75.05 ± 1.58 ^{*, a, f}
100% MPS B	83.54 ± 1.10 ^{*, c, f}	86.83 ± 0.90 ^{*, e, f}
50% MPS C	72.72 ± 3.18 ^{*, b, g}	77.81 ± 1.34 [*]
100% MPS C	86.90 ± 1.54 ^{*, d, g}	89.29 ± 0.50 [*]

Note: Statistical differences among tested solution families:

*: $p < 0.0001$ for each MPS vs. PBS within the same strain,

^a: $p < 0.0001$ for 50% MPS A vs. 50% MPS B within the same strain,

^b: $p < 0.0001$ for 50% MPS A vs. 50% MPS C within the same strain,

^c: $p < 0.0001$ for 100% MPS A vs. 100% MPS B within the same strain,

^d: $p < 0.0001$ for 100% MPS A vs. 100% MPS C within the same strain,

^e: $p < 0.01$ for 100% MPS A vs. 100% MPS B within the same strain,

^f: $p < 0.0001$ for 50% MPS B vs. 100% MPS B within the same strain, and

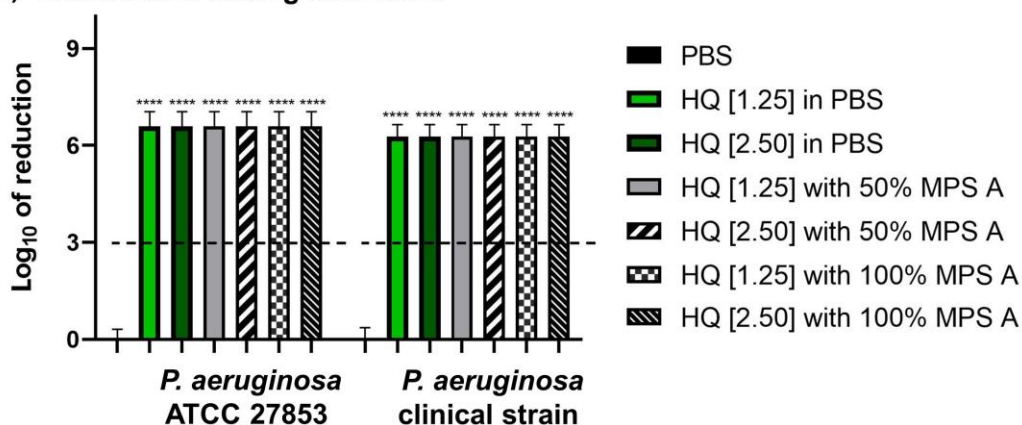
^g: $p < 0.05$ for 50% MPS C vs. 100% MPS C within the same strain,

3.4 Anti-bacterial activity of hydroquinine alone and in combination with MPSs

To investigate disinfection efficacy of the combination of hydroquinine with MPS A, hydroquinine solution at half-MIC and MIC (1.25 and 2.50 mg/mL) challenged *P. aeruginosa* strains for 6 and 24 h. The disinfection efficacy was determined by the calculation as the log reduction of bacterial growth.

The present study demonstrated the strong disinfection efficacy of the combination of MPS with hydroquinine. All tested solutions here met the ISO 14729 criteria. The result showed the log of reduction of bacterial growth at more than 6 log reduction (higher 99.9999 % killing) in both *P. aeruginosa* strains at 6 and 24 h contact times (Figure 35).

(A) Stand alone testing at 6 hours



(B) Stand alone testing at 24 hours

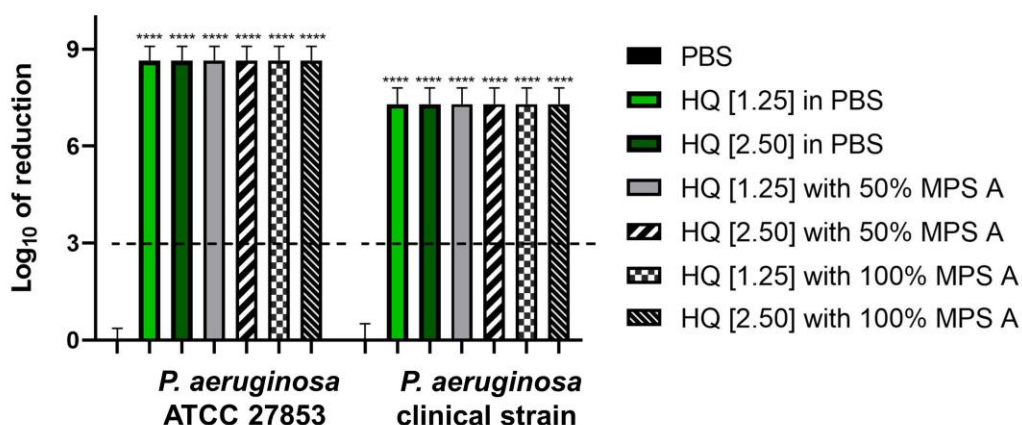


Figure 35 The log of reduction of the *P. aeruginosa* growth as a parameter of antibacterial efficacy of tested solutions at (A) 6 h and (B) 24 h contact time compared to the corresponding untreated controls (PBS).

The data was presented as mean \pm SD. The dashed line represented the ISO 14729 criteria (3 log of reduction). The asterisk **** symbol was $p < 0.0001$ compared to PBS at the same time point and within the same strain.

As the result mentioned above, even though the disinfection efficacies obviously differed from the untreated control (PBS), they did not differ among each tested solution. Therefore, the structure of *P. aeruginosa* strains using a field emission scanning electron microscope (FE-SEM) was also investigated. The structure of *P. aeruginosa* strain treated with 100% MPS A, hydroquinine at 2.50 mg/mL, and hydroquinine at 2.50 mg/mL with 100% MPS A are shown in Figure 4. The FE-SEM result demonstrated the dense clusters of viable cells when untreated with MPS and/or hydroquinine. The untreated bacterial structure still had intact structure such as a distinct border, a clear uniform (Figure 36A). However, *P. aeruginosa* was treated with MPS A and/or hydroquinine solutions, the number of bacterial cells was reduced (Figure 36B–D). The integrity of the cells was also affected by the combination of MPS and hydroquinine (Figure 36D).

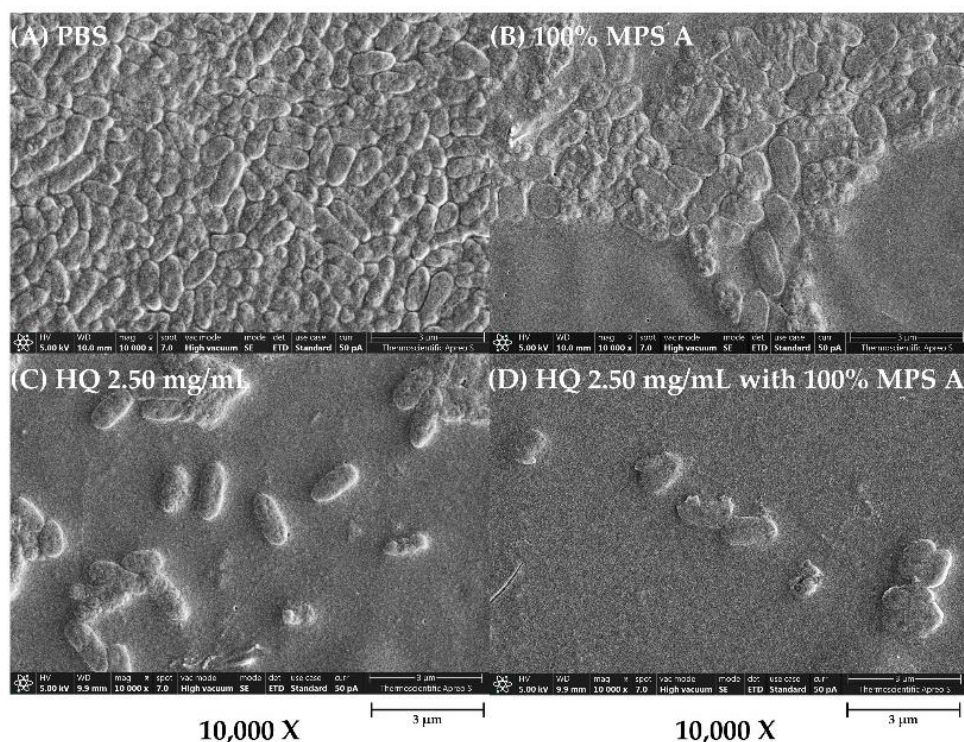


Figure 36 The structural characterization of *P. aeruginosa* ATCC 27853 as a representative strain in different tested solutions: (A) PBS, (B) 100% MPS A, (C) hydroquinine (HQ) 2.50 mg/mL, and (D) HQ 2.50 mg/mL with 100% MPS A.

The images were presented at magnification 10,000X using the FE-SEM.

3.5 Anti-adhesion efficacy of hydroquinine alone and in combination with MPSs

To investigate the combination of hydroquinine with MPS on anti-adhesion efficacy, the hydroquinine solutions challenged with both *P. aeruginosa* strains including *P. aeruginosa* ATCC 27853 and clinical *P. aeruginosa* strain at the same manner. The percentage of their anti-adhesion efficacy were shown in Table 16. Additionally, testing was conducted to determine the disinfection efficacy of hydroquinine alone and in combination on the surface of contact lenses (Figure 37).

Here, hydroquinine at 1.25 and 2.50 mg/mL had their effectiveness of anti-adhesion greater than 50% in both *P. aeruginosa* strains (between 54.84 and 59.56%). Interestingly, when using hydroquinine combined with MPS A, it significantly enhanced the anti-adhesion efficacy ($p < 0.0001$) compared with hydroquinine alone. The present study demonstrated that the percentages of anti-adhesion efficacy of the combination were between 95.59 and 97.91% in *P. aeruginosa* ATCC 27853 as well as between 92.23 and 93.64% in clinical *P. aeruginosa* strain (Table 16). Interestingly, the MPS A at half original concentration combined with hydroquinine was more anti-adhesion efficacy than original manufacturer's product (Table 15).

Table 16 Anti-adhesion efficacy of hydroquinine solutions and their combinations against *P. aeruginosa* strains

Test solutions	<i>P. aeruginosa</i> strains	
	PA-27853	PA-S4
PBS	00.00 ± 0.54	00.00 ± 0.63
HQ [1.25] in PBS	57.80 ± 0.41 ^{*,A}	54.84 ± 3.76 ^{*,C}
HQ [1.25] with 50% MPS A	95.59 ± 0.13 ^{*,a}	92.39 ± 0.55 ^{*,c}
HQ [1.25] with 100% MPS A	97.91 ± 0.21 ^{*,a}	93.64 ± 0.17 ^{*,c}
HQ [2.50] in PBS	59.56 ± 0.34 ^{*,B}	56.37 ± 1.27 ^{*,D}
HQ [2.50] with 50% MPS A	96.49 ± 0.22 ^{*,b}	92.23 ± 0.16 ^{*,d}
HQ [2.50] with 100% MPS A	97.16 ± 0.03 ^{*,b}	93.31 ± 0.20 ^{*,d}

Note: Statistical differences among tested solution families: * was $p < 0.0001$ for each tested solution vs. PBS within the same strain, ^{Aa}, ^{Bb}, ^{Cc}, and ^{Dd} were $p < 0.0001$ for comparing the hydroquinine alone (uppercases) with the combination (lowercases) at the same hydroquinine concentration and within the same strain.

3.6 Anti-adhesion efficacy on contact lens surface

To investigate whether MPS formulations containing hydroquinine exhibit disinfection efficacy on contact lens surfaces. All tested solutions reduced *P. aeruginosa* growth and adhesion on contact lens surfaces at disinfection time (6 hour) using ISO 18259 standard testing. The cell structure of *P. aeruginosa* ATCC 27853 strain was observed as a representative using the FE-SEM as shown in Figure 37. When untreated with hydroquinine, the microorganisms were tightly attached in packs on the contact lens surface. Furthermore, the untreated bacterial ordered and densely aggregated with cell-to-cell contact (Figure 37A). On the other hand, *P. aeruginosa* treated with 100% MPS A, hydroquinine alone or the combination showed a reduced number of cells and bacterial adhesion, as well as it was likely that the cellular arrangement was singly (Figure 37B–D). Moreover, the morphology of *P. aeruginosa* was changed such as losing cell membrane integrity (white arrow), showing an irregular shape, and reduced size.

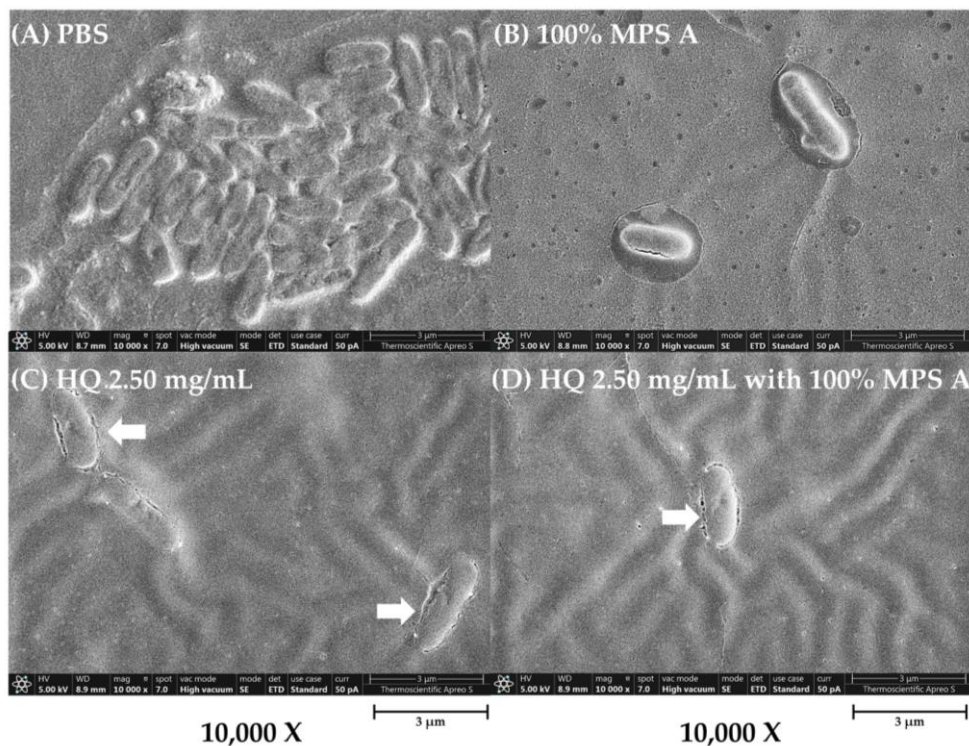


Figure 37 The adhesion of *P. aeruginosa* ATCC 27853 on contact lens surface as a representative strain in different tested solutions: (A) PBS, (B) 100% MPS A, (C) hydroquinine (HQ) 2.50 mg/mL, and (D) HQ 2.50 mg/mL with 100% MPS A.

The images were presented at magnification 10,000X using the FE-SEM. The white arrow represented the damaged cell membrane.

3.7 Destruction biofilm mass on contact lens surface

To determine the disinfection effectiveness of MPSs containing hydroquinine, testing was conducted to assess whether the combined solution could destroy biofilm mass on contact lenses. *P. aeruginosa* adhesion was simulated, allowing for biofilm formation over 24 h, and biofilm mass was then evaluated using FE-SEM.

When *P. aeruginosa* was untreated with tested solutions, the untreated microbial communities embedded in a 3D extracellular matrix (biofilm mass). The structure of *P. aeruginosa* biofilm mass was compact and packed cell-to-cell together (Figure 38B). On the other hand, 100% of MPS A destroyed a tiny quantity of biofilm mass (Figure 38C). Interestingly, either the combinations or hydroquinine solution demonstrated the extremely disinfection efficiency in removing biofilm mass from contact lens surface. For example, the biofilm mass was broken down and dispersed when treated with either hydroquinine alone or in combination with MPS A (Figure 38D–H).

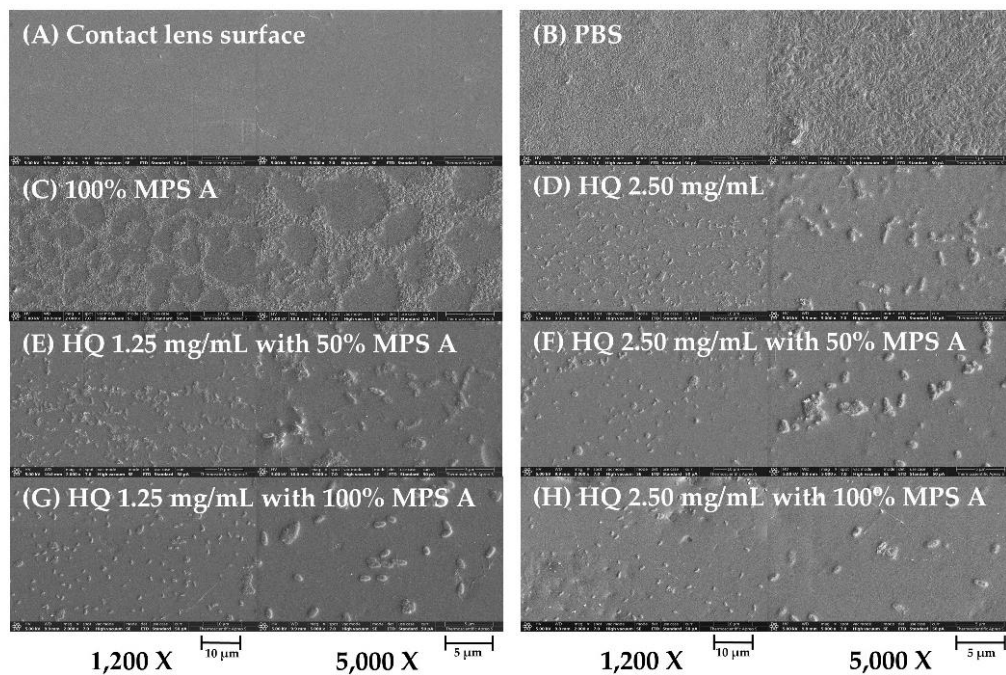


Figure 38 The biofilm mass of *P. aeruginosa* ATCC 27853 on contact lens surface as a representative strain in different tested solutions: **(A)** contact lens surface, **(B)** PBS, **(C)** 100% MPS A, **(D)** hydroquinine (HQ) 2.50 mg/mL, **(E)** HQ 1.25 mg/mL with 50% MPS A, **(F)** HQ 2.50 mg/mL with 50% MPS A, **(G)** HQ 1.25 mg/mL with 100% MPS A, and **(H)** HQ 2.50 mg/mL with 100% MPS A.

The images were presented at magnification 1,200X (left panels) and 5,000X (right panels) using the FE-SEM.

CHAPTER V

DISCUSSIONS AND CONCLUSIONS

Hydroquinine inhibits and kills MDR *P. aeruginosa* isolated from clinical samples

In the present study, strong evidence is presented showing that hydroquinine possesses bacteriostatic and bactericidal properties against clinical isolates of *P. aeruginosa* (Table 5). The isolates studied were obtained from different sources, including blood, pus, and sputum. These results are consistent with previous results showing killing efficacy of hydroquinine against *P. aeruginosa* reference strains (10). Hypothetically, clinical strains are expected to potentially adapt more readily to challenging conditions than reference strains because of virulence factors (e.g., adhesion, invasion, biofilm formation, etc.) (204). However, the presented research showed that hydroquinine inhibits all the clinical *P. aeruginosa* strains with a MIC of 2.50 mg/mL and kills the bacterium at an MBC of 5.00 mg/mL, including at least two MDR strains (Table 7). This is consistent with another previous study in which the same concentrations of hydroquinine inhibited bacterial growth and killing of a reference DS *P. aeruginosa* strain, ATCC 27853 (10). According to phenotypical antibiotic susceptibility profiles, only PA-S4 and PA-S5 strains are defined as clinical MDR pathogens due to showing resistance to more than three antimicrobial classes. Interestingly, these clinical MDR strains showed significant resistance to ceftazidime, with a high MIC (≥ 32 $\mu\text{g/mL}$). Moreover, PA-S5 was the only strain that resistant to imipenem and ciprofloxacin (Table 6). The MDR strains have many antibiotic resistance mechanisms, such as β -lactamase production, reduced outer membrane permeability, efflux pump overexpression, production of aminoglycoside-modifying enzymes, and target modification (205-207). These two MDR strains, therefore, were chosen to examine the combined activity of antibiotic alone and with hydroquinine. This study hypothesized that hydroquinine might show a synergistic effect with some anti-*P. aeruginosa* drugs against the tested MDR strains. The antibiotics namely, imipenem, ceftazidime, and ciprofloxacin, therefore, were selected to represent the antibiotic classes. In the combination treatments, hydroquinine had indifferent effects with imipenem and ciprofloxacin. However, when using imipenem or ciprofloxacin combined with hydroquinine, the MIC values of antibiotic decreased. Interestingly, this study demonstrated that hydroquinine had notable partial synergistic effects with ceftazidime against clinical MDR *P. aeruginosa* strains (Table 8). Ceftazidime, a third-generation cephalosporin, is one of the β -lactam antimicrobials that targets cell wall synthesis leading to bacterial cell death (208, 209). Hydroquinine may enhance the efficacy of ceftazidime by a yet unknown mechanism. Therefore, the mechanism of hydroquinine was investigated in the next investigation.

This is the first evidence report the antibacterial activity of hydroquinine in clinical strains. Moreover, this study discovered that hydroquinine could potentiate the activity of current anti-pseudomonal drugs against clinical *P. aeruginosa* strains including a MDR strain. However, this study has some limitations. The first limitation is the small number of clinical *P. aeruginosa* strains. This study investigates eight clinical strains. Moreover, there has only two MDR strains, therefore, the greater

sample sizes in MDR *P. aeruginosa* strains should be performed in the further investigation to ensure the anti-*P. aeruginosa* activity of hydroquinine. The second limitation is the small number of antibiotics. The synergistic activity was performed only three drugs, namely, imipenem, ceftazidime, and ciprofloxacin. For further investigation, it should identify whether hydroquinine could be used to enhance the effectiveness of other antibiotics. The larger hydroquinine and antibiotic combination screening should be performed seeking the most effective treatment against *P. aeruginosa*. Additionally, it is also suggested that the antimicrobial activity of hydroquinine against other clinical pathogenic microorganisms should be investigated such as *S. aureus* and *E. coli*.



Hydroquinine inhibits *P. aeruginosa* growth through decreased expression of ADI pathway-related genes

Previously work by Rattanachak *et al.* showed there were several changes in the transcriptomes of *P. aeruginosa* ATCC 27853 when treated with a hydroquinine concentration of 1.25 mg/mL for 1 h. Previously work revealed 157 upregulated and 97 downregulated genes in response to the treatment (173). Several differentially regulated genes have already been investigated relating to virulence factors, such as quorum sensing and flagella assembly. In this study, all the 254 DEGs were reassessed, and the top 15 significantly up- and downregulated genes were presented in the gene expression heatmap (Figure 26). Interestingly, four out of the fifteen most downregulated genes were integral to the ADI pathway namely, *arcA* (arginine deiminase; ADI), *arcB* (ornithine transcarbamylase; OTC), *arcC* (carbamate kinase; CK), and *arcD* (arginine/ornithine antiporter; AOA) genes (Table 11). This study therefore hypothesized whether the 1.25 mg/mL of hydroquinine treatment is sufficient to reduce the ADI pathway-related gene expression in *P. aeruginosa* strains.

To further validate these findings, the potential targeting of ADI pathway proteins by hydroquinine focused on molecular docking simulation was performed. The molecular docking results are mainly estimated by the minimum binding free energy (ΔG) between the ligand and the target (196, 210). Using MOE software and SwissDock web server, molecular docking results demonstrated the possibility of an interaction between the ADI pathway-related target proteins, including ADI, OTC, CK, and AOA. The 3D molecular interaction graphics showed that hydroquinine potentially interacts with the binding pockets of all target proteins (Figure 27). Furthermore, the 2D ligand interaction diagrams demonstrated that hydroquinine possibly interact with each ADI pathway-related proteins at quinoline ring and quinuclidine ring of hydroquinine (Figure 28–31). In this study, the researcher hypothesized that the structure of hydroquinine, cinchona alkaloid, especially, hydrogen and nitrogen in quinuclidine ring might be the considerable position which interacted with the target protein's structure. Interestingly, the S score and the ΔG values of hydroquinine binding with AOA protein was the lowest value compared to other target proteins which potentially correlating with the previous transcriptomic data (173).

Further investigation into the mRNA expression levels of all four genes were quantified using RT-qPCR. Following sub-MIC hydroquinine treatment, the expression levels of *arcA*, *arcB*, *arcC*, and *arcD* genes were significantly decreased. It also appears that the *arc* gene expression levels in clinical MDR *P. aeruginosa* isolates are affected to a greater extent than those in *P. aeruginosa* ATCC 27853. Interestingly, the mRNA levels of *arcA* in clinical MDR strains, PA-S4 and PA-S5, had the greatest downregulation of gene expression when compared with other genes (Figure 32).

Among the four *arc* genes, the *arcD* gene encodes a key membrane-bound transporter, the arginine/ornithine antiporter (AOA), which exchanges one molecule of L-arginine with one molecule of L-ornithine. In contrast, the *arcA*, *arcB*, and *arcC* genes encode the three important enzymes (namely, arginine deiminase (ADI), ornithine transcarbamylase (OTC), and carbamate kinase (CK), respectively) (Figure 39) (29-32).

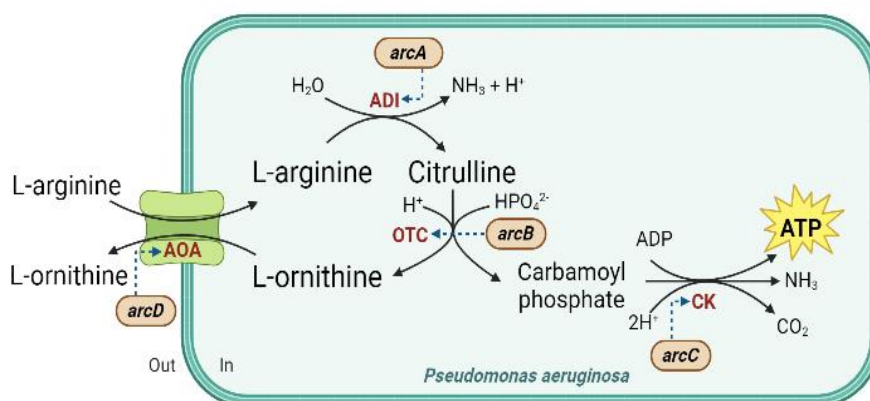


Figure 39 The schematic of the arginine deiminase (ADI) pathway.

The ADI pathway is conserved in a variety of bacteria, including *P. aeruginosa*. It produces one ATP mole from every mole of L-arginine consumed through three metabolic conversion steps (Figure 39). Firstly, L-arginine is catalyzed by ADI and converted into L-citrulline and ammonia. Secondly, the carbamoyl part of L-citrulline is then converted by OTC, resulting in L-ornithine and carbamoyl phosphate. The cluster of carbamoyl phosphate, which is a major metabolite in the ADI crossroad for both L-arginine catabolism and anabolism, is required for the initial step of pyrimidine biosynthesis (33). Subsequently, the phosphate moiety of carbamoyl phosphate is transferred to adenosine diphosphate (ADP) by the CK, yielding ATP, ammonia, and CO₂ (29-32). Overall, the ADI pathway allows the bacterial cells to sustain ATP production in the oxygen-dependent respiratory chain from carbamoyl phosphate (34) and produce ATP in anoxic environments (32, 35).

According to the RT-qPCR results in this study, hydroquinone reduced the expression levels of the *arc* genes in the *P. aeruginosa* strains of both DS and MDR (Figure 32). Interestingly, the ADI pathway may be one of the potential mechanisms by which hydroquinone inhibits *P. aeruginosa* growth. Here, this study proposed that hydroquinone may directly bind one of the proteins, AOA, while the expression levels of other proteins in the ADI pathway are also decreased. Validation of the downregulation of genes by RT-qPCR reveals that *arcA* expression is reduced to the greatest extent, particularly the MDR *P. aeruginosa* strain. The effect of inhibiting ADI pathway activity would suppress the subsequent generation of ATP via L-citrulline and carbamoyl phosphate metabolism. ATP production in *P. aeruginosa* is required for cell division and bacterial growth (211). The researcher hypothesized that hydroquinone may disturb metabolic energy generation by interrupting ATP production, which consequently reduces bacterial cell growth. Evidence for this is provided by Sandra *et al.* who showed that arginine fermentation provide sufficient energy for the growth of meat-spoiling *Pseudomonas* strains (35). Furthermore, ATP through the ADI pathway is required to maintain the membrane potential as well as to promote the motility of *P. aeruginosa* (212, 213). The ADI pathway normally supports protection from acidic stresses through intracellular ammonia production and from being involved in the microbial pathogenicity (28, 214). As a result, it is possible that hydroquinone may not only disturb the energy production effect but also affect ammonia generation via the ADI pathway. When ammonia production is

decreased, *P. aeruginosa* would be unable to tolerate this with acid stress and pH homeostasis, which is critical for survival in acidic conditions. It has been shown that intracellular acidification may affect bacterial growth and cell viability (28).

As mentioned previously, molecular docking simulations demonstrated the strongest potential binding energy of hydroquinine with AOA. Furthermore, it is consistent with the transcriptomic results that *arcD* transcripts were downregulated most by hydroquinine. Therefore, it is suggested that hydroquinine is most likely to interfere with AOA, resulting in the repression of other downstream proteins in the ADI pathway. Hypothetically, when AOA is affected by hydroquinine, L-arginine intake would likely also be reduced. In general, L-arginine in *P. aeruginosa* is an essential molecule in the regulation of biofilm formation (215). This supports the previous findings by Rattanachak *et al.* (173) that hydroquinine could suppress QS-related gene expression, reduce virulence factor production, and impair biofilm formation in *P. aeruginosa* (173). For another possible reason, hydroquinine may affect the production of carbamoyl phosphate, which is required for pyrimidine production (33). Theoretically, pyrimidine biosynthesis provides thymine, uracil, and cytosine nucleotides, which play a crucial role in DNA and RNA replication (216). Therefore, hydroquinine might have other specific mechanisms, like certain antibiotics, as a DNA synthesis inhibitor. This is supported by the structural evidence of a cinchona alkaloid (e.g., quinine, which has a DNA-binding capacity) possibly inhibiting the transcription and translation processes (217). So, hydroquinine might have a synergistic effect with other antibiotics via the inhibitions of the ADI pathway and DNA synthesis, as well as their own mechanisms of anti-pseudomonal drugs.

The present study is the first report that the ADI pathway could be a key target for hydroquinine and can be considered a target for anti-bacterial compounds capable of drug-resistant *P. aeruginosa*. Moreover, the ADI pathway plays an important role in the antibacterial mechanism of hydroquinine against the MDR *P. aeruginosa* strain.

There are some limitations that need to be addressed. Although, this study demonstrated that hydroquinine directly affected the ADI pathway in *P. aeruginosa*. However, this study only investigated in two MDR *P. aeruginosa* strains (PA-S4 and PA-S5). Therefore, a study with small sample size may not have the power to show the hydroquinine properties. The larger sample sizes are required in the further investigation. Moreover, although the molecular docking predicts the possible target sites of hydroquinine in individual genes, this study focuses on only the ADI pathway-related gene expression levels. Therefore, the protein expression level should be considered such as using western blotting method. For future investigations, the protein expression level might be performed using the PCR-based method such as site-directed mutagenesis and using the sodium dodecyl-sulfate polyacrylamide gel electrophoresis (SDS-PAGE) method to find out the exact target protein. Moreover, the reason why hydroquinine attenuates *arc* gene expression in MDR *P. aeruginosa* strains are still unknown. Understanding the role of the ADI pathway in bacterial growth may aid the development of novel antibacterial agents that might be effective in combating drug-resistant bacteria. For example, using hydroquinine as the ADI pathway inhibitor for targeting MDR *P. aeruginosa*. Further work will seek to determine the exact molecular target and exact mechanism of hydroquinine activity.

Hydroquinine enhances the effectiveness of contact lens solutions for inhibiting *Pseudomonas aeruginosa* adhesion and biofilm formation

In this study, hydroquinine had been shown to be effective in killing both clinical DS and MDR *P. aeruginosa* strains. Furthermore, hydroquinine attenuates *P. aeruginosa* growth by reducing flagella activity, pyocyanin production, and biofilm formation (173). In this study, it was hypothesised that hydroquinine might be efficacious in minimising bacterial adherence to contact lens surface and bacterial colonisation. *P. aeruginosa* is the most common pathogen which causes contact-lens-related microbial keratitis (CLMK) (1, 2, 105). Motility of *P. aeruginosa* is driven by two types of appendages which comprise a single polar flagella and multiple type IV pili. The flagellum operates as a rotor and generates forward movement via hydrodynamic force (139-141). In contrast, the type IV fimbriae or pili operate as linear actuators that pull the bacterium along a surface (139-141). For *P. aeruginosa*, the type IV pili are pilin-containing filaments on the surfaces that are associated with adhesion, motility, microcolony formation and secretion of proteases and colonization factors (141).

This study present evidence that hydroquinine downregulates genes involved in *P. aeruginosa* adhesion ability. Using RT-qPCR, the mRNA expression levels of *cgrC*, *cheY*, *cheZ*, *fimU*, and *pilV* genes were significantly decreased in response to hydroquinine treatment (Figure 33). Interestingly, expression of the *cgrC* gene was especially downregulated (relative expression levels of 0.05 ± 0.02 -fold). The *cgrC* gene encodes the *cupA* gene regulator C (CgrC) which controls the phase-variable expression of the *cupA* gene (218, 219). The *cup* gene cluster (chaperone-usheer pathway), in particular, *cupA*, encodes the components of *P. aeruginosa* assembly factors of the fimbrial structure (220, 221). These factors facilitate surface attachment, motility, and enable to form biofilm mass on abiotic surfaces (220, 221). Triggering *cgr* gene transcription results in activation of *cupA* gene expression (219). Therefore, the repression of *cgrC* gene by hydroquinine likely affects *cupA* gene expression, leading to the disruption of the fimbrial adhesins components in *P. aeruginosa*. Consistent with *cgrC*, the other genes including *cheY*, *cheZ*, *fimU*, and *pilV* were also significantly downregulated with hydroquinine treatment which may also have impacted bacterial motilities and their adhesion process. For example, the *cheY* and *cheZ* are related to chemotaxis (222). The *cheY* encodes two-component response regulator CheY, while the *cheZ* gene encodes chemotaxis protein CheZ. Chemotaxis is the directed movement in response to changes in the chemical environment. Bacteria can respond to the chemical gradients using chemosensory system coupled with flagella, fimbriae, or pili (223). The CheY and CheZ play a role in producing and transmitting the signals to flagellar motors, subsequently affecting the bacterial motility (222). For another example, the *fimU* and *pilV* encode type IV fimbrial biogenesis proteins, FimU and PilV, respectively (224, 225). The FimU and PilV are proteins which play an important role in biogenesis of type IV fimbrial proteins (224). The PilV possesses prepilin-like leader sequences (226). The FimU is required for both cleavage of the prepilin-like leader sequences and subsequent methylation of the mature protein in the biogenesis and function of type IV fimbriae in *P. aeruginosa* (226-228). These findings are the first evidence suggesting that hydroquinine inhibits the *P. aeruginosa* chemotaxis pathways by downregulating the expression levels of *cheY* and *cheZ* genes. Furthermore, hydroquinine also reduces the biogenesis of

bacterial surface organelles especially type IV fimbria by downregulating the expression levels of *fimU* and *pilV* genes. The reducing of surface organelles likely affecting bacterial microcolony formation and colony expansion (141). This is supported by previous research showing that deleting the appendage leads to deficiencies in cell attachment and growth (139). Several studies reported that both flagella and type IV pili influence the initial stages of biofilm formation in during bacterial transition from a free-swimming planktonic state to a surface-associated state, and subsequently microcolony formation (139, 229, 230). Additionally, the bacterial appendages facilitate its binding to various surfaces and twitching motility on surfaces (220, 224, 231). Therefore, hydroquinine might affect the *P. aeruginosa* motility through these adhesion-related genes. This is consistent with the previous study that hydroquinine had strong anti-motility effects in *P. aeruginosa*, affecting both swimming and swarming abilities (173).

According to its anti-bacterial efficacy, therefore, hydroquinine might show disinfection efficacy on contact lenses when included as part of commercial MPSs. To validate the hypothesis, the disinfection efficiency of all tested solutions via anti-bacterial activity, anti-adhesion efficacy, and anti-biofilm mass on contact lens were performed. In the present study, the researcher observed the efficacy of Opti-free® Replenish® solution (MPS A), Q-eye multipurpose solution (MPS B), and ReNu® solution (MPS C) which are available for sale in Thailand (Table 4). The MPSs and hydroquinine were tested with reference DS *P. aeruginosa* ATCC 27853 strain (PA-27853) and clinical MDR *P. aeruginosa* strain which isolated from pus obtained from eye infected patients (PA-S4).

It was discovered that these MPSs had the anti-bacterial capacity against the growth of both representatives from reference and clinical *P. aeruginosa* strains (PA-27853 and PA-S4, respectively) according to ISO 14729 criteria. Comparing MPSs, hydroquinine and its combination also reduced the growth of *P. aeruginosa* strains with similarity in reduction rates at more than 3 log of reduction (Figure 34–35). This is the first report that hydroquinine was as effective as commercially available MPSs. Therefore, hydroquinine might be used as a disinfecting contact lens solution like MPSs for inhibiting bacterial growth. Moreover, all MPSs also reduced the bacterial adhesion on contact lens surfaces (Table 15). It is interesting to note that MPS A displayed greater disinfection efficacy than others. Comparing the disinfectant agents, MPS A and MPS C composes of two biocides whereas MPS B contain only one. MPS A contain 0.001% polyquaternium-1 (PQ-1, as the predominant anti-bacterial agent, and 0.0005% myristamidopropyl dimethylamine (MAPD, as a broad spectrum antimicrobial agent (168)). MPS B contains only 0.0001% polyhexamethylene biguanide (PHMB, as the anti-bacterial agent (232)). MPS C contain 0.00015% PQ-1 and 0.0002% Alexidine dihydrochloride (AXD, as an antifungal agent (233)). PQ-1 and PHMB are agents in the family of quaternary ammonium compounds (QACs) (232). The QACs interact with bacterial outer membrane and then induce cytoplasmic membrane damage, resulting in loss of membrane integrity, intracellular component leakage, and cell lysis (168, 169). However, MPS A contains more ingredients e.g., MAPD, the dual biocides may be a reason why MPS A has more antimicrobial activity than others which is consistent with De Azevedo Magalhaes *et al.* (234). The higher concentrations of the QACs in MPS A may also explain the increased disinfection efficacy.

Interestingly, at half of their original concentration, the MPSs were still able to inhibit growth and reduce the adhesion. Previous research reported that the manufacturer's solutions at their original concentration (100%) containing biocides may cause some ocular adverse effects (170). To minimize the risk of ocular complications, it was hypothesized that half the original concentration of MPS A should have enough disinfection efficacy when combined with or without the hydroquinine on contact lenses. This study demonstrated that hydroquinine with commercial MPS showed the synergistic effects, reducing *P. aeruginosa* adhesion on contact lens surfaces (Table 16, Figure 37) and limiting biofilm formation (Figure 38). This study suggested that hydroquinine suppresses *P. aeruginosa* fimbrial activity by impairing surface attachment and interrupt their chemotaxis, resulting in prevention of biofilm formation. The hypothesis is supported by this previous study showing that hydroquinine could suppress L-arginine via the ADI pathway, resulting in decreased biofilm formation. This is also consistent with a previous study by Rattanachak *et al.* showing that hydroquinine could suppress QS-related gene expression, reduce virulence factor production, and impair biofilm formation in *P. aeruginosa* (173). Although, previous *in vitro* study demonstrated that commercially available disinfecting solutions were not effective against biofilms (117, 118), this study demonstrated that biofilm mass can be efficiently eradicated by either hydroquinone alone or in combination with commercial MPSs. The results indicate that the combinations were effective in inhibiting the formation of biofilm on the external surface of the contact lens.

The present study is the first strong evidence that the effectiveness of MPS combined with hydroquinine can inhibit *P. aeruginosa* adhesion and prevent biofilm formation on contact lens surfaces. Therefore, the researcher suggests that soaking contact lens in MPS containing with hydroquinine is possibly helpful in decreasing bacterial adhesion, preventing biofilm formation, and removing the existing biofilm mass. Further testing may be necessary to assess the safety of MPS formulations containing hydroquinine, thereby minimizing the risk of adverse ocular effects. Nevertheless, hydroquinine exhibits potential for use as part of a disinfectant to prevent bacterial growth on contact lenses. This potential development could contribute to the creation of new disinfectants from natural products, effectively combating *P. aeruginosa* infections and reducing the CLMK incidence.

There is limited available evidence regarding the disinfection efficacy of various contact lens types and materials. This study employed only polycarbonate materials. Additionally, this study focused on only *P. aeruginosa*. For further its application as preventive contact lens solution, the disinfection efficacy of hydroquinine with several different contact lens types is required. Moreover, the antimicrobial activity of hydroquinine against other CLMK related microorganisms such as *Acanthamoeba* spp. and *Staphylococcus* spp. should be performed. Additional environment conditions may be included in the future work, for example, an *in vitro* model under consumer-use conditions to closely mimic the real situation. In addition, the safety assessment of hydroquinine is now challenging. An *in vitro* cytotoxicity of hydroquinine in human cells and an *in vivo* in animal models should be investigated in the future to provide the useful data before moving forward to clinical trials.


From this study, the potential of hydroquinine to reduce the growth of clinical *P. aeruginosa* strains was performed and the potential molecular targets of hydroquinine were investigated. This study present new findings that hydroquinine has potential antibacterial properties against both clinically DS and MDR *P. aeruginosa* isolates. Using molecular docking and RT-qPCR, downregulation of the arginine deiminase (ADI) pathway is predicted to be the mode of action of hydroquinine against drug-resistant *P. aeruginosa*. Furthermore, the potential of disinfection efficacy of hydroquinine and its application were investigated in this study. Hydroquinine directly affected the expression levels of adhesion-related genes. The effectiveness of MPS combined with hydroquinine was effective at inhibiting *P. aeruginosa* adhesion and destroying biofilms. This study presented new findings that hydroquinine had potential as a part of contact lens disinfecting solution for adhesion inhibition and biofilm destruction which contribute to the development of new disinfectant that is effective in combating microorganisms, especially *P. aeruginosa*.

In conclusion, this research demonstrated the anti-bacterial properties of hydroquinine for combating with *P. aeruginosa*. Additionally, the findings of study may be used to explore a novel bioactive compound for developing alternative drugs against antibiotic resistant bacteria in the future. Further work will seek to determine hydroquinine safety profiles.

ABBREVIATION LIST

Abbreviation	Meaning
°C	Degree Celsius
µg	Microgram
µg/mL	Microgram per milliliter
µL	Microliter
µM	Micromolar
ADI	Arginine deiminase
ADP	Adenosine diphosphate
Ala	Alanine
AOA	Arginine/ornithine antiporter
Arg	Arginine
AST	Antibiotic susceptibility testing
ATCC	American Type Culture Collection
ATP	Adenosine triphosphate
AXD	Alexidine dihydrochloride
β	Beta
BLAST	Basic Local Alignment Search Tool
BSC	Biosafety cabinet
CDC	Centers for Disease Control and Prevention
cDNA	Complementary DNA
CFU/mL	Colony-forming units per milliliter
CIP	Ciprofloxacin
CK	Carbamate kinase
CLMK	Contact-lens-related microbial keratitis
CLSI	Clinical and Laboratory Standards
Comb	Combination
CO ₂	Carbon dioxide
Ct	Cycle threshold
CV	Crystal violet
DAVID	Database for Annotation, Visualization, and Integrated Discovery
DEGs	Differentially expressed genes
DMSO	Dimethyl sulfoxide
DNA	Deoxyribonucleic acid
DS	Drug-sensitive
eDNA	Extracellular DNA
eNEEs	Ethanollic nest entrance extracts
EPS	Extracellular polymeric substances
ERK	Extracellular signal-regulated kinase
FC	Fold change

FDR	False discovery rate
FE-SEM	Field emission scanning electron microscope
FF	Full Fitness
FICI	Fractional Inhibitory Concentration (FIC) Index
FPKM	Fragments per kilobase of transcript per million
GO	Gene ontology
h	Hour, hours
HQ	Hydroquinine
IL-1 β	Interleukin-1 beta
IM	Imipenem
ISO	International Organization for Standardization
kb	Kilobase
kDa	Kilo Dalton
KEGG	Kyoto Encyclopedia of Genes and Genomes
LB	Luria Bertani
log	Logarithm
LPS	Lipopolysaccharide
M	Molar (mol/L)
MAPD	Myristamidopropyl dimethylamine
MBC	Minimum bactericidal concentration
MDR	Multidrug-resistant
mg	Milligram
mg/mL	Milligram per milliliter
MHA	Mueller Hinton agar
MHB	Mueller Hinton broth
MIC	Minimum inhibitory concentration
min	Minute
ml	Milliliter
MOE	Molecular Operating Environment
MPS	Multipurpose solution
NADH	Reduced nicotinamide adenine dinucleotide
NCBI	National Center for Biotechnology Information
ng	Nanogram
nm	Nanometer
nM	Nanomolar
NNIS	National Nosocomial Infections Surveillance
NSS	Normal saline solution
OTC	Ornithine transcarbamylase
PA	<i>Pseudomonas aeruginosa</i>
PBS	Phosphate buffer saline
PDB	Protein databank
pH	Positive potential of the Hydrogen ions
PHMB	Polyhexamethylene biguanide
PQ-1	Polyquaternium-1



QACs	Quaternary ammonium compounds
QC	Quality control
QS	Quorum sensing
RCSB	Research Collaboratory for Structural Bioinformatics
Ref	Reference
RNA	Ribonucleic acid
RND	Resistance nodulation division
rpm	Revolutions per minute
RT-qPCR	Quantitative reverse transcription polymerase chain reaction
s	Second
T _a	Annealing temperature
TLR	Toll-like receptor
T _m	Melting temperature
TNF- α	Tumor necrosis factor-alpha
TSA	Tryptone Soya agar
TSB	Tryptone Soya broth
T3SS	Type 3 secretion system
T4P	Type IV pilus
UCSF	University of California San Francisco
UTI	Urinary tract infections
vs	Versus
v/v	Volume per volume
w/v	Weight per volume
2D	Two-dimension
3D	Three-dimension



REFERENCES

1. Stapleton F, Carnt N. Contact lens-related microbial keratitis: how have epidemiology and genetics helped us with pathogenesis and prophylaxis. *Eye (Lond)*. 2012;26(2):185-93.
2. Cohen EJ, Laibson PR, Arentsen JJ, Clemons CS. Corneal ulcers associated with cosmetic extended wear soft contact lenses. *Ophthalmology*. 1987;94(2):109-14.
3. Gonelimali FD, Lin J, Miao W, Xuan J, Charles F, Chen M, et al. Antimicrobial properties and mechanism of action of some plant extracts against food pathogens and spoilage microorganisms. *Front Microbiol*. 2018;9:1-9.
4. Bouyahya A, Chamkhi I, Balahbib A, Rebezov M, Shariati MA, Wilairatana P, et al. Mechanisms, anti-quorum-sensing actions, and clinical trials of medicinal plant bioactive compounds against bacteria: A comprehensive review. *Molecules*. 2022;27(5).
5. Siriyong T, Srimanote P, Chusri S, Yingyongnarongkul BE, Suaisom C, Tipmanee V, et al. Conessine as a novel inhibitor of multidrug efflux pump systems in *Pseudomonas aeruginosa*. *BMC Complement Altern Med*. 2017;17(1):1-7.
6. Jongjitvimol T, Kraikongjit S, Paensuwan P, Jongjitwimol J. *In vitro* biological profiles and chemical contents of ethanolic nest entrance extracts of thai stingless bees *Tetrigona apicalis*. *Online J Biol Sci*. 2020;20(3):157-65.
7. National Center for Advancing Translation Science; NIH. Inxigt: Drugs, Hydroquinine 31J30Q51T6L. [Internet]. [cited 02 Aug 2023]. Available from: <https://drugs.ncats.io/substance/31J30Q51T6L>.
8. Kraikongjit S, Jongjitvimol T, Mianjinda N, Sirithep N, Kaewbor T, Jumroon N, et al. Antibacterial effect of plant resin collected from *Tetrigona apicalis* (Smith, 1857) in Thung Salaeng Luang National Park, Phitsanulok. *Walailak J Sci & Tech*. 2017;15(8):599-607.
9. Khameneh B, Iranshahy M, Soheili V, Fazly Bazzaz BS. Review on plant antimicrobials: a mechanistic viewpoint. *Antimicrob Resist Infect Control*. 2019;8:1-28.
10. Rattanachak N, Weawsiangsang S, Jongjitvimol T, Baldock RA, Jongjitwimol J. Hydroquinine possesses antibacterial activity, and at half the MIC, Induces the overexpression of RND-type efflux pumps using multiplex digital PCR in *Pseudomonas aeruginosa*. *Trop Med Infect Dis*. 2022;7(8):156.
11. CLSI. Methods for dilution antimicrobial susceptibility tests for bacteria that grow aerobically; approved Standard—Ninth Edition. Wayne, PA: Clinical and Laboratory Standards Institute; 2012. p. 19087-1898.
12. National Health Care Institute. Hydroquinine (Inhibin®) for patients with nocturnal muscle cramps 2020 [Available from: <https://english.zorginstituutnederland.nl/publications/reports/2020/03/04/hydroquinine-inhibin-for-patients-with-nocturnal-muscle-cramps>].
13. Jansen PH, Veenhuizen KC, Wesseling AI, de Boo T, Verbeek AL. Randomised controlled trial of hydroquinine in muscle cramps. *The Lancet*. 1997;349(9051):528-32.
14. Kanteev M, Goldfeder M, Fishman A. Structure-function correlations in tyrosinases. *Protein Sci*. 2015;24(9):1360-9.
15. Nontprasert A, Pukrittayakamee S, Kyle DE, Vanijanonta S, White NJ. Antimalarial activity and interactions between quinine, dihydroquinine and 3-hydroxyquinine against *Plasmodium falciparum* *in vitro*. *Trans R Soc Trop Med Hyg*. 1996;90(5):553-5.

16. Polet H, Barr CF. Chloroquine and Dihydroquinine *in vitro* studies of thesis antimalarial effect upon. *Plasmodium knowlesi*. J Pharmacol Exp Ther. 1968;164(2):380-6.
17. Warhurst DC, Craig JC, Adagu IS, Meyer DJ, Lee SY. The relationship of physico-chemical properties and structure to the differential antiplasmodial activity of the cinchona alkaloids. Malar J. 2003;2(1):26.
18. Sullivan DJ. Cinchona alkaloids: quinine and quinidine. In: Staines HM, Krishna S, editors. Treatment and prevention of malaria: Antimalarial drug chemistry, action and use. Basel.: Springer Basel; 2012. p. 45-68.
19. Andersson L. A new revision of *Joosia* (Rubiaceae-Cinchoneae). Brittonia. 1997;49(1):24-44.
20. Kacprzak KM. Natural products: phytochemistry, botany and metabolism of alkaloids, phenolics and terpenes. Nat Prod. 2013:605-41.
21. Marella A, Tanwar OP, Saha R, Ali MR, Srivastava S, Akhter M, et al. Quinoline: A versatile heterocyclic. Saudi Pharm J. 2013;21(1):1-12.
22. Achan J, Talisuna AO, Erhart A, Yeka A, Tibenderana JK, Baliraine FN, et al. Quinine, an old anti-malarial drug in a modern world: role in the treatment of malaria. Malar J. 2011;144(10):1-12.
23. Edwards G. Antimalarial chemotherapy: Mechanisms of action, resistance and new directions in drug discovery. Br J Clin Pharmacol. 2001;52(4):461-4.
24. Ning X, He J, Shi Xe, Yang G. Regulation of adipogenesis by quinine through the ERK/S6 Pathway. Int J Mol Sci. 2016;17(4):1-15.
25. Krishnaveni M, K S. Induction of apoptosis by quinine in human laryngeal carcinoma cell line. Int J Curr. 2015;3(3):169-78.
26. Antika LD, Triana D, Ernawati T. Antimicrobial activity of quinine derivatives against human pathogenic bacteria. IOP Conf Ser Earth Environ Sci. 2020;462:1-8.
27. Jongjitwimol J, Baldock RA. Hydroquinine: a potential new avenue in drug discovery for drug-resistant bacteria? Expert Opin Drug Discov. 2023;18(3):227-9.
28. Casiano-Colón A, Marquis RE. Role of the arginine deiminase system in protecting oral bacteria and an enzymatic basis for acid tolerance. Appl Environ Microbiol. 1988;54(6):1318-24.
29. Xiong L, Teng JL, Botelho MG, Lo RC, Lau SK, Woo PC. Arginine metabolism in bacterial pathogenesis and cancer therapy. Int J Mol Sci. 2016;17(3):363.
30. Mercenier A, Simon JP, Vander Wauven C, Haas D, Stalon V. Regulation of enzyme synthesis in the arginine deiminase pathway of *Pseudomonas aeruginosa*. J Bacteriol. 1980;144(1):159-63.
31. Lu CD, Winteler H, Abdelal A, Haas D. The ArgR regulatory protein, a helper to the anaerobic regulator ANR during transcriptional activation of the *arcD* promoter in *Pseudomonas aeruginosa*. J Bacteriol. 1999;181(8):2459-64.
32. Vander Wauven C, Piérard A, Kley-Raymann M, Haas D. *Pseudomonas aeruginosa* mutants affected in anaerobic growth on arginine: evidence for a four-gene cluster encoding the arginine deiminase pathway. J Bacteriol Res. 1984;160(3):928-34.
33. Müsken M, Di Fiore S, Dötsch A, Fischer R, Häussler S. Genetic determinants of *Pseudomonas aeruginosa* biofilm establishment. Microbiology. 2010;156(Pt 2):431-41.
34. Scribani Rossi C, Barrientos-Moreno L, Paone A, Cutruzzola F, Paiardini A, Espinosa-Urgel M, et al. Nutrient sensing and biofilm modulation: the example of L-

arginine in *Pseudomonas*. Int J Mol Sci. 2022;23(8).

35. Sandra Kolbeck MA, Maik Hilgarth, Rudi F Vogel,. Comparative proteomics reveals the anaerobic lifestyle of meat-spoiling *Pseudomonas* species. Front Microbiol. 2021;12.
36. Yan Y, Li X, Zhang C, Lv L, Gao B, Li M. Research progress on antibacterial activities and mechanisms of natural alkaloids: A review. Antibiotics. 2021;10(3):3-30.
37. Elisabetsky E, Costa-Campos L. The alkaloid alstonine: a review of its pharmacological properties. Evid Based Complementary Altern Med. 2006;3(1):39-48.
38. Zhang Q, Lyu Y, Huang J, Zhang X, Yu N, Wen Z, et al. Antibacterial activity and mechanism of sanguinarine against *Providencia rettgeri* in vitro. PeerJ. 2020;8:1-19.
39. Salton MRJ. Structure and function of bacterial cell membranes. Annu Rev Microbiol. 1967;21(1):417-42.
40. RNA Functions [Internet]. Nature Education 2008 [cited 2022 Aug 26]. Available from: <https://www.nature.com/scitable/topicpage/rna-functions-352/>.
41. Othman L, Sleiman A, Abdel-Massih RM. Antimicrobial activity of polyphenols and alkaloids in middle eastern plants. Front Microbiol. 2019;10:1-28.
42. Maxwell A. DNA gyrase as a drug target. Trends Microbiol. 1997;5(3):102-9.
43. Heeb S, Fletcher MP, Chhabra SR, Diggle SP, Williams P, Cámara M. Quinolones: from antibiotics to autoinducers. FEMS Microbiol Rev. 2011;35(2):247-74.
44. Rukachaisirikul T, Prabpai S, Champung P, Suksamrarn A. Chabamide, a novel piperine dimer from stems of *Piper chaba*. Planta Med. 2002;68(9):853-5.
45. Bendaif H, Melhaoui A, Ramdani M, Elmsellem H, Douez C, El Ouadi Y. Antibacterial activity and virtual screening by molecular docking of lycorine from *Pancreaticum foetidum* Pom (Moroccan endemic Amaryllidaceae). Microb Pathog. 2018;115:138-45.
46. Levenfors JJ, Nord C, Bjerketorp J, Ståhlberg J, Larsson R, Guss B, et al. Antibacterial pyrrolidinyl and piperidinyl substituted 2,4-diacetylphloroglucinols from *Pseudomonas protegens* UP46. J Antibiot Res. 2020;73(11):739-47.
47. Barrows JM, Goley ED. FtsZ dynamics in bacterial division: What, how, and why? Curr Opin Cell Biol. 2021;68:163-72.
48. Silhavy TJ, Kahne D, Walker S. The bacterial cell envelope. Cold Spring Harb Perspect Biol. 2010;2(5):a000414.
49. Hummels KR, Berry SP, Li Z, Taguchi A, Min JK, Walker S, et al. Coordination of bacterial cell wall and outer membrane biosynthesis. Nature. 2023;615(7951):300-4.
50. Cao X, van Putten JPM, Wösten MMSM. Chapter Two - Biological functions of bacterial lysophospholipids. In: Poole RK, Kelly DJ, editors. Adv Microb Physiol. 82: Academic Press; 2023. p. 129-54.
51. Qian LH TY, Xie J. Antibacterial mechanism of tea polyphenols against *Staphylococcus aureus* and *Pseudomonas aeruginosa*. Microbiol Rev. 2010;37:1628-33.
52. Lan WQ XJ, Hou WF, Li DW. Antibacterial activity and mechanism of compound biological preservatives against *Staphylococcus squirrel*. Res Dve Nat Prod. 2012;24:741-6.
53. Hara S, Yamakawa M. Moricin, a novel type of antibacterial peptide isolated from the silkworm, *Bombyx mori*. J Biol Chem. 1995;270(50):29923-27.
54. Dvorač Z, Sovadinová I, Bláha L, Giesy JP, Ulrichová J. Quaternary benzo[c]phenathridine alkaloids sanguinarine and chelerythrine do not affect

transcriptional activity of aryl hydrocarbon receptor: analyses in rat hepatoma cell line H4IIE.luc. *Food Chem Toxicol.* 2006;44(9):1466-73.

55. Wang Y, Shou JW, Li XY, Zhao ZX, Fu J, He CY, et al. Berberine-induced bioactive metabolites of the gut microbiota improve energy metabolism. *Metabolism.* 2017;70:72-84.

56. Bonora M, Patergnani S, Rimessi A, De Marchi E, Suski JM, Bononi A, et al. ATP synthesis and storage. *Purinergic Signal.* 2012;8(3):343-57.

57. Rajendran M, Dane E, Conley J, Tantama M. Imaging Adenosine Triphosphate (ATP). *Biol Bull.* 2016;231(1):73-84.

58. Sobti M, Ishmukhametov R, Stewart AG. ATP synthase: expression, purification, and function. *Methods Mol Biol.* 2020;2073:73-84.

59. Van Bambeke F, Balzi E, Tulkens PM. Antibiotic efflux pumps. *Biochem Pharmacol.* 2000;60(4):457-70.

60. Webber MA, Piddock LJ. The importance of efflux pumps in bacterial antibiotic resistance. *J Antimicrob Chemother.* 2003;51(1):9-11.

61. Lomovskaya O, Warren MS, Lee A, Galazzo J, Fronko R, Lee M, et al. Identification and characterization of inhibitors of multidrug resistance efflux pumps in *Pseudomonas aeruginosa*: novel agents for combination therapy. *Antimicrob Agents Chemother.* 2001;45(1):105-16.

62. Wei JT QJ, Su QLY, Liu ZX, Wang XL, Wang YP. Research progress on the mechanism of bacterial biofilm induced drug resistance and the effect of antimicrobial peptide LL-37 on biofilm. *J Hexi Univ.* 2020;36:38-43.

63. Paulsen IT, Brown MH, Skurray RA. Proton-dependent multidrug efflux systems. *Microbiol Rev.* 1996;60(4):575-608.

64. Siriyong T, Chusri S, Srimanote P, Tipmanee V, Voravuthikunchai SP. *Holarrhena antidysenterica* extract and its steroidal alkaloid, conessine, as resistance-modifying agents against extensively drug-resistant *Acinetobacter baumannii*. *Microb Drug Resist.* 2016;22(4):273-82.

65. Mabhiza D, Chitemerere T, Mukanganyama S. Antibacterial properties of alkaloid extracts from *Callistemon citrinus* and *Vernonia adoensis* against *Staphylococcus aureus* and *Pseudomonas aeruginosa*. *Int J Med Chem.* 2016;2016:1-7.

66. Hooper DC. Efflux pumps and nosocomial antibiotic resistance: a primer for hospital epidemiologists. *Clin Infect Dis.* 2005;40(12):1811-17.

67. World Health Organization. antimicrobial resistance. Global Report on Surveillance. Geneva 2014. [Internet]. [cited 2022 Aug 23]. Available from: <https://www.who.int/home/search?indexCatalogue=genericsearchindex1&searchQuery=Antimicrobial%20resistance&wordsMode=AllWords>.

68. Centers for disease control and prevention. antibiotic resistance threats in the United States, 2013. [Internet]. [cited 2022 Aug 24]. Available from: <http://www.cdc.gov/drugresistance/threat-report-2013>.

69. Ventola CL. The antibiotic resistance crisis: part 1: causes and threats. *P T.* 2015;40(4):277-83.

70. Pang Z, Raudonis R, Glick BR, Lin TJ, Cheng Z. Antibiotic resistance in *Pseudomonas aeruginosa*: mechanisms and alternative therapeutic strategies. *Biotechnol Adv.* 2019;37(1):177-92.

71. *Pseudomonas aeruginosa*. [Internet]. [cited 2022 Aug 25]. Available from: <http://www.antimicrobe.org/b112-index.asp>.

72. Livermore DM. Multiple mechanisms of antimicrobial resistance in *Pseudomonas aeruginosa*: our worst nightmare? *Clin Infect Dis*. 2002;34(5):634-40.
73. Cohen AL, Calfee D, Fridkin SK, Huang SS, Jernigan JA, Lautenbach E, et al. Recommendations for metrics for multidrug-resistant organisms in healthcare settings: SHEA/HICPAC position paper. *Infect Control Hosp Epidemiol*. 2008;29(10):901-13.
74. Falagas ME, Koletsi PK, Bliziotis IA. The diversity of definitions of multidrug-resistant (MDR) and pandrug-resistant (PDR) *Acinetobacter baumannii* and *Pseudomonas aeruginosa*. *J Med Microbiol*. 2006;55(12):1619-29.
75. Kallen AJ, Hidron AI, Patel J, Srinivasan A. Multidrug resistance among gram-negative pathogens that caused healthcare-associated infections reported to the national healthcare safety network, 2006-2008. *Infect Control Hosp Epidemiol*. 2010;31(5):528-31.
76. Critchley IA, Draghi DC, Sahm DF, Thornsberry C, Jones ME, Karlowsky JA. Activity of daptomycin against susceptible and multidrug-resistant Gram-positive pathogens collected in the SECURE study (Europe) during 2000-2001. *J Antimicrob Chemother*. 2003;51(3):639-49.
77. Richards MJ, Edwards JR, Culver DH, Gaynes RP. Nosocomial infections in medical intensive care units in the United States. National nosocomial infections surveillance system. *Crit Care Med*. 1999;27(5):887-92.
78. Mirzaei B, Bazgir ZN, Goli HR, Iranpour F, Mohammadi F, Babaei R. Prevalence of multi-drug resistant (MDR) and extensively drug-resistant (XDR) phenotypes of *Pseudomonas aeruginosa* and *Acinetobacter baumannii* isolated in clinical samples from Northeast of Iran. *BMC Res Notes*. 2020;13(1):1-6.
79. Killough MR, A. M., Ingram, R. J. *Pseudomonas aeruginosa* recent advances in vaccine development. *Vaccines*. 2022;10(7).
80. Silby MW, Winstanley C, Godfrey SA, Levy SB, Jackson RW. *Pseudomonas genomes*: diverse and adaptable. *FEMS Microbiol Rev*. 2011;35(4):652-80.
81. Anjum H, Arefin M, Jahan N, Jannat Oishee M, Nahar S, Islam S, et al. Roles of intrinsic and acquired resistance determinants in multidrug-resistant clinical *Pseudomonas aeruginosa* in Bangladesh. *BJMS*. 2023.
82. Cobos-Triguero N, Zboromyrska Y, Morata L, Alejo I, De La Calle C, Vergara A, et al. Time-to-positivity, type of culture media and oxidase test performed on positive blood culture vials to predict *Pseudomonas aeruginosa* in patients with Gram-negative bacilli bacteraemia. *Rev Esp Quimioter*. 2017;30(1):9-13.
83. LaBauve AE, Wargo MJ. Growth and laboratory maintenance of *Pseudomonas aeruginosa*. *Curr Protoc Microbiol*. 2012:2-11.
84. Schobert M, Jahn D. Anaerobic physiology of *Pseudomonas aeruginosa* in the cystic fibrosis lung. *Int J Med Microbiol*. 2010;300(8):549-56.
85. Mazhar Ali N, Rehman S, Abdullah Mazhar S, Liaqat I, Mazhar B. *Pseudomonas aeruginosa*-Associated acute and chronic pulmonary infections. In: Sahara Kirmusaoglu, Bhardwaj SB, editors. *Pathogenic Bacteria*. London: IntechOpen; 2020. p. 1-21.
86. Iglewski. BH. *Pseudomonas*. 1996 [cited 2022 Aug 27]. In: *Medical Microbiology* [Internet]. Galveston: University of Texas Medical Branch at Galveston. 4th ed. [cited 2022 Aug 27]. Available from: <https://www.ncbi.nlm.nih.gov/books/NBK8326/>.
87. Al-Mujaini A, Al-Kharusi N, Thakral A, Wali UK. Bacterial keratitis:

perspective on epidemiology, clinico-pathogenesis, diagnosis and treatment. Sultan Qaboos Univ Med J. 2009;9(2):184-95.

88. Whitcher JP, Srinivasan M, Upadhyay MP. Corneal blindness: a global perspective. Bull World Health Organ. 2001;79(3):214-21.

89. Cabrera-Aguas M, Khoo P, Watson SL. Infectious keratitis: A review. Clin Exp Ophthalmol. 2022;50(5):543-62.

90. Sridhar MS. Anatomy of cornea and ocular surface. Indian J Ophthalmol. 2018;66(2):190-4.

91. DelMonte DW, Kim T. Anatomy and physiology of the cornea. J Cataract Refract Surg. 2011;37(3):588-98.

92. Ahearne M, Lynch A. Early observation of extracellular matrix-derived hydrogels for corneal stroma regeneration. Tissue engineering Part C, Methods. 2015;21.

93. Laibson PR. Cornea and sclera. Arch Ophthalmol. 1972;88(5):553-74.

94. Zhang L, Anderson MC, Liu CY. The role of corneal stroma: A potential nutritional source for the cornea. J Nat Sci. 2017;3(8).

95. Dua HS, Faraj LA, Said DG, Gray T, Lowe J. Human corneal anatomy redefined: a novel pre-Descemet's layer (Dua's layer). Ophthalmology. 2013;120(9):1778-85.

96. Eghrari AO, Riazuddin SA, Gottsch JD. Overview of the cornea: structure, function, and development. Prog Mol Biol Transl Sci. 2015;134:7-23.

97. Chen Z, You J, Liu X, Cooper S, Hodge C, Sutton G, et al. Biomaterials for corneal bioengineering. Biomed Mater. 2018;13(3):032002.

98. Wiley L, SundarRaj N, Sun TT, Thoft RA. Regional heterogeneity in human corneal and limbal epithelia: an immunohistochemical evaluation. Invest Ophthalmol Vis Sci. 1991;32(3):594-602.

99. Wilson SE, Medeiros CS, Santhiago MR. Pathophysiology of corneal scarring in persistent epithelial defects after PRK and other corneal injuries. J Refract Surg. 2018;34(1):59-64.

100. Robaei D, Watson S. Corneal blindness: a global problem. Clin Exp Ophthalmol. 2014;42(3):213-4.

101. Resnikoff S, Pascolini D, Etya'ale D, Kocur I, Pararajasegaram R, Pokharel GP, et al. Global data on visual impairment in the year 2002. Bull World Health Organ. 2004;82(11):844-51.

102. Carnt N, Samarawickrama C, White A, Stapleton F. The diagnosis and management of contact lens-related microbial keratitis. Clin Exp Optom. 2017;100(5):482-93.

103. Burton MJ. Prevention, treatment and rehabilitation. Community Eye Health. 2009;22(71):33-5.

104. Eltis M. Contact-lens-related microbial keratitis: case report and review. J Optom. 2011;4(4):122-7.

105. Preechawat P, Ratananikom U, Lerdvitayasakul R, Kunavisarut S. Contact lens-related microbial keratitis. J Med Assoc Thai. 2007;90(4):737-43.

106. Kopeček J. Hydrogels from soft contact lenses and implants to self-assembled nanomaterials. J Polym Sci A Polym Chem. 2009;47(22):5929-46.

107. Fukuda K, Ishida W, Fukushima A, Nishida T. Corneal fibroblasts as sentinel cells and local immune modulators in infectious keratitis. Int J Mol Sci. 2017;18(9).

108. Simmons KT, Xiao Y, Pflugfelder SC, de Paiva CS. Inflammatory response to lipopolysaccharide on the ocular surface in a murine dry eye model. *Invest Ophthalmol Vis Sci.* 2016;57(6):2443-51.
109. Moreddu R, Vigolo D, Yetisen AK. Contact lens technology: from fundamentals to applications. *Adv Healthc Mater.* 2019;8(15):e1900368.
110. Lim CHL, Stapleton F, Mehta JS. Review of contact lens-related complications. *Eye Contact Lens.* 2018;44 Suppl 2:S1-s10.
111. Forister JF, Forister EF, Yeung KK, Ye P, Chung MY, Tsui A, et al. Prevalence of contact lens-related complications: UCLA contact lens study. *Eye Contact Lens.* 2009;35(4):176-80.
112. Eltis M. Contact-lens-related microbial keratitis: case report and review. *Journal of Optometry.* 2011;4(4):122-7.
113. Dart JKG, Stapleton F, Minassian D, Dart JKG. Contact lenses and other risk factors in microbial keratitis. *The Lancet.* 1991;338(8768):650-3.
114. Fleiszig SMJ, Kroken AR, Nieto V, Grosser MR, Wan SJ, Metruccio MME, et al. Contact lens-related corneal infection: Intrinsic resistance and its compromise. *Prog Retin Eye Res.* 2020;76:100804.
115. Robertson DM. The effects of silicone hydrogel lens wear on the corneal epithelium and risk for microbial keratitis. *Eye Contact Lens.* 2013;39(1):67-72.
116. ISO. ISO 14729 Ophthalmic optics—Contact lens care products—Microbiological requirements and test methods for products and regimens for hygienic management of contact lenses. 2001.
117. McAnally C, Walters R, Campolo A, Harris V, King J, Thomas M, et al. Antimicrobial efficacy of contact lens solutions assessed by ISO standards. *Microorganisms.* 2021;9(10).
118. Szczotka-Flynn LB, Imamura Y, Chandra J, Yu C, Mukherjee PK, Pearlman E, et al. Increased resistance of contact lens-related bacterial biofilms to antimicrobial activity of soft contact lens care solutions. *Cornea.* 2009;28(8):918-26.
119. Kilvington S, Huang L, Kao E, Powell CH. Development of a new contact lens multipurpose solution: Comparative analysis of microbiological, biological and clinical performance. *J Optom.* 2010;3(3):134-42.
120. Niederkorn JY. Cornea: window to ocular immunology. *Curr Immunol Rev.* 2011;7(3):328-35.
121. Tam C, LeDue J, Mun JJ, Herzmark P, Robey EA, Evans DJ, et al. 3D quantitative imaging of unprocessed live tissue reveals epithelial defense against bacterial adhesion and subsequent traversal requires MyD88. *PLoS One.* 2011;6(8):e24008.
122. Li J, Metruccio MME, Evans DJ, Fleiszig SMJ. Mucosal fluid glycoprotein DMBT1 suppresses twitching motility and virulence of the opportunistic pathogen *Pseudomonas aeruginosa*. *PLOS Pathogens.* 2017;13(5):e1006392.
123. Keay L, Stapleton F. Development and evaluation of evidence-based guidelines on contact lens-related microbial keratitis. *Cont Lens Anterior Eye.* 2008;31(1):3-12.
124. Edwards K, Keay L, Naduvilath T, Snibson G, Taylor H, Stapleton F. Characteristics of and risk factors for contact lens-related microbial keratitis in a tertiary referral hospital. *Eye (Lond).* 2009;23(1):153-60.
125. Lim CH, Carnt NA, Farook M, Lam J, Tan DT, Mehta JS, et al. Risk factors for contact lens-related microbial keratitis in Singapore. *Eye (Lond).* 2016;30(3):447-55.

126. Radford CF, Lehmann OJ, Dart JK. Acanthamoeba keratitis: multicentre survey in England 1992-6. National Acanthamoeba Keratitis Study Group. Br J Ophthalmol. 1998;82(12):1387-92.
127. Phillips SP. Defining and measuring gender: a social determinant of health whose time has come. Int J Equity Health. 2005;4:11.
128. Jimena A-V, Raul ER-L, Julio CH-C, Alejandro R-G. Contact lens-associated infectious keratitis: update on diagnosis and therapy. In: Alejandro R-G, Julio CH-C, editors. Infectious Eye Diseases. Rijeka: IntechOpen; 2021. p. Ch. 1.
129. Dart JK, Radford CF, Minassian D, Verma S, Stapleton F. Risk factors for microbial keratitis with contemporary contact lenses: A case-control study. Ophthalmology. 2008;115(10):1647-54, 54.e1-3.
130. Stapleton F, Keay L, Edwards K, Naduvilath T, Dart JK, Brian G, et al. The incidence of contact lens-related microbial keratitis in Australia. Ophthalmology. 2008;115(10):1655-62.
131. Carnt N, Hoffman JM, Verma S, Hau S, Radford CF, Minassian DC, et al. Acanthamoeba keratitis: confirmation of the UK outbreak and a prospective case-control study identifying contributing risk factors. Br J Ophthalmol. 2018;102(12):1621-8.
132. Keay L, Edwards K, Naduvilath T, Taylor HR, Snibson GR, Forde K, et al. Microbial keratitis predisposing factors and morbidity. Ophthalmology. 2006;113(1):109-16.
133. Mun JJ, Tam C, Evans DJ, Fleiszig SM. Modulation of epithelial immunity by mucosal fluid. Sci Rep. 2011;1:8.
134. Willcox MD, Holden BA. Contact lens related corneal infections. Biosci Rep. 2001;21(4):445-61.
135. Zaidi T, Mowrey-McKee M, Pier GB. Hypoxia increases corneal cell expression of CFTR leading to increased *Pseudomonas aeruginosa* binding, internalization, and initiation of inflammation. Invest Ophthalmol Vis Sci. 2004;45(11):4066-74.
136. Vilaplana L, Marco MP. Phenazines as potential biomarkers of *Pseudomonas aeruginosa* infections: synthesis regulation, pathogenesis and analytical methods for their detection. Anal Bioanal Chem. 2020;412(24):5897-912.
137. Nikolaidis M, Mossialos D, Oliver S, Amoutzias G. Comparative analysis of the core proteomes among the *Pseudomonas* major evolutionary groups reveals species-specific adaptations for *Pseudomonas aeruginosa* and *Pseudomonas chlororaphis*. Diversity. 2020;12:289.
138. Diggle SP, Whiteley M. Microbe Profile: *Pseudomonas aeruginosa*: opportunistic pathogen and lab rat. Microbiology. 2020;166(1):30-3.
139. Conrad JC, Gibiansky ML, Jin F, Gordon VD, Motto DA, Mathewson MA, et al. Flagella and pili-mediated near-surface single-cell motility mechanisms in *P. aeruginosa*. Biophys J. 2011;100(7):1608-16.
140. Berg HC. The rotary motor of bacterial flagella. Annu Rev Biochem. 2003;72:19-54.
141. Craig L, Li J. Type IV pili: paradoxes in form and function. Curr Opin Struct Biol. 2008;18(2):267-77.
142. King JD, Kocíncová D, Westman EL, Lam JS. Review: lipopolysaccharide biosynthesis in *Pseudomonas aeruginosa*. Innate Immun. 2009;15(5):261-312.
143. Diggle SP, Griffin AS, Campbell GS, West SA. Cooperation and conflict in

quorum-sensing bacterial populations. *Nature*. 2007;450(7168):411-4.

144. Schwarzer C, Fischer H, Machen TE. Chemotaxis and binding of *Pseudomonas aeruginosa* to scratch-wounded human cystic fibrosis airway epithelial cells. *PLoS One*. 2016;11(3):e0150109.

145. Feldman M, Bryan R, Rajan S, Scheffler L, Brunnert S, Tang H, et al. Role of flagella in pathogenesis of *Pseudomonas aeruginosa* pulmonary infection. *Infect Immun*. 1998;66(1):43-51.

146. Campolo A, Pifer R, Shannon P, Crary M. Microbial adherence to contact lenses and *Pseudomonas aeruginosa* as a model organism for microbial keratitis. *Pathogens*. 2022;11(11).

147. Melville S, Craig L. Type IV pili in Gram-positive bacteria. *Microbiol Mol Biol Rev*. 2013;77(3):323-41.

148. Gold VAM, Salzer R, Averhoff B, Kühlbrandt W. Structure of a type IV pilus machinery in the open and closed state. *eLife*. 2015;4:e07380.

149. Suzuki T, Inoue H. Mechanisms underlying contact lens-related keratitis caused by *Pseudomonas aeruginosa*. *Eye Contact Lens*. 2022;48(3):134-7.

150. Williams P, Cámara M. Quorum sensing and environmental adaptation in *Pseudomonas aeruginosa*: a tale of regulatory networks and multifunctional signal molecules. *Curr Opin Microbiol*. 2009;12(2):182-91.

151. Morlon-Guyot J, Méré J, Bonhoure A, Beaumelle B. Processing of *Pseudomonas aeruginosa* exotoxin A is dispensable for cell intoxication. *Infect Immun*. 2009;77(7):3090-9.

152. Jaffar-Bandjee MC, Lazdunski A, Bally M, Carrère J, Chazalotte JP, Galabert C. Production of elastase, exotoxin A, and alkaline protease in sputa during pulmonary exacerbation of cystic fibrosis in patients chronically infected by *Pseudomonas aeruginosa*. *J Clin Microbiol*. 1995;33(4):924-9.

153. Dutta D, Cole N, Willcox M. Factors influencing bacterial adhesion to contact lenses. *Mol Vis*. 2012;18:14-21.

154. Thi MTT, Wibowo D, Rehm BHA. *Pseudomonas aeruginosa* Biofilms. *Int J Mol Sci*. 2020;21(22).

155. Høiby N, Bjarnsholt T, Givskov M, Molin S, Ciofu O. Antibiotic resistance of bacterial biofilms. *Int J Antimicrob Agents*. 2010;35(4):322-32.

156. Elder MJ, Stapleton F, Evans E, Dart JK. Biofilm-related infections in ophthalmology. *Eye (Lond)*. 1995;9 (Pt 1):102-9.

157. Mordmuang A, Udomwech L, Karnjana K. Influence of contact lens materials and cleaning procedures on bacterial adhesion and biofilm formation. *Clin Ophthalmol*. 2021;15:2391-402.

158. Klotz SA, Misra RP, Butrus SI. Contact lens wear enhances adherence of *Pseudomonas aeruginosa* and binding of lectins to the cornea. *Cornea*. 1990;9(3):266-70.

159. Ibrahim YW, Boase DL, Cree IA. How could contact lens wearers be at risk of *Acanthamoeba* infection? A review. *J Optom*. 2009;2(2):60-6.

160. McLaughlin-Borlace L, Stapleton F, Matheson M, Dart JK. Bacterial biofilm on contact lenses and lens storage cases in wearers with microbial keratitis. *J Appl Microbiol*. 1998;84(5):827-38.

161. Ruffin M, Brochiero E. Repair process impairment by *Pseudomonas aeruginosa* in epithelial tissues: major features and potential therapeutic avenues. *Front Cell Infect*

Microbiol. 2019;9:182.

162. Saillard J, Spiesser-Robelet L, Gohier P, Briot T. Bacterial keratitis treated by strengthened antibiotic eye drops: An 18 months review of clinical cases and antibiotic susceptibilities. *Ann Pharm.* 2018;76(2):107-13.

163. Austin A, Lietman T, Rose-Nussbaumer J. Update on the management of infectious keratitis. *Ophthalmology.* 2017;124(11):1678-89.

164. Chen AMH, Straw A. Chapter 29: Prevention of contact lens-related disorders. *Handbook of Nonprescription Drugs: An Interactive Approach to Self-Care*, 20th Edition: The American Pharmacists Association; 2020.

165. Donshik PC, Ehlers WH, Anderson LD, Suchecki JK. Strategies to better engage, educate, and empower patient compliance and safe lens wear: compliance: what we know, what we do not know, and what we need to know. *Eye Contact Lens.* 2007;33(6 Pt 2):430-3; discussion 4.

166. Jones IA, Joshi LT. Biocide Use in the Antimicrobial Era: A Review. *Molecules* [Internet]. 2021; 26(8).

167. Jiao Y, Niu L-n, Ma S, Li J, Tay FR, Chen J-h. Quaternary ammonium-based biomedical materials: State-of-the-art, toxicological aspects and antimicrobial resistance. *Prog Polym Sci.* 2017;71:53-90.

168. Codling CE, Maillard JY, Russell AD. Aspects of the antimicrobial mechanisms of action of a polyquaternium and an amidoamine. *J Antimicrob Chemother.* 2003;51(5):1153-8.

169. Salton MR. Lytic agents, cell permeability, and monolayer penetrability. *J Gen Physiol.* 1968;52(1):227-52.

170. Bradley CS, Sicks LA, Pucker AD. Common ophthalmic preservatives in soft contact lens care products: benefits, complications, and a comparison to non-preserved solutions. *Clin Optom (Auckl).* 2021;13:271-85.

171. Maillard J-Y, Pascoe M. Disinfectants and antiseptics: mechanisms of action and resistance. *Nature Reviews Microbiology.* 2024;22(1):4-17.

172. Craig WA, Gerber AU. Pharmacokinetics of cefoperazone: a review. *Drugs.* 1981;22(1):35-45.

173. Rattanachak N, Weawsiangsang S, Daowtak K, Thongsri Y, Ross S, Ross G, et al. High-throughput transcriptomic profiling reveals the inhibitory effect of hydroquinine on virulence factors in *Pseudomonas aeruginosa*. *Antibiotics.* 2022;11(10):1436.

174. CLSI. Performance standards for antimicrobial susceptibility testing. 30th ed. CLSI supplement M100. Wayne, PA: Clinical and Laboratory Standards Institute; 2020.

175. Cohen AL, Calfee D, Fridkin SK, Huang SS, Jernigan JA, Lautenbach E, et al. Recommendations for metrics for multidrug-resistant organisms in healthcare settings: SHEA/HICPAC position paper. *Infect Control Hosp Epidemiol.* 2008;29(10):901-13.

176. Falagas ME, Koletsi PK, Bliziotis IA. The diversity of definitions of multidrug-resistant (MDR) and pandrug-resistant (PDR) *Acinetobacter baumannii* and *Pseudomonas aeruginosa*. *J Med Microbiol.* 2006;55(12):1619-29.

177. Kallen AJ, Hidron AI, Patel J, Srinivasan A. Multidrug resistance among gram-negative pathogens that caused healthcare-associated infections reported to the National Healthcare Safety Network, 2006-2008. *Infect Control Hosp Epidemiol.* 2010;31(5):528-31.

178. Critchley IA, Draghi DC, Sahm DF, Thornsberry C, Jones ME, Karlowsky JA.

Activity of daptomycin against susceptible and multidrug-resistant gram-positive pathogens collected in the SECURE study (Europe) during 2000-2001. *J Antimicrob Chemother.* 2003;51(3):639-49.

179. American Type Culture Collection (ATCC). *Pseudomonas aeruginosa* (Schroeter) Migula BAA-2108™ [Internet]. [cited 2022 Sep 7]. Available from: <https://www.atcc.org/products/baa-2108>.

180. Fratini F, Mancini S, Turchi B, Friscia E, Pistelli L, Giusti G, et al. A novel interpretation of the Fractional Inhibitory Concentration Index: The case *Origanum vulgare* L. and *Leptospermum scoparium* J. R. et G. Forst essential oils against *Staphylococcus aureus* strains. *Microbiol Res.* 2016;195.

181. Cheypratub P LW, Eumkeb G. The synergy and mode of action of *Cyperus rotundus* L. extract plus ampicillin against ampicillin-resistant *Staphylococcus aureus*. *Evid Based Complementary Altern Med.* 2018;2018.

182. Cha JD, Lee JH, Choi KM, Choi SM, Park JH. Synergistic effect between cryptotanshinone and antibiotics against clinic methicillin and vancomycin-resistant *Staphylococcus aureus*. *Evid Based Complementary Altern Med.* 2014;2014:450572.

183. Rakholiya KD, Kaneria MJ, Chanda SV. Chapter 11-Medicinal plants as alternative sources of therapeutics against multidrug-resistant pathogenic microorganisms based on their antimicrobial potential and synergistic properties. In: Rai M, Kon K, editors. *Fighting multidrug resistance with herbal extracts, essential oils and their components*. San Diego: Academic Press; 2013. p. 165-79.

184. Bassolé IH, Lamien-Meda A, Bayala B, Obame LC, Ilboudo AJ, Franz C, et al. Chemical composition and antimicrobial activity of *Cymbopogon citratus* and *Cymbopogon giganteus* essential oils alone and in combination. *Phytomedicine.* 2011;18(12):1070-4.

185. King E, Aitchison E, Li H, Luo R. Recent developments in free energy calculations for drug discovery. *Front Mol Biosci.* 2021;8.

186. Hall R, Dixon T, Dickson A. On calculating free energy differences using ensembles of transition paths. *Front Mol Biosci.* 2020;7.

187. Grosdidier A, Zoete V, Michielin O. SwissDock, a protein-small molecule docking web service based on EADock DSS. *Nucleic Acids Res.* 2011;39(Web Server issue):W270-7.

188. Varadi M, Anyango S, Deshpande M, Nair S, Natassia C, Yordanova G, et al. AlphaFold protein structure database: massively expanding the structural coverage of protein-sequence space with high-accuracy models. *Nucleic Acids Res.* 2022;50(D1):D439-D44.

189. Jumper J, Evans R, Pritzel A, Green T, Figurnov M, Ronneberger O, et al. Highly accurate protein structure prediction with AlphaFold. *Nature.* 2021;596(7873):583-9.

190. Madeira F, Pearce M, Tivey ARN, Basutkar P, Lee J, Edbali O, et al. Search and sequence analysis tools services from EMBL-EBI in 2022. *Nucleic Acids Res.* 2022;50(W1):W276-W9.

191. Pettersen EF, Goddard TD, Huang CC, Couch GS, Greenblatt DM, Meng EC, et al. UCSF Chimera--a visualization system for exploratory research and analysis. *J Comput Chem.* 2004;25(13):1605-12.

192. Kumar S, Kashyap P, Chowdhury S, Kumar S, Panwar A, Kumar A. Identification of phytochemicals as potential therapeutic agents that binds to Nsp15

protein target of coronavirus (SARS-CoV-2) that are capable of inhibiting virus replication. *Phytomedicine*. 2021;85:153317.

193. Peluso P, Chankvetadze B. Recent developments in molecular modeling tools and applications related to pharmaceutical and biomedical research. *J Pharm Biomed Anal*. 2023;238:115836.

194. Murugan NA, Muvva C, Jeyarajpandian C, Jeyakanthan J, Subramanian V. Performance of Force-Field- and Machine Learning-Based Scoring Functions in Ranking MAO-B Protein-Inhibitor Complexes in Relevance to Developing Parkinson's Therapeutics. *Int J Mol Sci*. 2020;21(20).

195. Kadela-Tomanek M, Jastrzębska M, Marciniak K, Chrobak E, Bębenek E, Boryczka S. Lipophilicity, pharmacokinetic properties, and molecular docking study on SARS-CoV-2 target for betulin triazole derivatives with attached 1,4-quinone. *Pharmaceutics*. 2021;13(6).

196. Chen S, Li B, Chen L, Jiang H. Uncovering the mechanism of resveratrol in the treatment of diabetic kidney disease based on network pharmacology, molecular docking, and experimental validation. *J Transl Med*. 2023;21(1):380.

197. Ccgi M. Molecular operating environment (MOE), 2013.08. Chemical Computing Group, Inc. 2016;354.

198. Vilar S, Cozza G, Moro S. Medicinal chemistry and the Molecular Operating Environment (MOE): application of QSAR and molecular docking to drug discovery. *Curr Top Med Chem*. 2008;8(18):1555-72.

199. Clark AM, Labute P. 2D depiction of protein-ligand complexes. *J Chem Inf Model*. 2007;47(5):1933-44.

200. Han Y, Lafleur RPM, Zhou J, Xu W, Lin Z, Richardson JJ, et al. Role of molecular interactions in supramolecular polypeptide–polyphenol networks for engineering functional materials. *J Am Chem Soc*. 2022;144(27):12510-9.

201. Premier biosoft: accelerating research in life scienc. PCR primer design guidelines [Internet]. [cited 2022 Aug 21]. Available from: http://www.premierbiosoft.com/tech_notes/PCR_Primer_Design.html.

202. Weawsiangsang S, Rattanachak N, Jongjitvimol T, Jaifoo T, Charoensit P, Viyoch J, et al. Hydroquinine inhibits the growth of multidrug-resistant *Pseudomonas aeruginosa* via the suppression of the arginine deiminase pathway genes. *Int J Mol Sci*. 2023;24(18):13914.

203. ISO. ISO 18259 Ophthalmic optics—contact lens care products—method to assess contact lens care products with contact lenses in a lens case, challenged with bacterial and fungal organisms. 2014.

204. Del Mar Cendra M, Torrents E. Differential adaptability between reference strains and clinical isolates of *Pseudomonas aeruginosa* into the lung epithelium intracellular lifestyle. *Virulence*. 2020;11(1):862-76.

205. Moradali MF, Ghods S, Rehm BH. *Pseudomonas aeruginosa* lifestyle: A paradigm for adaptation, survival, and persistence. *Front Cell Infect Microbiol*. 2017;7:39.

206. Pachori P, Gothwal R, Gandhi P. Emergence of antibiotic resistance *Pseudomonas aeruginosa* in intensive care unit; a critical review. *Genes Dis*. 2019;6(2):109-19.

207. Livermore DM. Multiple mechanisms of antimicrobial resistance in *Pseudomonas aeruginosa*: our worst nightmare? *Clin Infect Dis*. 2002;34(5):634-40.

208. Richards DM, Brogden RN. Ceftazidime. A review of its antibacterial activity, pharmacokinetic properties and therapeutic use. *Drugs*. 1985;29(2):105-61.
209. Shirley M. Ceftazidime-Avibactam: A review in the treatment of serious gram-negative bacterial infections. *Drugs*. 2018;78(6):675-92.
210. Huang X, Pearce R, Omenn GS, Zhang Y. Identification of 13 guanidinobenzoyl- or aminidinobenzoyl-containing drugs to potentially inhibit TMPRSS2 for COVID-19 treatment. *Int J Mol Sci*. 2021;22(13).
211. Arai H. Regulation and function of versatile aerobic and anaerobic respiratory metabolism in *Pseudomonas aeruginosa*. *Front Microbiol*. 2011;2:103.
212. Armitage JP, Evans MC. The motile and tactic behaviour of *Pseudomonas aeruginosa* in anaerobic environments. *FEBS Lett*. 1983;156(1):113-8.
213. Shoesmith JH, Sherris JC. Studies on the mechanism of arginine-activated motility in a *Pseudomonas* strain. *J Gen Microbiol*. 1960;22:10-24.
214. Hirose Y, Yamaguchi M, Sumitomo T, Nakata M, Hanada T, Okuzaki D, et al. *Streptococcus pyogenes* upregulates arginine catabolism to exert its pathogenesis on the skin surface. *Cell Rep*. 2021;34(13):108924.
215. Bernier SP, Ha D-G, Khan W, Merritt JH, O'Toole GA. Modulation of *Pseudomonas aeruginosa* surface-associated group behaviors by individual amino acids through c-di-GMP signaling. *Res Microbiol*. 2011;162(7):680-8.
216. Goncheva MI, Chin D, Heinrichs DE. Nucleotide biosynthesis: the base of bacterial pathogenesis. *Trends Microbiol*. 2022;30(8):793-804.
217. Punihaole D, Workman RJ, Upadhyay S, Van Bruggen C, Schmitz AJ, Reineke TM, et al. New insights into quinine-DNA binding using raman spectroscopy and molecular dynamics simulations. *J Phys Chem B*. 2018;122(43):9840-51.
218. Vallet-Gely I, Sharp JS, Dove SL. Local and global regulators linking anaerobiosis to *cupA* fimbrial gene expression in *Pseudomonas aeruginosa*. *J Bacteriol*. 2007;189(23):8667-76.
219. Giraud C, de Bentzmann S. Inside the complex regulation of *Pseudomonas aeruginosa* chaperone usher systems. *Environ Microbiol*. 2012;14(8):1805-16.
220. Vallet I, Olson JW, Lory S, Lazdunski A, Filloux A. The chaperone/usher pathways of *Pseudomonas aeruginosa*: identification of fimbrial gene clusters (*cup*) and their involvement in biofilm formation. *Proc Natl Acad Sci U S A*. 2001;98(12):6911-6.
221. McManus Heather R, Dove Simon L. The CgrA and CgrC proteins form a complex that positively regulates *cupA* fimbrial gene expression in *Pseudomonas aeruginosa*. *J Bacteriol*. 2011;193(22):6152-61.
222. Kuo SC, Koshland DE, Jr. Roles of *cheY* and *cheZ* gene products in controlling flagellar rotation in bacterial chemotaxis of *Escherichia coli*. *J Bacteriol*. 1987;169(3):1307-14.
223. Sampedro I, Parales RE, Krell T, Hill JE. *Pseudomonas* chemotaxis. *FEMS Microbiology Reviews*. 2015;39(1):17-46.
224. Han X, Kennan RM, Parker D, Davies JK, Rood JI. Type IV fimbrial biogenesis is required for protease secretion and natural transformation in *Dichelobacter nodosus*. *J Bacteriol*. 2007;189(14):5022-33.
225. Giltner CL, Nguyen Y, Burrows LL. Type IV pilin proteins: versatile molecular modules. *Microbiol Mol Biol Rev*. 2012;76(4):740-72.
226. Alm RA, Mattick JS. Identification of a gene, *pilV*, required for type 4 fimbrial biogenesis in *Pseudomonas aeruginosa*, whose product possesses a pre-pilin-like leader

sequence. *Mol Microbiol.* 1995;16(3):485-96.

227. Strom MS, Nunn DN, Lory S. A single bifunctional enzyme, PilD, catalyzes cleavage and N-methylation of proteins belonging to the type IV pilin family. *Proc Natl Acad Sci U S A.* 1993;90(6):2404-8.

228. Alm RA, Mattick JS. Identification of two genes with prepilin-like leader sequences involved in type 4 fimbrial biogenesis in *Pseudomonas aeruginosa*. *J Bacteriol.* 1996;178(13):3809-17.

229. O'Toole GA, Kolter R. Flagellar and twitching motility are necessary for *Pseudomonas aeruginosa* biofilm development. *Mol Microbiol.* 1998;30(2):295-304.

230. Barken KB, Pamp SJ, Yang L, Gjermansen M, Bertrand JJ, Klausen M, et al. Roles of type IV pili, flagellum-mediated motility and extracellular DNA in the formation of mature multicellular structures in *Pseudomonas aeruginosa* biofilms. *Environ Microbiol.* 2008;10(9):2331-43.

231. Chiang P, Habash M, Burrows LL. Disparate subcellular localization patterns of *Pseudomonas aeruginosa* type IV pilus ATPases involved in twitching motility. *J Bacteriol.* 2005;187(3):829-39.

232. Jones IA, Joshi LT. Biocide use in the antimicrobial era: A review. *Molecules.* 2021;26(8).

233. Mamouei Z, Alqarihi A, Singh S, Xu S, Mansour MK, Ibrahim AS, et al. Alexidine dihydrochloride has broad-spectrum activities against diverse fungal pathogens. *mSphere.* 2018;3(5).

234. de Azevedo Magalhães O, Ribeiro Dos Santos D, Coch Broetto BG, Corção G. Polyhexamethylene biguanide multipurpose solutions on bacterial disinfection: A comparison study of effectiveness in a developing country. *Eye Contact Lens.* 2023;49(4):139-42.